



NATIONAL & KAPODISTRIAN
UNIVERSITY OF
ATHENS
SCHOOL OF SCIENCE
FACULTY OF GEOLOGY &
GEOENVIRONMENT

TECHNOLOGICAL INSTITUTE
OF SERRES
FACULTY OF
CEOMETICS AND
SYRVEING



Postgraduate Study Program in Physical Disasters

Master thesis

Pallikarakis Aggelos I.N. 2907

Faculty of Geology & Geoenvironment U.O.A.

*“ Study of an active fault in the Corinth canal, through
paleoenvironmental interpretations and borehole data.
Implications for seismic hazard”*

Thesis Committee

Migiros Georgios
Papanikolaou Ioannis
Triantaphyllou Maria

Professor (Supervisor)
As. Professor
Assoc. Professor

Athens

December 2011



ΥΠΟΥΡΓΕΙΟ ΕΘΝΙΚΗΣ ΠΑΙΔΕΙΑΣ ΚΑΙ ΘΡΗΣΚΕΥΜΑΤΩΝ
ΕΙΔΙΚΗ ΥΠΗΡΕΣΙΑ ΔΙΑΧΕΙΡΙΣΗΣ ΕΠΕΑΕΚ



ΕΥΡΩΠΑΪΚΗ ΕΝΩΣΗ
ΣΥΓΧΡΗΜΑΤΟΔΟΤΗΣΗ
ΕΥΡΩΠΑΪΚΟ ΚΟΙΝΩΝΙΚΟ ΤΑΜΕΙΟ



Η ΠΑΙΔΕΙΑ ΣΤΗΝ ΚΟΡΥΦΗ
Επιχειρησιακό Πρόγραμμα
Εκπαίδευσης και Αρχικής
Επαγγελματικής Κατάρτισης



**ΕΘΝΙΚΟ ΚΑΙ ΚΑΠΟΔΙΣΤΡΙΑΚΟ
ΠΑΝΕΠΙΣΤΗΜΙΟ ΑΘΗΝΩΝ**

**ΣΧΟΛΗ ΘΕΤΙΚΩΝ
ΕΠΙΣΤΗΜΩΝ
ΤΜΗΜΑ ΓΕΩΛΟΓΙΑΣ ΚΑΙ
ΓΕΩΠΕΡΙΒΑΛΛΟΝΤΟΣ**

**ΤΕΧΝΟΛΟΓΙΚΟ ΕΚΠΑΙΔΕΥΤΙΚΟ
ΙΔΡΥΜΑ ΣΕΡΡΩΝ**

**ΤΜΗΜΑ
ΓΕΩΠΛΗΡΟΦΟΡΙΚΗΣ
& ΤΟΠΟΓΡΑΦΙΑΣ**



**ΔΙ-ΙΔΡΥΜΑΤΙΚΟ ΠΡΟΓΡΑΜΜΑ ΜΕΤΑΠΤΥΧΙΑΚΩΝ ΣΠΟΥΔΩΝ
«ΠΡΟΛΗΨΗ ΚΑΙ ΔΙΑΧΕΙΡΙΣΗ ΦΥΣΙΚΩΝ ΚΑΤΑΣΤΡΟΦΩΝ»**

ΜΕΤΑΠΤΥΧΙΑΚΗ ΔΙΑΤΡΙΒΗ ΕΙΔΙΚΕΥΣΗΣ

Παλληκαράκης Άγγελος Α.Μ. 2907

Τμήμα Γεωλογίας & Γεωπεριβάλλοντος Ε.Κ.Π.Α.

“Η μελέτη ενός ρήγματος στον Ισθμό της Κορίνθου μέσω ανάλυσης του παλαιοπεριβάλλοντος και γεωτρήσεων. Εκτίμηση της σεισμικής επικινδυνότητας. ”

ΤΡΙΜΕΛΗΣ ΕΠΙΤΡΟΠΗ

**Μιγκίρος Γεώργιος
Παπανικολάου Ιωάννης
Τριανταφύλλου Μαρία**

**Καθηγητής (Επιβλέπων)
Επ. Καθηγητής
Αν. Καθηγήτρια**

ΑΘΗΝΑ

Δεκέμβριος 2011



**ΥΠΟΥΡΓΕΙΟ ΕΘΝΙΚΗΣ ΠΑΙΔΕΙΑΣ ΚΑΙ ΘΡΗΣΚΕΥΜΑΤΩΝ
ΕΙΔΙΚΗ ΥΠΗΡΕΣΙΑ ΔΙΑΧΕΙΡΙΣΗΣ ΕΠΕΑΕΚ**

**ΕΥΡΩΠΑΪΚΗ ΕΝΩΣΗ
ΣΥΓΧΡΗΜΑΤΟΔΟΤΗΣΗ
ΕΥΡΩΠΑΪΚΟ ΚΟΙΝΩΝΙΚΟ ΤΑΜΕΙΟ**



Η ΠΑΙΔΕΙΑ ΣΤΗΝ ΚΟΡΥΦΗ
Επιχειρησιακό Πρόγραμμα
Εκπαίδευσης και Αρχικής
Επαγγελματικής Κατάρτισης

Abstract

A fault that intersects the Corinth canal has been studied in detail, based on several boreholes that were recovered from the hangingwall and the footwall of the fault. Lithostratigraphic units were described within these boreholes. Due to the lateral stratigraphic variations that were encountered, it was difficult to determine the accumulative displacement, as well as the slip rate of the fault. In order to overcome this problem micropaleontological analysis was performed.

Foraminiferal assemblages were picked from approximately 100 samples from boreholes 3 and 7 from the footwall and the hangingwall respectively. Species were identified and grouped into seven subcategories. Through them, the paleoenvironment was estimated within the boreholes and it was feasible to correlate horizons of borehole 3 with borehole 7. A colony of *Cladocora* corals that has been found in situ was used in order to estimate vertical offset between these two boreholes. Taking under consideration the known uplift rate for the Isthmus and global glacioeustatic sea level curve relative dates for these layers could be estimated.. Afterwards according to these dates and the measured fault's offset, the throw rate of the fault was estimated.

Using empirical relationships concerning fault's geometrical features and the estimated throw rate for a certain period of time, the seismic hazard posed from this fault has been assessed. Moreover, the seismic hazard over the entire Corinth canal posed from the neighboring major active faults was also assessed. The same procedure was repeated for other significant faults that influence the area. Loutraki, Kechries, Agios Vasilios and South Alkyonides faults system were examined in detail in order to determine how hazardous are for the area. For these faults earthquake recurrence was estimated using the throw rate that has already been calculated. Geological formations can amplify or lessen the expected intensity from an earthquake. As a result seismic hazard maps from geological data were compiled showing expected seismic intensities in the area.

Περίληψη

Η μελέτη ενός ενεργού ρήγματος το οποίο τέμνει τον Ισθμό της Κορίνθου, πραγματοποιήθηκε μέσω γεωτρήσεων στο ανερχόμενο και στο κατερχόμενο τέμαχος του. Στους πυρήνες όπου πάρθηκαν έγινε λιθοστρωματογραφική ανάλυση. Λόγο των πλευρικών διαφοροποιήσεων που παρατηρήθηκαν στην γεωτρήσεις, δεν ήταν δυνατή η συσχέτιση των οριζόντων μεταξύ τους. Για αυτό τον λόγο αναλύθηκαν οι γεωτρήσεις ως προς το περιεχόμενό τους σε μικροπανίδα

Περίπου 100 δείγματα λήφθηκαν από τους πυρήνες αυτούς, με σκοπό την μικροπαλαιοντολογική τους ανάλυση. Τα δείγματα αυτά εξετάστηκαν και ταξινομήθηκαν σε 7 υποκατηγορίες. Μέσω των αποτελεσμάτων αυτών εκτιμήθηκε το παλαιοπεριβάλλον και με τον τρόπο αυτό, συσχετίστηκαν οι οριζόντες στις γεωτρήσεις 3 και 7. Η θέση κοραλλιών τα οποία βρέθηκαν *in situ* στις δυο αυτές γεωτρήσεις, χρησιμοποιήθηκε για να υπολογιστεί το κατακόρυφο άλμα του ρήγματος. Αφού συνυπολογίστηκε η μεταβολή της στάθμης της θάλασσας και η ταχύτητα ανύψωσης του Ισθμού της Κορίνθου, εκτιμήθηκε η σχετική ηλικία των στρωμάτων αυτών. Με βάση αυτή την ηλικία και το κατακόρυφο άλμα για την συγκεκριμένη περίοδο, υπολογίστηκε ο ρυθμός ολίσθησης του ρήγματος.

Στην συνέχεια, μέσω εμπειρικών σχέσεων όσον αφορά τα γεωμετρικά χαρακτηριστικά ενός ρήγματος και τον ρυθμό ολίσθησής του, εκτιμήθηκε η σεισμική επικινδυνότητα στον Ισθμό από την πιθανή ενεργοποίηση του συγκεκριμένου ρήγματος. Για την καλύτερη εκτίμηση της επικινδυνότητας στην ευρύτερη περιοχή, συνυπολογίστηκε η επίδραση μεγαλύτερων ρηγμάτων που είναι περιμετρικά από τον Ισθμό και επηρεάζουν την περιοχή. Έτσι υπολογίστηκε η σεισμική επικινδυνότητα για το ρήγμα του Λουτρακίου, των Κεχριών, των Αλκυονίδων και του Αγίου Βασιλείου. Για κάθε ένα ρήγμα από αυτό, υπολογίστηκε η επαναληψιμότητα ενός σεισμικού γεγονότος, καθώς και η επίδραση που έχει η γεωλογία στον καθορισμό της μέγιστης αναμενόμενης έντασης. Το αποτέλεσμα ήταν η εκτίμηση της σεισμικής επικινδυνότητας στην περιοχή από τα μεγαλύτερα ρήγματα που μπορούν να την επηρεάσουν.

Acknowledgements

I would like to express my gratitude to the advisory committee Dr. Migiros Georgios, Dr Papanikolaou Ioannis and Dr Triantaphyllou Maria. Without their helpful supporting and guidance, this thesis would not have been achieved.

I would also like to thank Dr. Dimiza Margarita and the laboratory of Historical Geology-Paleontology Department, for their permission to use Leica APO S8 stereoscope and the scanning electron microscope analysis (SEM Jeol JSM 6360). I would also like to appreciate them for their assistance and their instructions, as far as concerns paleoenvironmental analysis. I would like to thank Msc Deligiannakis Georgios and other anonymous researchers for their helpful comments.

Finally, I would like to thank the Academy of Athens for their financial support, offering me a scholarship.

Table of contents

Abstract.....	2
Περίληψη.....	3
Acknowledgements	4
1. Introduction	7
2. Previous work.....	10
2.1 Corinth Gulf.....	10
2.2 Paleoenvironment, Boreholes and Slip rate.....	16
2.3 Seismic Hazard assessment	20
3. Description of the study area.....	22
3.1 Studied fault	22
3.2 Corinth Isthmus	25
3.3 Geology of the area.....	27
4. Borehole data.....	31
4.1 Introduction	31
4.2 Lithostratigraphic units.....	31
4.2.1 Description	31
4.2.2 Interpretation	40
4.3 Methodology.....	44
4.4 Micropaleontological analysis.....	45
4.4.1 Description	45
4.4.2 Interpretation	50
5. Paleoenvironmental Analysis	51
5.1 Description.....	51
5.2 Interpretation	55

6.	Seismic hazard assessment.....	63
6.1	Introduction	63
6.2	Slip rate	64
6.3	Methodology	65
6.4	Seismic Hazard maps	68
6.4.1	Kalamaki fault.....	68
6.4.2	The Kechries fault.....	73
6.4.3	The Loutraki fault	77
6.4.4	The South Alkyonides fault system	81
6.4.5	The Agios Vasilios fault	86
7.	Discussion	90
7.1	Effects from the studied fault.....	90
7.2	Seismic hazard of Corinth canal.....	93
7.3	Paleoenvironmental reconstruction	100
8.	Conclusions	104
9.	References	106
	List of figures.....	114

1. Introduction

The Gulf of Corinth is a 115 km long and 30 km wide structure in central Greece. It is considered to be the most active tectonically area of and one of fastest extending regions in the world (Billiris et al. 1991; Briole et al. 2000). Corinth Gulf is extending towards its center at a 20 mm/yr rate that decreases eastwards at 8 to 4 mm/yr. To the eastern end of the gulf has been constructed the Corinth canal one of the most famous infrastructures in Greece (Figure 1.1(A)).

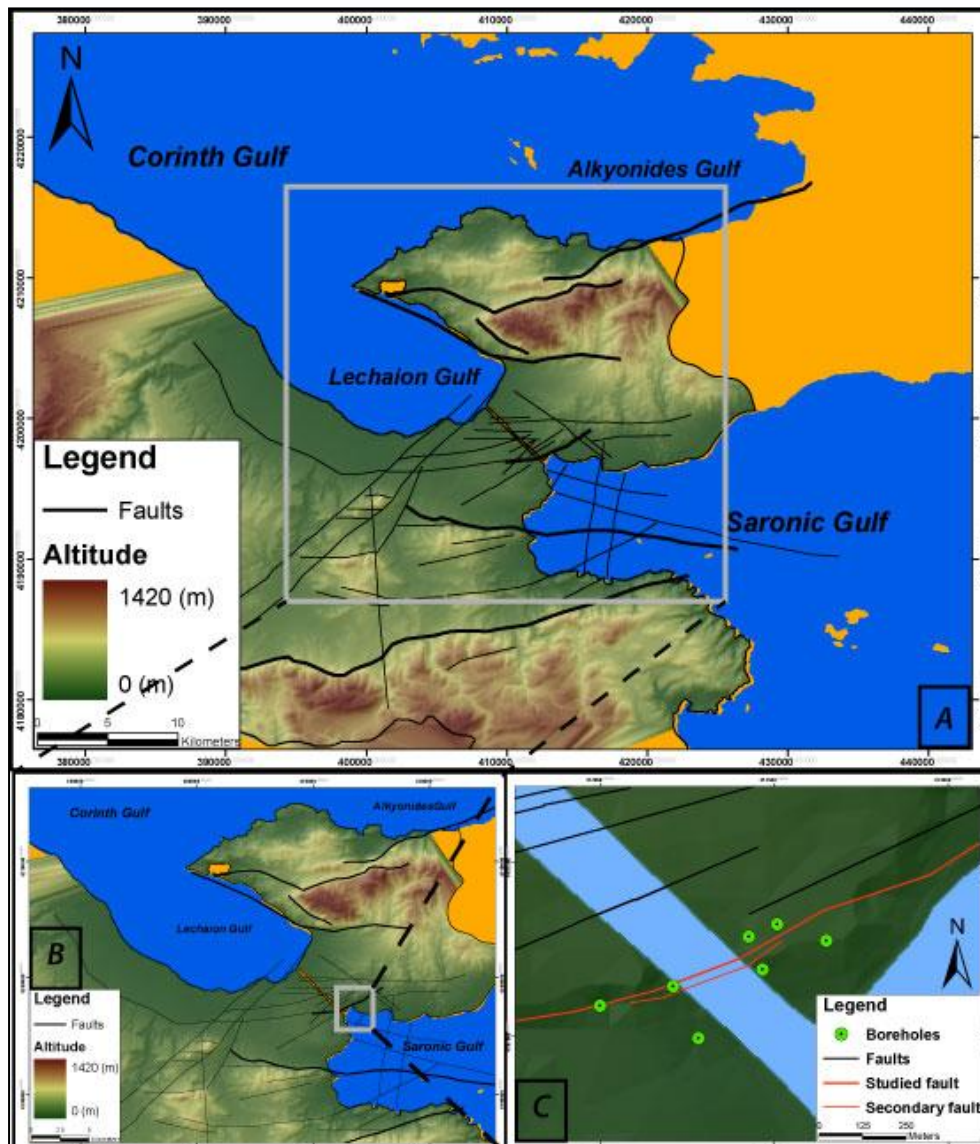


Fig. 1.1 The eastern end of Corinth Gulf (A), where the Corinth canal is (B) and the boreholes were drilled (C)

The canal is operational since 1893 connecting Corinth Gulf with Saronic Gulf. This 6.5 km long mega-trench offers a unique opportunity to observe more than 52 faults and strata sequence. Since the age of these strata is more or less known, it is an excellent opportunity to determine the activity of the faults. Several of them intersect only Pliocene sediments and are clearly inactive, while others intersect Pleistocene sediments up to the surface and are characterized as active. None of these faults though, have significantly displaced the topography. The only fault that has created topographic variations near the Kalamaki village is located to the easternmost tip of the Corinth Isthmus (Figure 1.1 (B, C)). This 5.5 km long fault, which trends ENE-WSW, seems to be the most active in the canal area (Collier et al. 1991, Papanikolaou et al. 2011).

Foraminiferal and other marine species have been used before in order to specify the paleoenvironment of an area. For instance, the presence of foraminifera such as *Haynesina* spp. and small-sized *Ammonia* imply that this is a closed lagoon environment, while the presence of miliolids and full marine species indicate that this is a pure marine system (Koukousioura et al. 2011, Goiran et al. 2010, Triantaphyllou et al. 2003, 2010). Boreholes that were recovered towards the hangingwall and the footwall of the fault were examined regarding foraminiferal assemblages. Through them the paleoenvironment can be reconsidered. In order to examine them, foraminifera were grouped to *Haynesina* spp., *Aubignina*, small and large sized *Ammonia*, *Elphidium* spp., Miliolids and full marine species. Some of these that were identified within boreholes indicate a lagoonal environment, while others indicate a deeper marine environment. These alterations are thought to be the product of interplay between the rate of global sea-level change and the rate of tectonic uplift of the area. Through this procedure the throw rate of this fault has been estimated.

Researchers in order to estimate seismic hazard threat in an area, evaluated recorded historical earthquakes. They statistically analyzed them and through this procedure they estimated earthquake recurrence in an area and how imminent an oncoming event is. This methodology though is not completely sufficient. Catalogues of historical earthquakes are incomplete. Furthermore, recorded earthquakes by instruments are available only for the last 60 years.

In order to overcome this problem, several researchers have used faults slip-rate and their geometrical characteristics in order to estimate and map the seismic hazard in an area. Faults with higher rates, are activated more frequently and therefore pose greater threat. Furthermore, the magnitude of an earthquake is related with the length of a fault that has been ruptured. Evaluating these data, someone can specify the seismic hazard in an area.

The result of this thesis are maps that determine which area of the canal is under greater hazard, where maximum intensities are expected, which fault mostly threatens the area and how often can one of these faults shake the area and with what consequences. Furthermore, back on paleoenvironmental results extracted from this study, evaluating the tectonic uplift and the global sea level changes, the paleogeographical evolution of the study area was reconstructed.

2. Previous work

2.1 *Corinth Gulf*

The Corinth Gulf is one of the fastest extending regions of the world and this has provoked a plethora of researchers to study the area. Especially after the 1981 earthquake sequence that occurred at the Perachora peninsula, many authors have described the active faults of the area, the morphology and the paleogeography of the area, the environmental alterations and how the paleoenvironment evolves during time. Other researchers have identified and describe marine microfauna found in the area, from foraminifera to corals.

Lykousis et al. (2007), have examined through geophysical methods, surface observations and cores the stratigraphy and the tectonic structure of the central and eastern part of Corinth Gulf. They have dated sediments found in cores, in order to specify their age. They have also found different depositional environments, since they have spotted the transition from marine to lacustrine sediments. Through them they were able to determine sedimentation rates at the Corinth gulf. The most important though, was that after they have traced offshore faults at the seabed, they were able to calculate displacements caused from their activity and their slip rates. Finally, they have made implications about the evolution of the Gulf during Quaternary.

Zygouri et al. (2008), have thoroughly mapped and examined 136 offshore and onshore faults, located at the Corinth Gulf. They have analyzed fault length and throw, in order to study the scaling properties of 136 well determined offshore and onshore faults. They have compiled an extended database, of these fault's length, throw and slip rate. They have calculated the displacement/length ratio of these faults and through this they have made implications about fault growth and linkage in Corinth Gulf.

Papantoniou et al. (2008), had studied the geological conditions and slope failures along the Corinth canal. After they have mapped geological formations, paying more attentions to the excavated debris from the Canal, they were able to determine which

area was under greater risk. Three areas were highlighted after their study, the villages of Isthmia and Posidonia and the intersection with the national railroad.

Anagnostopoulos et al. (1990), have thoroughly examined the marl formations that compile the area of Isthmus. Geotechnical investigation was performed with an extensive laboratory testing program. They have concluded that these marls have a brittle geotechnical behavior, high stiffness and significant cohesion..

Rondoyanni & Marinos (2008), have examined the seismic hazard assessment of the Corinth highway, at Kakia Skala area. More specific, they have estimated the threat that Kakia Skala fault poses at the Corinth highway. Rondoyanni et al. 2008, have examined the geological structure and the active tectonic of the eastern tip of Corinth Gulf. After they have analysed the geological formations that structured the area, they have identified and described the most important active faults that affect the area. Among them are the Loutraki, the Schinos-Pisia and the Kechries faults. Finally they have made implications about the seismic threat posed by these faults and how can affect infrastructures.

Maroukian et al. (2008), have described the effects of fault propagation on drainage system. The area that they have examined is the westernmost section of Perachora peninsula and the Schinos-Pisia faults segments. They have analyzed the geomorphology of the drainage system, where they have marked the presence of wind gaps. After that they have mapped marine terraces from the isotope stage 5, they have concluded that the drainage system is not only affected by these faults, but by regional uplift as well. Finally they have reconstructed the paleogeography of the area, during the last 125.000 years.

Gaki-Papanastasiou et al. (1996), made geomorphic observations caused by earthquakes such as raised coastal notches and beachrocks, at Peloponnesus. Firstly they have taken into account paleoseismological data, concerning Sparta, Mycenae, Eliki and Perachora. At the eastern tip of the Gulf, the researchers have mapped raised notches, shorelines and beachrocks. They have found beachrocks at the ancient Diolkos 0.80 m higher than the present sea level and through this, estimated uplift throw. For each of these areas, recorded historical earthquakes have been correlated with these effects.

Collier & Dart (1991), have examined in detail the area of the Corinth Isthmus. They have thoroughly described the lithological formations that exist in the area and have made assumptions about the paleoenvironment of each one of them. The oldest formation that they mention is from the lower Pliocene. They have identified several faults that intersect the area, where many of them are active. The Kalamaki fault that has been studied in detail in this thesis, was described there even though that they have not extended southern from the canal. Finally, authors have implied that the basin is uplifted, from observations that were made to marine terraces.

Morewood & Roberts (1997), have mapped seventy eight faults segments to the westernmost segment of Perachora peninsula. The geometry, kinematics and rates of deformation of these segments have been investigated.

Morewood & Roberts (1999), have meticulously mapped the paleoshorelines and marine terraces to the southern bay of Perachora peninsula. Marine terraces have been correlated with the sea level change. This correlation gives uplift rates of the bay. Taking all these under consideration they calculated when drainage system was cut by SAFS propagation. They were also able to determine a propagation rate approximately of 12.1 ± 16.7 mm/yr over at least the last 330.000 years. Finally they made paleogeographical implications, about the evolution of the SAFS, the drainage system and entire area of Perachora during the last 330.000 years.

Roberts (1996), showed that the Corinth Gulf can be divided into fault segments and he has mapped several faults to the Gulf. He has also mapped fault displacements, where he implied that more obvious topographic variations are observed towards the center of the faults. Roberts (1996), has shown that the central part of a fault slips faster than its tip. Finally he implied that spatial variations in fault kinematics can be used for estimating the seismic hazard assessment of an area.

Leeder et al. (2002), used geophysical methods in order to investigate the offshore segment of the South Alkyonides system fault. They were able to describe the bathymetry of the Alkyonides Gulf and they have found the traces of the offshore faults of East, West Alkyonides fault and the offshore segment of Psatha fault. Taking under consideration the sea level change during the upper Pleistocene and the fact that Corinth Gulf was lake during the last glaciation, they have estimated the displacement

at the tip of the Psatha fault. They have estimated a slip rate approximately 0.8 mm/yr during the Holocene. Furthermore, taking consideration raised Holocene coastal notches located at the footwall of SAFS, they calculated the footwall uplift at 0.2 mm/yr and the hangingwall subsidence at 0.6 mm/yr.

Several researchers have tried to estimate the uplift rate of the eastern tip of Corinth Gulf. Different rates have been estimated for Corinth Isthmus, Lechaion Gulf and Perachora peninsula. There is a controversy though about the reasoning and the rate of this uplift. Some of them (Turner et al. 2010, Leeder et al. 2003), imply there is regional uplift due to the subduction of the African plate beneath Peloponnesus. On the contrary, other researchers (Armijo et al. 1996, Roberts et al. 2009), claim that uplift has also to do with active faults which affect the area.

Leeder et al. (2003), have mapped diagnostic shoreline features such as beachface deposits, marine terraces and coastal notches, they have dated corals and correlated them with the sea level change, in order to determine their age. They suggested that Perachora, Lechaion, Isthmus region are regionally uplifted and it is inconsistent with the movement of Xylokastro or Alkyonides fault. They implied that this uplift is due to the subduction zone of the African plate beneath Peloponnesus.

Turner et al. (2010), tested various rival hypothesis concerning the evolution of the eastern tip of Corinth and the uplift of this area. These hypotheses are tested by comparing predicted spatial uplift trends with those observed. They have thoroughly mapped raised paleoshorelines and have correlated the results with the global glacioeustatic sea level change compiled by Thompson & Goldstein (2006). They have proposed that 0.31 mm/yr uplift rate at Lechaion Gulf could be explained as displacement on the footwall of active faults. They have also proposed that the north coast of Lechaion Gulf uplift cannot be explained by footwall uplift but it is due to isostatic uplift that probably affects the whole of the southern Gulf of Corinth rift.

Collier & Thompson (1991), have examined in detail sedimentary facies across the Corinth canal. They have identified and described transverse and linear dunes. They have dated corals that were found in situ, 1.5 km southwards the canal and have placed them in isotope stage 7 At 200.000 years. With this age they have estimated the uplift rate there approximately at 0.44 mm/yr. Through the analysis of the

sediments and the date of these strata, authors were able not only to reconstruct the paleogeography of Corinth 200.000 years ago, but state the fact that Corinth and Saronic Gulf, could communicate then.

Corals have been used by Collier et al. (1992), for estimating the date of sediments in more than one paper. According to Collier et al. 1992, the uplift rate of the Corinth Isthmus and of the area southern from it, has been estimated by using corals. Several samples were taken from colonies which were found in situ. After they have date them, they estimated their age at 205.000 years. The age of corals that were found in Examilia was also at 205.000 years. They have co estimated the relative change of the sea level and specified the rate in which the area is uplifted. The central part of Corinth is uplifted with a 0.30 mm/yr rate during the last 200.000 years, where the area south and westwards is uplifted with a 0.44 mm/yr rate during the same period.

Dia et al. (1997), estimated the uplift rate at the eastern tip of Corinth Gulf, at Perachora peninsula. After that they have dated corals that they found in situ, relative ages have been estimated. The age of the samples that were taken from the isthmus canal was at approximately 200.000 years. The age of the samples that were taken from Examilia was approximately at 323.000 years. Taking under consideration the sea level change, they determine the uplift rates for the Corinth canal, Examilia, Perachora and Alepochori. Finally, these ages were correlated with other author's work such as Collier. It interesting to mention that samples were taken close the boreholes area, implied that uplift rate corresponds with Collier's work¹. On the contrary dates from Examilia samples were not in correspondence.

Armijo et al. (1996), have thoroughly examined the Corinth Gulf and more specific the Xylokastro fault. They have mapped the marine terraces about for 30 km long and up to 400 m altitude. They have implied that risen terraces are constantly uplifted during the Pleistocene. They have also found terraces of Late Pleistocene to Holocene 400 m height around the Lechaion. They have implied that this uplift is related with the migration of north-dipping fault systems.

¹ Collier has found that corals' age was approximately 200.000 years and the uplift rate was 0.3 mm/yr.

Roberts et al. (2009) and Cooper et al. (2007) have examined raised paleoshorelines to north bay of Lechaion Gulf. According to Cooper et al. (2007), the southern section of Perachora peninsula is constantly uplifted during the last 125.000 years. They have mapped and examined three notches and through ^{14}C ages on notch fauna, their age was estimated. They have also mapped the paleoshoreline of 125.000 years, which was previously dated with corals that were found in situ. Finally they have estimated the uplift rate during the Holocene from the highest notches up to 0.55mm/yr. Roberts et al. 2009, have also mapped and examined the raised paleoshorelines and marine terraces at the footwall of the South Alkyonides fault system. Apart from notches, they have also dated *Cladocora* corals that were found in situ. Results have been correlated with the global glacioeustatic sea level curve and through this procedure the uplift rate was estimated. According to them, the southernmost area of Perachora peninsula, was uplifted with a rate approximately 0.15 mm/yr during the Pleistocene till the last 200.000 years. From then till today, SASF has accelerated and the area is uplifted with a 0.51 mm/yr rate. Finally they tried to determine the paleomorphology of Corinth gulf and how it has evolved during the last 340.000 year.

Houghton et al. (2003), estimated uplift rates at the westernmost section of Corinth Gulf, near the Rio Straits. In the footwall of Psathopyrgos fault they mapped marine terraces, where corals were found in situ. After dating these corals, relative ages were estimated and through them was determined the uplift rate. The global sea level change was also taken under consideration. The 0.7-0.8 mm/yr uplift rate during the last 175.000 years that was estimated was correlated with rates estimated by other authors along the Gulf. Finally, implications were made concerning the mechanical/kinematics models between the eastern and the western section of Corinth Gulf.

The 1981 earthquake sequence, has spurred several researchers to examine the Gulf, as it was an excellent opportunity to observe the effects from an earthquake sequence. Three seismic events occurred within 20 days, where it is supported that one event might have triggered the others (Hubert et al. 1996).

Jackson et al. (1982) and Mariolakos et al. (1982), were among the first have mapped and described the effects from these earthquakes. They have identified surface ruptures in Kaparelli fault and Schinos-Pisia faults which are segments of the

SAFS. They have traced surface ruptures that were approximately 25 km long. Maximum displacements that have been observed were at 1.5 m high. They have also plotted the epicenters of these earthquakes.

Hubert et al. (1996), have described and mapped the effects from these shakes, at the north section of the Perachora peninsula. They have modeled vertical displacement caused by the shakes and Coulomb stress transfer due to the earthquakes. Finally, they have implied that the first earthquake might have triggered the others.

Pantosti et al. (1996), have tried to estimate the vertical slip rate at SAFS, through trenching. For this reasons, has been selected an active alluvial fan at Bambakies. This is located approximately at the center of the fault system and more specifically at the easternmost end of the Schinos surface rupture. A trench has been excavated in order to identify paleosols. Three such surfaces were identified and have been dated. These surfaces were attributes to paleoearthquakes at 1295 AD and at 590 AD. Vertical slip rate has been estimated, at minimum of 1 mm/yr.

Collier et al. (1998), had repeated the procedure, two years afterwards at the same area of Bambakies fan. This time though, has excavated two more trenches close to the previous one. The second trench was excavated in April 1996 and was located 40 m east of the active channel on the Bambakies Fan, where the fault has displaced fan surface 2 by 3.5 - 5.0 m. The third trench was excavated at an antithetic fault to the north. From these trenches paleoseismological events were estimated. Earthquake recurrence is estimated from 700 years (trench 1), to 330 years (trench 3). Displacement per event has been estimated at 0.5 m, while vertical slip rate has been calculated to 2-3 mm/yr.

2.2 Paleoenvironment, Boreholes and Slip rate

Several researchers have used boreholes cores before, to estimate the paleoenvironment of an area, since paleoenvironmental analysis can be proved very helpful in order to examine an area. The keystone for estimating the paleoenvironment is assemblages of each foraminiferal species, or other marine microfauna.

Koukousioura et al. (2011), performed boreholes to three different locations in Greece with three different environments. In Lafrouda in Thrace, there is a modern closed lagoon with salinity ranging between 29.0 and 29.5 psu. In Vravron in Attica, there is a recent open lagoon where salinity ranges between 29.6 and 32.7 psu and to the coast of Alykes in Kitros, there is a modern coastal environment with salinity between 36.7 and 37.5 psu. Samples that were taken were analyzed for foraminifera and assemblages were grouped into two categories. The one group contains foraminifera that represent a closed lagoon environment (consists solely of *A. tepida* and *H. Germanica* species), while the other represents an open lagoon environment (consists from *A. perlucida*, miliolids, *Elphidium* spp., *A. beccarii*, *A. parkinsoniana*, accompanied by *P. pertusus*, *Bolivina* spp. and other small epiphytic rotaliids (*Rosalina* spp., *L. lobatula*, *A. planorbis*).

. Goiran et al. (2011), used cores from 10 boreholes drilled around Piraeus in order to validate the hypothesis that it was an island during the past. They took samples from these cores which were analyzed for microfaunal content. Species that were found represent alterations between marine foraminiferal species. These species were grouped into 7 categories, where assemblages of each species, indicated the paleoenvironment that fluctuated from shallow marine to lagoonal oligohaline. . Through them, these researchers could imply the paleogeographical evolution of the area.

Triantafyllou et al. (2010), performed the same procedure in order to estimate the paleoenvironment in Vravron, an area near Athens. Apart from foraminiferal assemblages though, they used palynological analysis and ostracods assemblages that were found into the drilled boreholes. Through them, they could identify several alterations to the paleoenvironment. Triantaphyllou et al. (2003), investigated the microfauna that was recovered from the coastal plain of Marathon. Three biofacies were identified based on foraminifera and ostracoda assemblages: the shallow mesohaline-oligohaline biofacies, the shallow oligohaline-fresh waters biofacies suggesting an approximate elevation of 20 cm above mean sea level and finally the mesohaline-oligohaline to oligohaline-freshwater biofacies characteristic of an intermediate mesohaline-oligohaline to oligohaline-freshwater lagoonal environment.

Pavlopoulos et al. (2006) determined the sequence of depositional environments and the sea level changes recorded in the coastal plain of Marathon for about the last 6000 yr, using micromorphological and micropalaeontological methods in addition to AMS radiocarbon datings. The same author, Pavlopoulos et al. (2010), used the same methodology in Palamari bay in Skyros, in order to estimate the paleoenvironmental evolution. Samples that were taken from boreholes and from trenches were analyzed. Foraminiferal assemblages, ostracods and pollen were used in order to determine the paleoenvironment and after radiocarbon method the date of these layers was determined. Evaluating these data the paleogeography of the area was reconstructed.

Evelpidou et al. (2010), used foraminiferal assemblages that were found in boreholes so as to estimate the paleogeography of Naxos island. After radiocarbon dating they were able to determine the exact age of these strata. In combination with the expected paleoenvironment, as it was found through micropaleontological analysis, these researchers determine the paleogeographical evolution of the area.

Theodorakopoulou et al. (2009), used foraminiferal assemblages, pollen analyses and ostracods, in order to determine the paleoenvironment in Istron in Crete. The ^{14}C method was used to date charred and plant material from layers of the sedimentary sequence. These data were correlated with the sea level change during the last thousand years and through this the paleogeography of the area was estimated. Pollen analysis with boreholes in order to estimate the paleoenvironment, has been used by Kouli et al. (2009), in the coastal plain of Marathon.

Trikolas et al. (2004), have mapped marine terraces towards the westernmost section of Corinth Gulf, near Aigio. Firstly, they have taken samples from several terraces. Afterwards, they have described the sediments and they have analysed the microfauna that was found (foraminifera, ostracods, shells even corals). They have dated several samples and through these ages, they have identified the paleoenvironment during the Pleistocene. Finally, they have estimated the uplift rate of the area approximately at 2.5 mm/yr.

Boreholes and paleoenvironmental analysis have been used before in order to determine slip rate. Ferranti et al. (2011), drilled boreholes at the area of the ancient town Sybaris, south Italy in order to examine different vertical displacements rates.

The entire area is constantly uplifted, while the area where the city is has been subsided at least during the Upper Pleistocene. Boreholes cores were used in order to correlate different horizons, where samples were dated. Microfauna that were found within the boreholes was used to determine the paleoenvironment. Finally the sea level changes were co estimated in order to determine the vertical displacements and their rates. Authors were able to determine various rates not only spatially, but within the boreholes, where they implied that maximum subsidence was during the Early Holocene. Local subsidence is attributed according to the authors in sediments compaction.

Yasuhara et al. (2005), used boreholes in order to determine the vertical displacement at the Median Tectonic Line in Iyo-nada Bay, in western Japan, Several boreholes were recovered at the footwall and at the hangingwall of this fault. From the cores, samples were taken which were thoroughly examined as far as concern their ostracods assemblages. They have used sensitive microfossils to reconstruct changes in water depths caused by seabed fault movement. Through them implication about the paleoenvironment were made, which were used afterwards to construct a local sea level change curve. This curve was afterwards correlated with another one from an area that is considered to be relative stable tectonically. Differences that were found, were considered to be the displacement caused due to this fault and they have managed to estimate vertical displacements during the Mid- Holocene.

Murata et al. (2001), have tried to estimate vertical offset and average slip rate of the Nojima Fault on Awaji Island in Japan. Several boreholes were drilled to that fault zone, as a part of a drilling project. Different lithological formations were encountered and described within the boreholes. Through lithostratigraphic description, layers have been correlated and vertical displacements were calculated. Afterwards, maximum displacement was estimated and taking under consideration that faults are active approximately from 1.2 Ma, average vertical displacement can be estimated.

Hayward et al. (2006), have used micropaleontological evidence in southern Hawke's Bay at New Zealand. Several boreholes were recovered, where 147 samples were taken. These, were analyzed as regards their foraminiferal and diatoms assemblages. From these assemblages, implications about the paleoenvironment and the past elevations were made Foraminiferal fauna was grouped according the

paleoenvironment. Furthermore, radiometric carbon dates were done on shell and plant material, where relative ages were estimated. The fact the tidal affected the area, has lead into several different depositional environments during the Holocene. Authors could estimate different elevations with high accuracy due to tidal effects. Since they estimated pale elevations of the area, they have reconstructed the paleoenvironment during the last 6.500 years. Finally, they were able not to estimate vertical displacements since the Mid –Holocene, but due to the fact that they have previously estimated different elevations with high accuracy, they identified possible seismic events.

2.3 Seismic Hazard assessment

Traditionally, in order to estimate seismic hazard of an area, researchers counted on paleoseismological data and historical earthquakes that have been recorded in this area. Tsapanos et al. (2011), has estimated the seismic hazard of Corinth taking under consideration, all major event from 550 BC till recently, as they have been recorded by Papazachos & Papazachou (1997). Afterwards they have tried to locate these epicenters that surround Corinth within a radius of 30 km and a larger one of 50 km, in order to co estimated big seismic event that might have also affected the city. 25 epicenters have been estimated, 12 within the 30-km radius circle and 13 at the 50-km radius circle. After using statistical and empirical relationships, they have concluded that the City of Corinth can experience an earthquake of maximum magnitude 6.7 Ms within the 30 km radius and 7 Ms within the 50 km radius. An event of 6.5 or bigger is expected every 100 years more or less.

These results can only show the expected magnitude of an earthquake, not the expected intensity. Geology was not taken under consideration. Only after that someone co estimates the geological factor in an area, can determine the seismic risk there. In order to do that someone must evaluate the faults which might affect this area, how often can these fault ruptures and finally co estimate the influence that geology has to the expected intensity.

Roberts et al. (2004), determined the seismic risk in the Lazio-Abruzzo Apennines in central Italy. They have meticulously mapped all active faults that threaten the area and they have estimated their slip rates. They have combined fault throw-rates with expected earthquake magnitudes, coseismic slip magnitudes, earthquake rupture lengths and the expected intensity of IX caused from these faults in MCS scale. Throw rates of the last 18.000 years have been transformed into hypothetical epicenters through empirical relationships, which were plotted at the hangingwalls of the faults. Afterwards they have co estimated the influence geology has to the expected intensity. The combined earthquake recurrence and geological amplification, has highlighted area that are considered to under greater threat.

Papanikolaou et al. (2011), used more or less the same methodology for estimating the seismic threat in Sparta. Westwards from the city a 70 km long fault, is located. In this case throw rates of the last 15.000 ± 3.000 have transformed into hypothetical epicenters which afterwards were plotted at the hangingwall. Geology was also taken under consideration in order to produce seismic maps. Furthermore, Taking under consideration earthquake recurrence and the last recorded time that this fault has ruptured, researchers have estimated the time depending probability of an imminent event the following 30 and 50 years.

This thesis is probably the first that has estimated seismic hazard in Corinth area, not by analyzing seismological data, but by examination of the geological and tectonic characteristics of the area. Paleoenvironmental evolution and micropaleontological analysis at the Corinth Isthmus have been done by several researchers before. This thesis though, is probably the only that has taken under consideration boreholes so deep (the deepest drilling was till 70 m depth).

3. Description of the study area

3.1 Studied fault

The fault that has been studied in detail lies to the eastern tip of the canal (Figure 3.1). It is located in the hangingwall of Loutraki and Kechries fault and in the footwall of the South Alkyonides fault. Its total length is approximately 5.5 km where is extended for at least 1 km southwards from the canal and for 4.5 km northwards from the canal. It strikes at 075°-255° (ENE-WSW trending) and is a high angle normal fault dipping at 65° towards the SSE. It has created topography variations approximately 150 m height towards its center, between the footwall and its hanging wall (Collier & Dart 1991).

Undoubtedly, this fault is active. Apart from the fact that it bounds recent alluvial sediments, it has offset layers from the Upper Pleistocene and exhibits a clear fault plane (Figure 3.2). Furthermore strata in the immediate footwall of the fault are dipping about 10-20° to the NNW, indicating also that this tilt is due to the recent fault activity. On the fault plane striations have been measured, which are plunging at 55° towards the SE (145°), confirming that it is an almost pure normal fault.



Fig. 3.1 View from Google Earth, where Kechries and the studied fault are shown. The area where boreholes were drilled is also shown (redrawn from Roberts et al. 2011)



Fig. 3.2 View of the main fault plane about 50m northwards the Canal. On this plane striations have been measured. This is a high angle normal fault dipping 65o towards the SSE.

Southwards from the Corinth canal the fault has been traced again (Figure 3.3). Now, it trends at 070o-250o and dips 70o towards the SSE. Apart from the main fault, to the NW of the main fault plane and over a 350m distance several fault planes parallel to the main fault have been identified. A clear secondary active fault plane has also been mapped, located in the immediate hangingwall of the main fault (Figure 3.4). Its length is approximately at 350 m long. Looking at the canal, it is clear that this minor fault intersects the entire lithostratigraphic column. In figure 3.4 a landslide has occurred there that the fault plane of this secondary fault is. Taking under consideration this minor fault, the fault zone is extending at 50 m. Based on the characteristics of these faults, implications can be made that the fault activity has progressively migrated eastwards towards from the studied fault.

Near to the canal, seven boreholes were drilled, two at the footwall and the rest at the hangingwall (Figure 3.1). The entire area is characterized by the presence of semicohesive Upper Pleistocene sediments of variable grain sizes (from cm thick pebbles to clay), conglomerate and gravels. Microfauna that was found in the area, indicates a shallow marine to brackish-oligohaline environment. Several researchers

have identified corals, gastropods, foraminifera and an abundance of ostracods (Freyberg 1973, Krstic & Dermizakis, 1981, Collier et al. 1991, Papanikolaou et al. 2011).



Fig. 3.3 View of the fault about 650m southwards the Canal. Arrows point to the fault plane displayed in the photo towards the right. It trends 070o-250o and dips 70o towards the SSE.

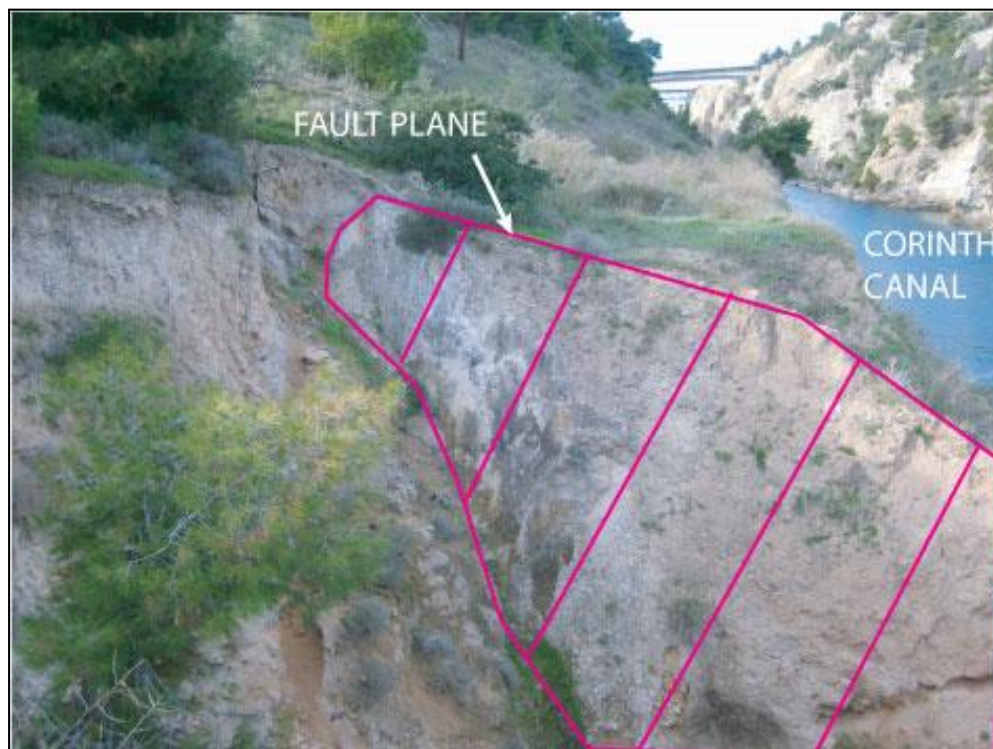


Fig. 3.4 View of the secondary fault plane of the principal fault on the southern part of the Canal. It also created a landslide in the past.

3.2 Corinth Isthmus

In order to examine more properly the Corinth canal, the nearby area must be taken under consideration as well. It has been studied in detail the easternmost tip of the Gulf of Corinth, the Corinth canal, the Lechaion Gulf and the Perachora peninsula. With the use of ArcGis 9.3 ESRI 2008, the Digital Elevation Model of the area has been created. Highest altitude that was observed in the area was in Perachora peninsula at the northernmost section of map in figure 3.5 (1060 meters). The central section of map, where the Corinth canal is, is characterized by milder topographic variations that do not exceed 150- 200 m. High altitude also has been recorded at the southernmost area of the map, where Kechries fault and Acrocorinth is.

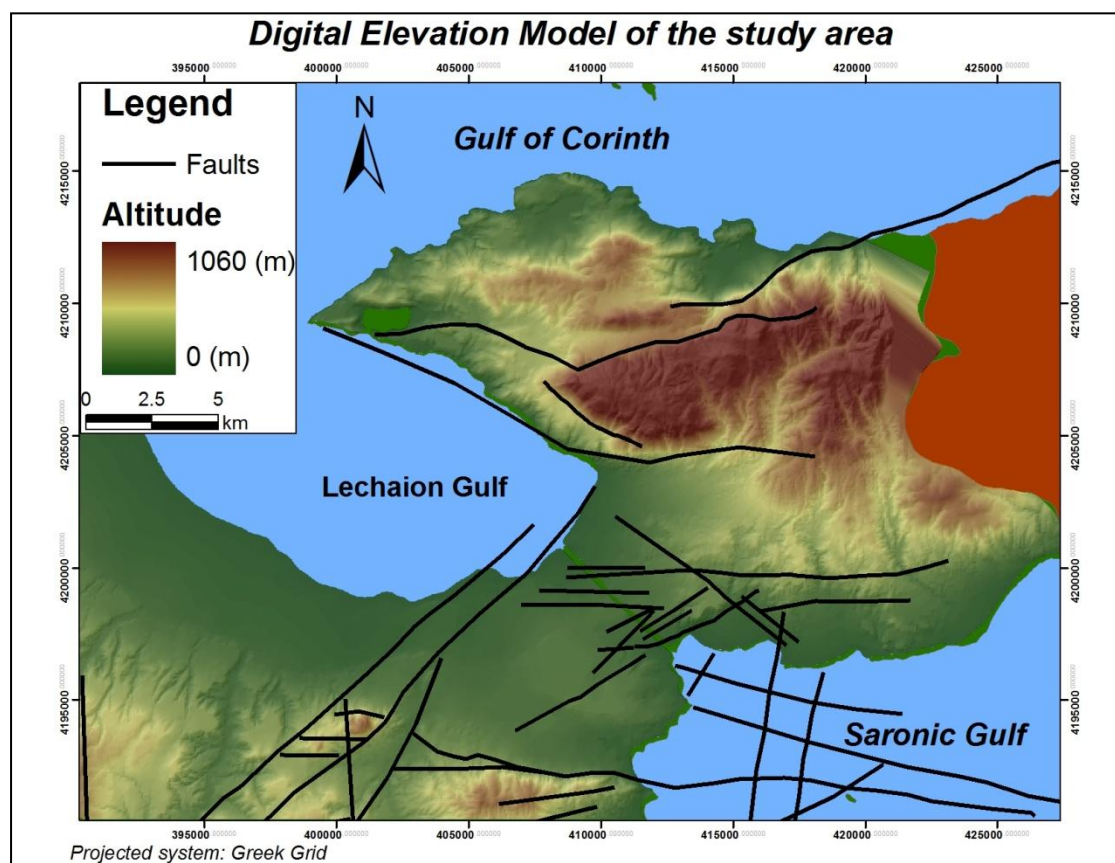


Fig. 3.5 DEM of the area.

Topographic variations can also be depicted in slope map of figure 3.6. Generally the southern and central section of the area has milder slope inclinations than the north area. If it was not the area of Acrocorinth² and Kechries, slope inclination would not be more than 20°. On the contrary, to Perachora peninsula slopes are much steeper.

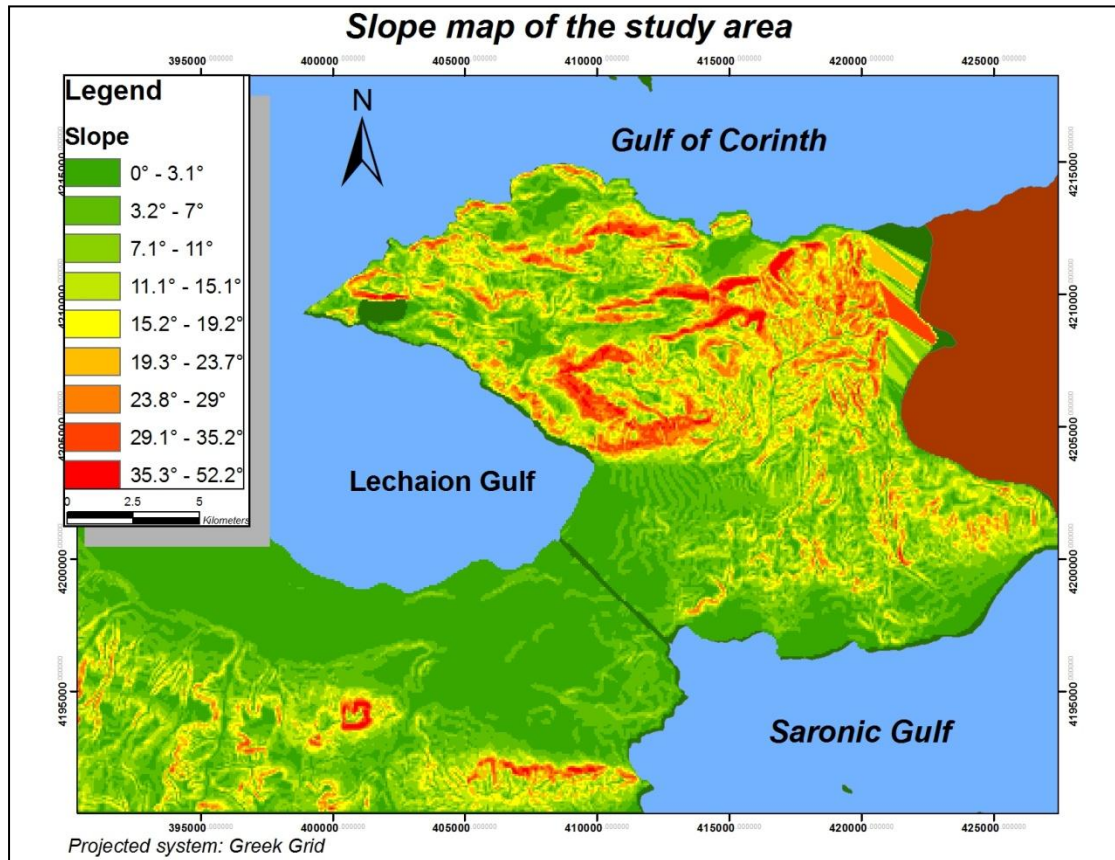


Fig. 3.6 *Slope map of study area. The north section is much steeper than the central and south part.*

² It was not irrelevant that Acrocorinth, was used during ancient times as a fort

3.3 Geology of the area

The area has a complicated geological structure with several lithological formations. The north section of the study area is composed by limestones, ophiolites, flysch, Pliocene and Quaternary sediments, Holocene sediments and igneous formations mostly andesites. The central section, where the Isthmus canal is, has a more simple structure. Sediments are mainly from Pliocene and Quaternary and there are few igneous formations. Limestones, flysch and ophiolites were not found. Southwards, structure is mainly composed by Pliocene – Quaternary sediments and limestones. Simplified and homogenized geology is shown in figure 3.3.

Boeotian zone

The most typical layer of this zone is flysch. It is from upper Jurassic to lower Cretaceous and is composed by alterations of limestones often with silex, sandstones, radiolarites and shales. This complex is intensely microfolded. The clastic sediments that consist flysch, originate from ophiolites, radiolarites and other metamorphic rocks. Beneath this, a layer of Jurassic limestones has been observed. From middle Jurassic to middle Triassic stratigraphy is composed by limestones, partially dolomitized to the lower members of the column.

Ophiolites

Ophiolites are mostly found at the north part of the area. These are mainly composed by Peridotites, Serpentinites and other basic rock that are common to this complex. In some places limestone blocks are locally observed of Triassic to Jurassic age. Apart from this, schist-cherts are observed. These formations occur mainly at the base of the ophiolitic complex, to the Gerania Mountains.

Neogene

Neogene sediments dominate the central part of Corinth. The most common lithological formation in this area is marl. Pliocene formations can be distinguished to several parts. Typical strata that can be found to the Corinth canal are Charalampos marl and conglomerate formation, followed by white marl formation, Kitrinovouni sand formation and Koudounistra – Drosia conglomerate formation. Trapeza -Isthmus formation has overlain these strata and only in central Corinth can someone observe

them (Collier & Dart 1991). Westwards from the canal, Pliocene sediments are mainly marls, sands and fewer conglomerates.

At Charalampos formation the lower member of this formation consists of yellow to grey strata, with alterations of brown clay and sand. Right above them there are conglomerate with well rounded pebbles. The white marl formation consists of approximately 200 meters thick calcareous siltstone with alterations of sandstone. Kitrinovouni is separated in two categories. The first one is composed by cohesive sandstone and the other one is composed by sandstone and calcareous siltstone. Koudounistra and Drosia formation consists of poorly sorted conglomerates, alternating with thin sandstone intercalations. Trapeza- Isthmus formation marks the transition from Pliocene to Pleistocene sediments and consists mainly by alternations of marine and brackish deposits of yellow to white marls, sandy and silty marls.

Igneous formations

Pliocene sediments are intruded and overlain by volcanic rocks, mostly dacites and andesites. Igneous formations are mainly northwards of Isthmus canal, according Freyberg (1973) and Collier (1991). Collier has dated igneous rocks, similar to these that were found by Freyberg. Their age is approximately at 3.62 ± 0.18 Ma suggesting that were formed in one face more or less at 3.5 to 4 Ma. These rocks are typical of calcalkaline volcanicity of the Hellenic volcanic arc and are consider being the westernmost outcrops of the arc.

Quaternary

Pleistocene and Holocene sediments are predominant in study area, since consists more than 50 % of the area. Pleistocene sediments are mostly composed by cohesive or not sandstones, conglomerates, sands clays and marls. They can be divided into several subcategories. Many of these depositions used to be alluvial fans and are formed by pebbles of limestone and ophiolites, not well rounded and from sand. More or less the same lithology is encountered to old river terraces but here pebbles are rounded. Another subcategory is marine terraces that exist mostly westwards from Corinth canal. These terraces are significant due to the fact were used in order to determine the uplift rate of the area (Collier et al.1991; Houghton et al.2003).

Holocene sediments are mostly recent talus cones and screes, elluvial and alluvial deposits and coastal sand and pebbles. Another subcategory of Holocene formations is debris that have been artificial created. After the excavation of the canal, all this material has been thrown near the Isthmus. The area that these debris overlain can be mapped.

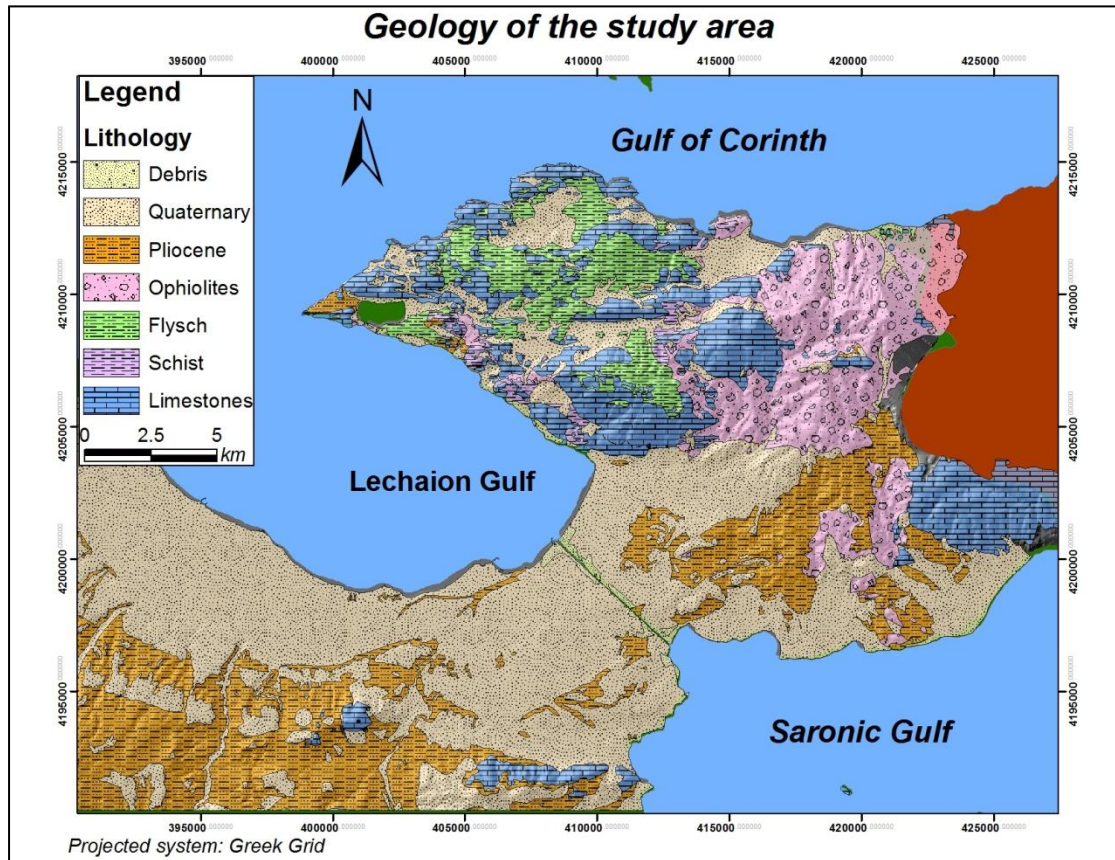


Fig. 3.7 Simplified geology of study area.

In figure 3.7, it is clearly depicted that lithological formations vary mostly to the north section of the map, where limestone and ophiolites prevail. Quaternary and Pliocene sediments are mostly at the central and southern part of the map, while the southern section of the area is constructed mostly by marls and limestones. In figure 3.4 lithological formations are correlated with slope inclination. It is obvious that steeper inclinations are associated with formations that are not susceptible to erosion

such as limestones and igneous rocks³. Furthermore, active faults are also responsible for topographic variations. It is clear in figure 3.8 that Kechries, Loutraki and South Alkyonides fault system are associated with steep slope inclinations. This is a sign that these faults are active tectonically at least during the Pleistocene.

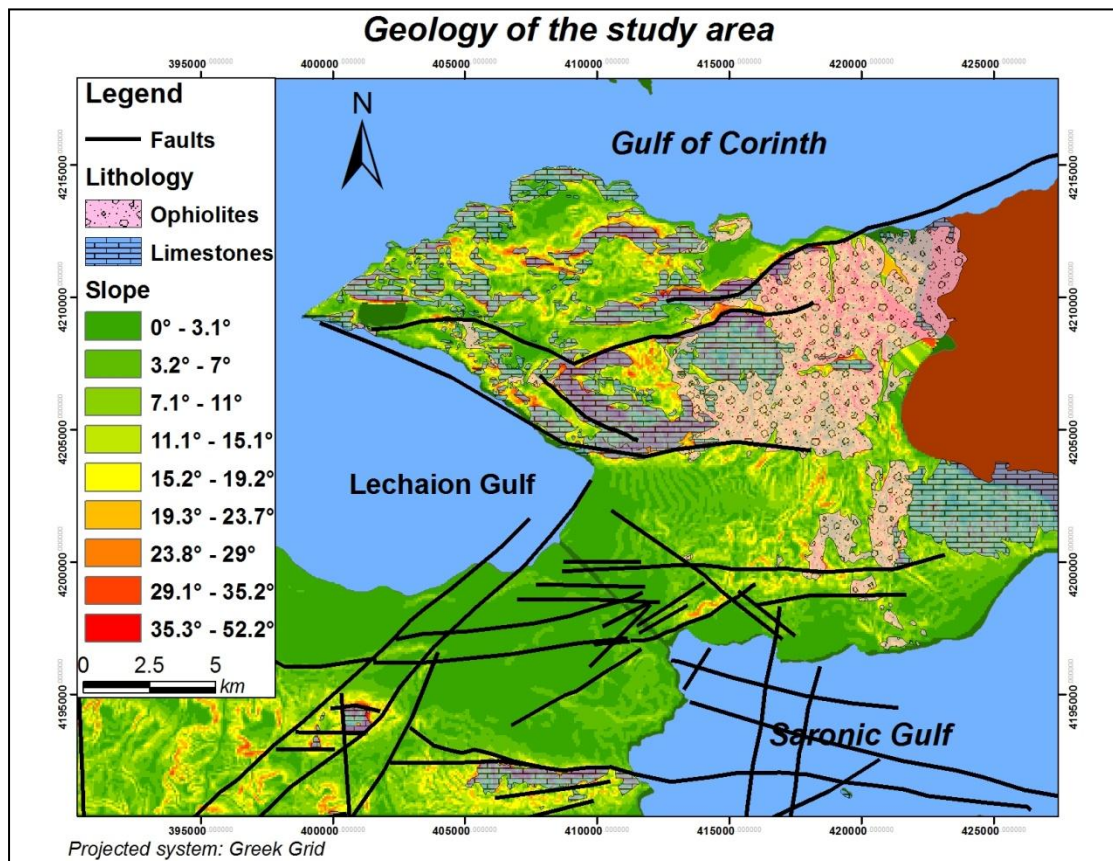


Fig. 3.8 Active faults and lithological formations resistant to erosion are clearly associated with steep slopes.

³ As igneous rocks have been characterized ophiolites, dacites and andesites that exist in the area

4. Borehole data

4.1 Introduction

Seven boreholes have been recovered on the eastern side of the Corinth Canal; two of them at the hanging wall and five at the footwall. These at the hanging wall were boreholes 3, and 6, where boreholes 1, 2, 5, 4, 7 were at the footwall. From these, Bh 7 was up to 70 meters deep and Bh 3 up to 57 meters deep and were selected for detailed micropaleontological-paleoenvironmental analyses, where the rest were maintained for geotechnical analyses. Apart from Bh-5 that was destroyed, lithostratigraphic units of the other boreholes were described. Foraminiferal species were picked and counted through a specific procedure, in samples that were taken from Bh-3 and 7. Microfauna was identified and counted in genera and species level, where possible, with them the paleoenvironment of the area has been reconstructed

4.2 Lithostratigraphic units

4.2.1 Description

Bh-3

Lithological alterations of sand, clay, clayed sand, conglomerate, marl, fractions of limestone, even topsoil have been recognized. More specifically the first 4,7 meters was described as brown-beige sand or clayed sand with no or low cohesion. From 4,70 up to 5,70 meters depth was described as clay while up to 22,40 meters depth was characterized as sand, clayed sand with low cohesive. A colony of *Cladocora* corals was found there in situ. Beneath this layer stratigraphy has altered to more cohesive and rock like formations. Conglomerate and gravels with grit and sand extended up to

31.20 meters depth. From 31,20 up to 34,00 meters depth was described as clayed sand, where the following 3 meters thick layer was a mixed rock-soil sand with gravels. Beneath this layer, clay extended up to 39,60 meters depth, followed by a 10 meters thick layer composed from gravels and grit. Up to 66,00 meters depth layers were described as sand or clayed sand. Between 56 and 60 meters depth sand was cohesive enough to be described as sandstone. A Cladocora colony was found here also, but not in situ. Fragments of corals were found transferred and destroyed. Up to the end of Bh-3, sand with gravel layer was described.

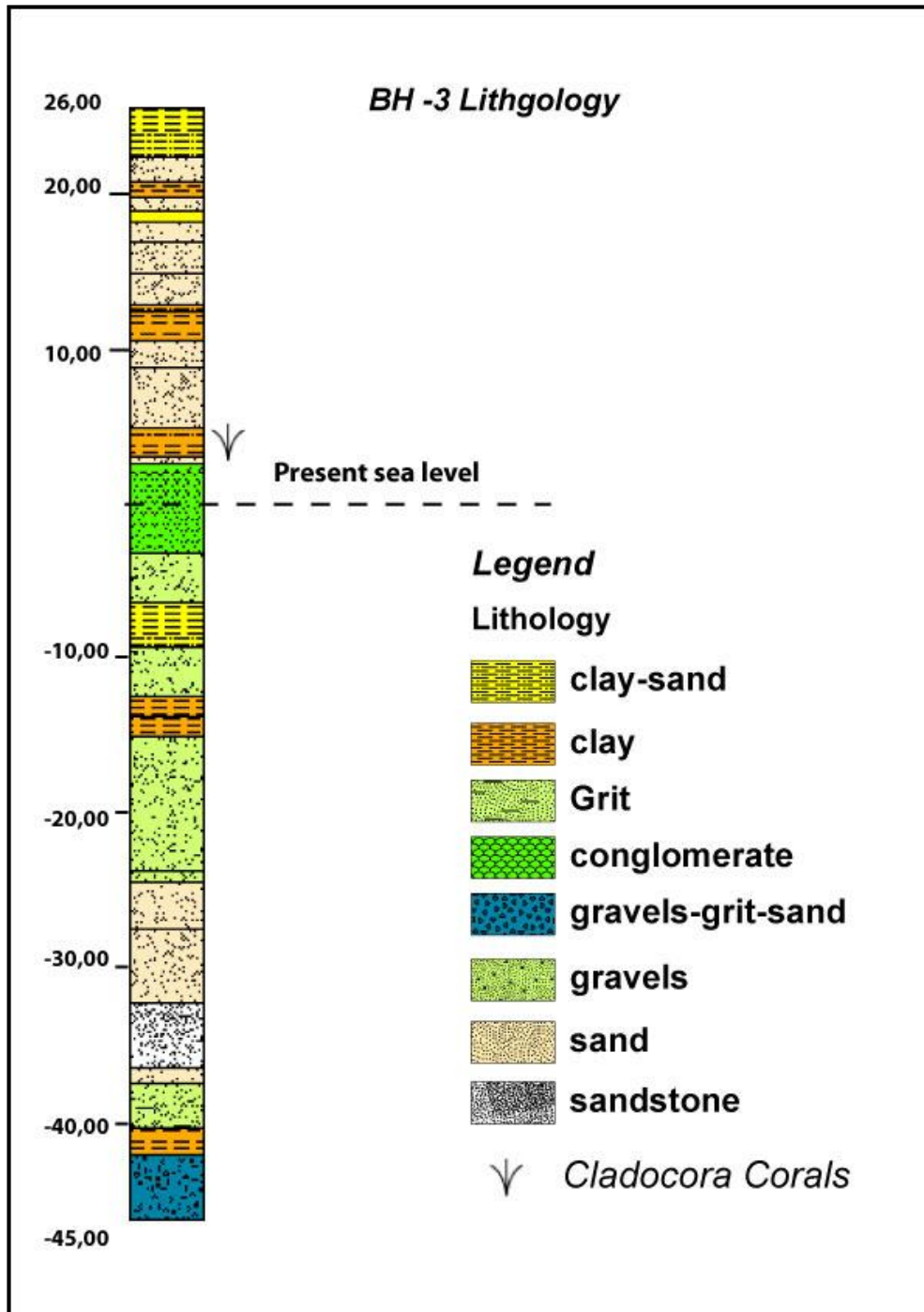


Fig. 4.1 Lithostratigraphic view of borehole 3. Borehole was 70.00 m deep

Bh-7

In borehole 7, lithology was more or less similar to Bh-3. The first 9 meters were described as sand with low or no cohesion, interrupted by a thin layer of topsoil at 5 meters. This factor clearly indicates that the entire area was above the sea level at that

specific time. A layer of grit and gravels was found afterwards and again sand with no cohesion up to 18 meters depth. Up to 19 meters a layer of clay with silt was encountered, including a colony of *Cladocora* corals. From 19 to 23 meters the layers were described as sand with cohesion as rock. Right afterwards lithology alters from a thin layer of clay to a conglomerate strata up to 26,50 meters. From that point until 33 meters depth lithology was described as sand with medium cohesion including a thin layer of gravels. Under 33 meters depth the deformation zone of the fault has begun. Firstly a layer of silty sand has been identified. The fault was found at 36 meters depth. The layer from 39 to 44,50 meters was described as cataclasites, and exactly there the deformation zone ended. From that point until the end of the borehole alterations of cohesive, sand and grit with gravels were encountered.

. Apart from boreholes 3 and 7, other 5 boreholes were recovered for more detailed analysis. Unfortunately these boreholes were destroyed during the geotechnical analysis, thus only their lithology was described. Boreholes 1 and 4 were at the hanging wall, while boreholes 2, 5 and 6 were at the foot wall. Data for borehole 5 were not recorded due to the fact that they were destroyed completely.

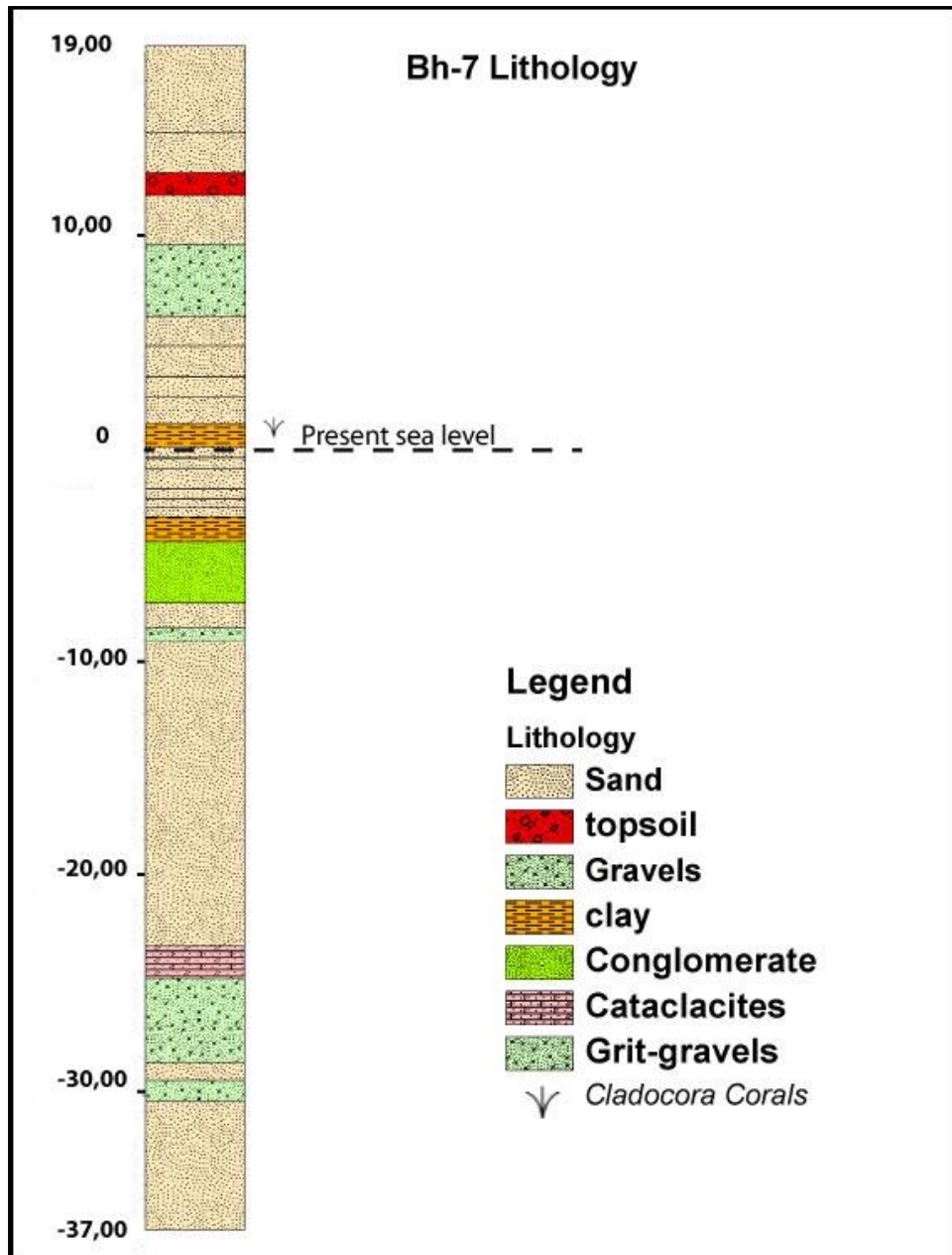


Fig. 4.2 Lithostratigraphic view of borehole 7. Borehole was 56.00 m deep.

Bh-1

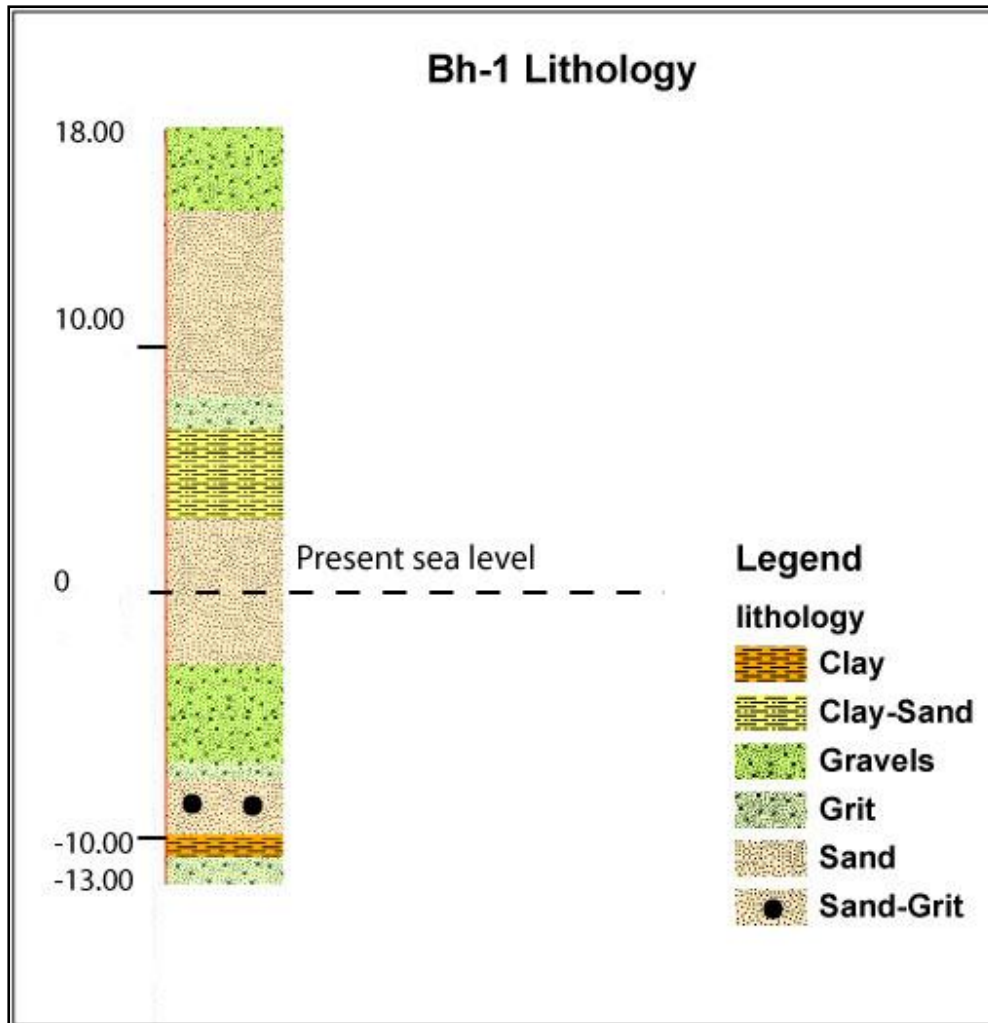


Fig. 4.3 Lithostratigraphic view of borehole 1. Borehole was 31.00 m deep.

Borehole 1 was up to 31 meters deep. The first 3,00 meters were described as gravels with cohesive sand. Layers up to 11,00 meters were described as sand medium to low cohesion, partially containing grit. From there until 12,30 meters grit prevailed. Strata until 22,0 meters were characterized as sand containing grit with medium cohesion. Up to 25,80 meters lithology has altered to conglomerate with sand and clay. After that a layer of grit was described, followed by a layer of sand and silt with medium cohesion. Borehole has ended with a layer of clay, followed by a layer of grit.

Bh-2

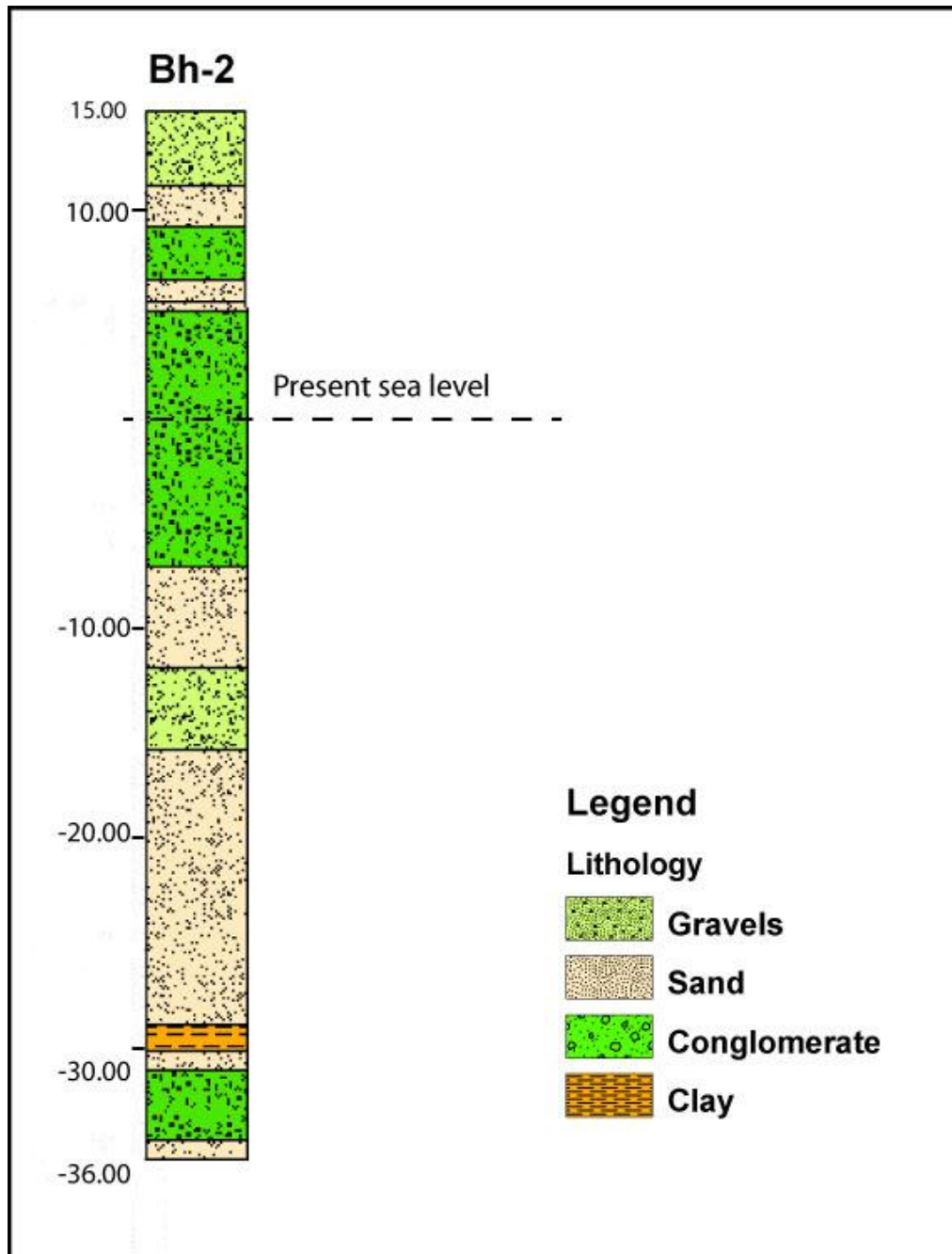


Fig. 4.4 Lithostratigraphic view of borehole 2. Borehole was 50.00 m deep

Borehole's 2 lithology was significant different compared with the others. Conglomerate and gravels prevailed, while sand and clay were fewer. More specific

the first 3,70 meters were described as gravels with no cohesion, followed by sand with silt. From 5,40 until 21,80 strata were described as conglomerate containing grit. This layer has been interrupted by a thin layer of sand and sandstone at 8 meters. After conglomerate a layer of sand was encountered until 26,60 meters depth, followed by a layer of gravels. From 30,60 until 43,60 meters depth was characterized as sand with silt. Afterwards it was described as a layer of clay with silt, followed by a layer of cohesive sand. Boreholes ended with a layer of conglomerates followed by sand with silt. Borehole's depth was at 50,00 meters.

Bh-4

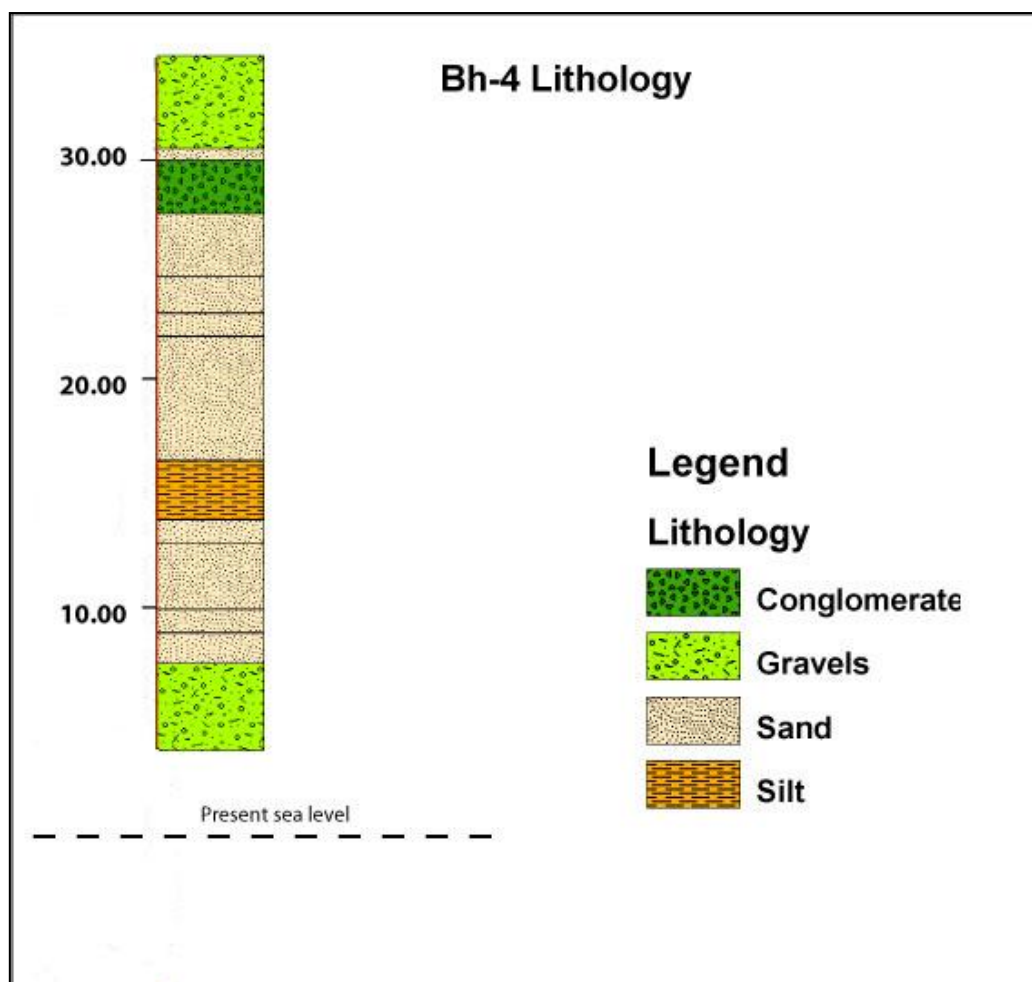


Fig. 4.5 Lithostratigraphic view of borehole 4. Borehole was 30.50 m deep.

Borehole 4 had no significant lithological alterations. The first 4 meters were characterized as gravels with sand followed by a thin layer of sand. From 4,50 up to 6,90 meters a layer of conglomerate was encountered. From this point up to 26,50

meters depth strata were characterized as sand partially with silt or grit, with medium or no cohesion. This layer was interrupted only by a thin layer of silt from 17,80 to 20,30 meters depth. Until the end of Bh-4 at 30,50 meters strata were described as gravels with sand with low cohesion.

Bh-6

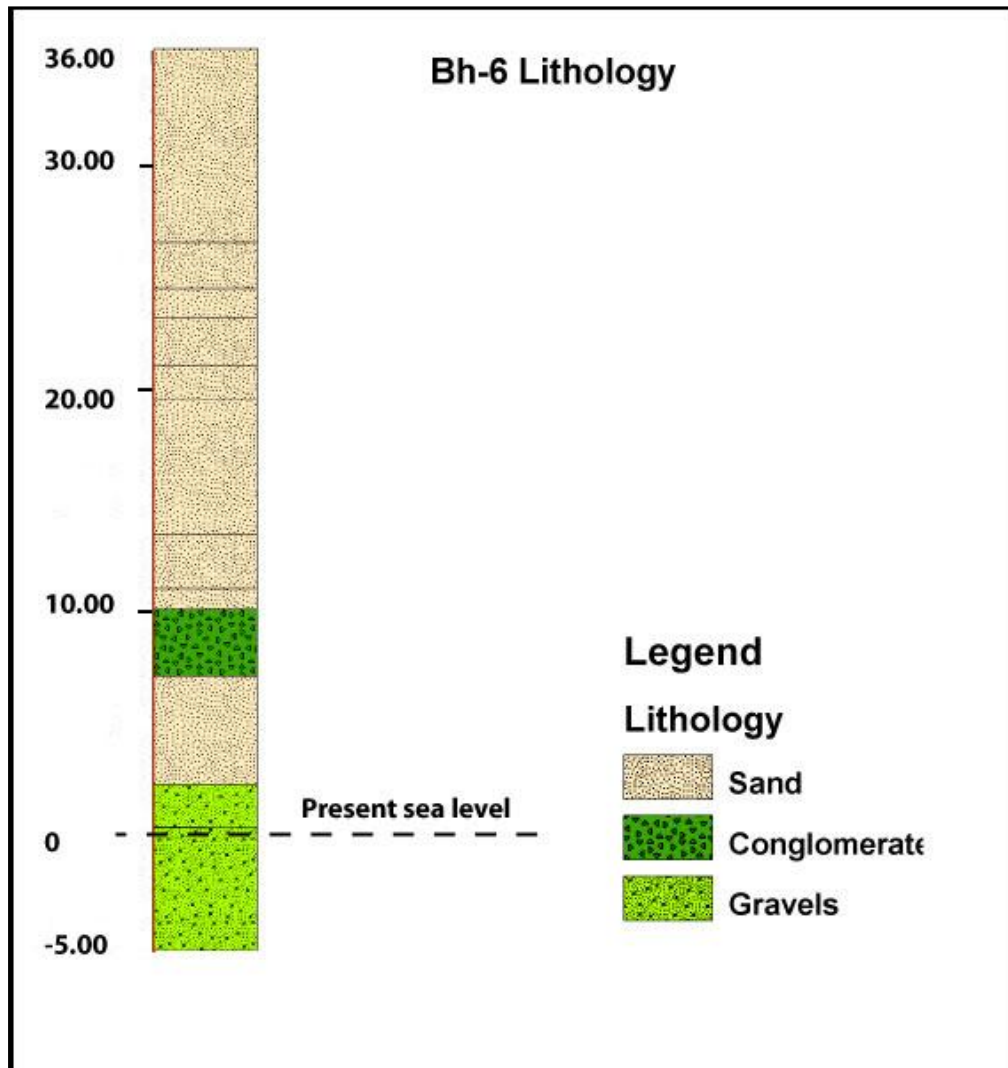


Fig. 4.6 Lithostratigraphic view of borehole 6. Borehole was 40.50 m deep.

Borehole 6 was 40,50 meters deep. Up to 25.20 meters depth strata were characterized as sand with minor variations. Cohesion varied from low to no cohesion and some layers contain grit and silt. From 25,20 to 28,10 meters depth strata were characterized as conglomerate, followed by sand highly cohesive up to 33,00 meters

depth. Until the end of borehole at 40,50 meters depth layers of gravels were encountered, partially containing grit.

4.2.2 Interpretation

It is obvious from the description that no significant correlation can be done among these boreholes. Differentiations are not only observed between boreholes at the hangingwall and the footwall, something that it is expected more or less. Several variations in lithology take place among boreholes that are at the same side of the fault. For instance, borehole 3 and borehole 6 are both at the footwall and the distance between them is not more than 100 meters. Nevertheless, as it is shown in figures 1 and 6, there are many lithological variations. The same can be implied, up to certain degree, for the lithology of the other boreholes as well. The exact location of each borehole is shown in figure 7. The distance between borehole 1 and 4 is approximately 580 meters and the distance between borehole 7 and 6 is 145 meters. So many lithological variations in such a limited area strongly indicate that there are major lateral alterations and stratigraphic variations. Lithostratigraphic variations imply paleoenvironmental variations as well. Sand or clay corresponds to a marine paleoenvironment, while conglomerate represent a subaerial paleoenvironment.

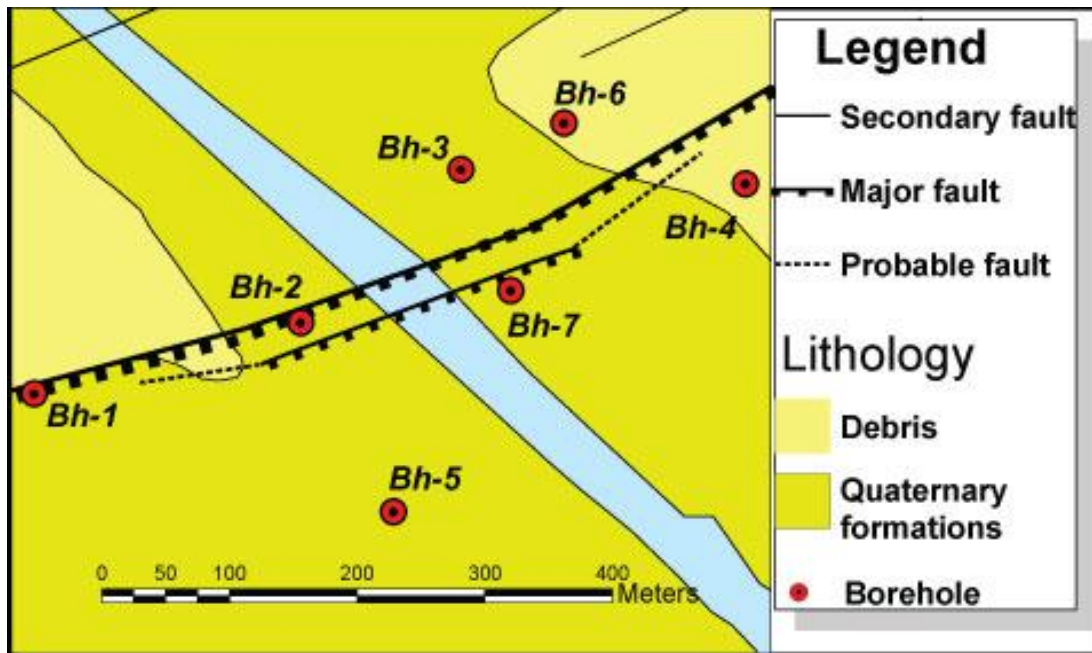


Fig. 4.7 The exact location of each borehole. The distance between Bh-1 to Bh-4 is 580 meters and from Bh-6 to Bh-7 is 145 meters

Due to lithological variations that were found in boreholes, correlation between layers is difficult. Bh-3 is at the footwall while Bh-7 is at the hangingwall. Nevertheless, only a layer of conglomerate seems to be the only common strata in both boreholes. Consequently, it is not possible to specify the displacement of the fault block or the throw rate and the slip rate.

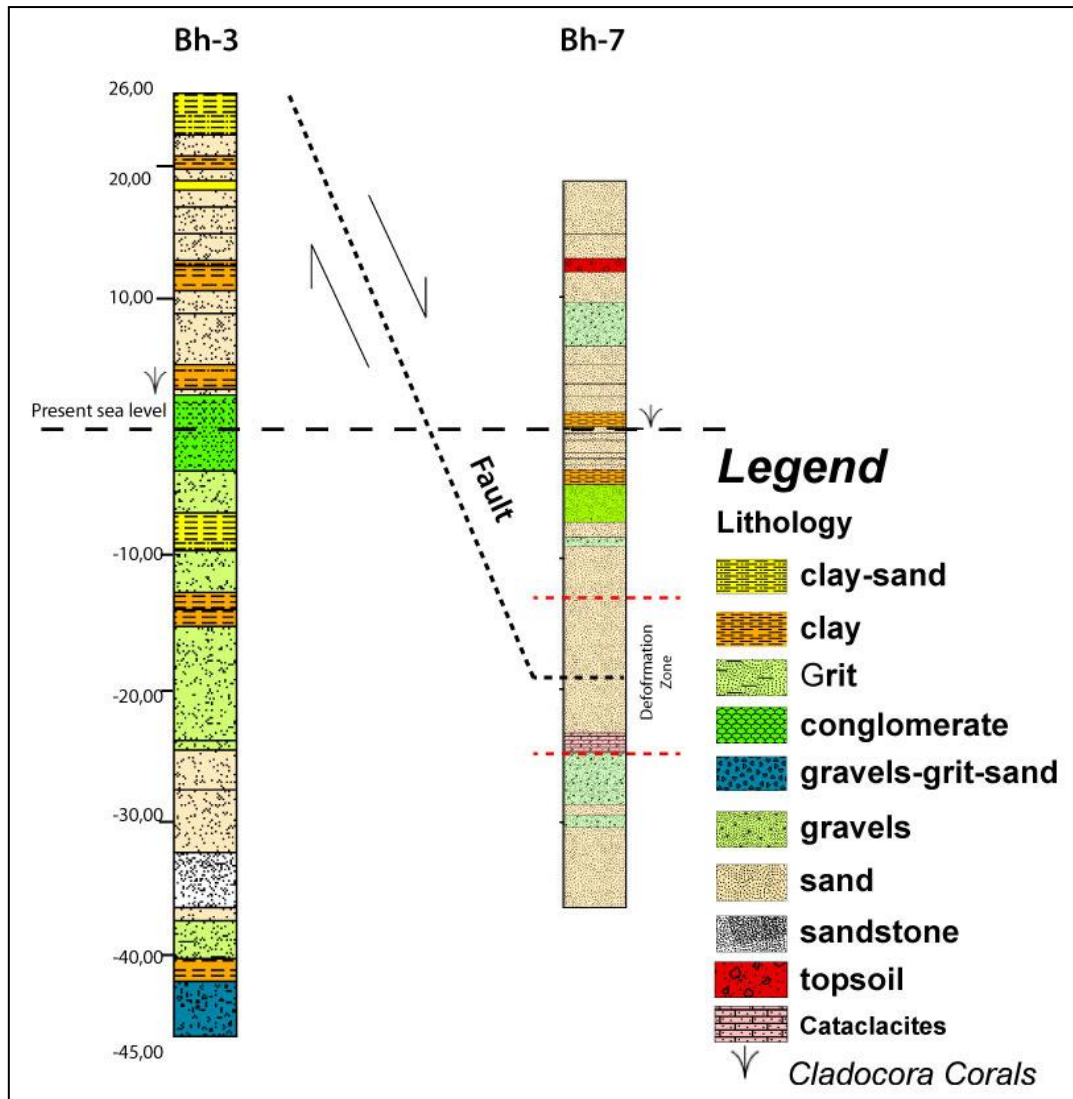


Fig. 4.8 View of the stratigraphic columns of borehole 3 located on the immediate footwall and borehole 7 located on the immediate hangingwall of the studied fault.

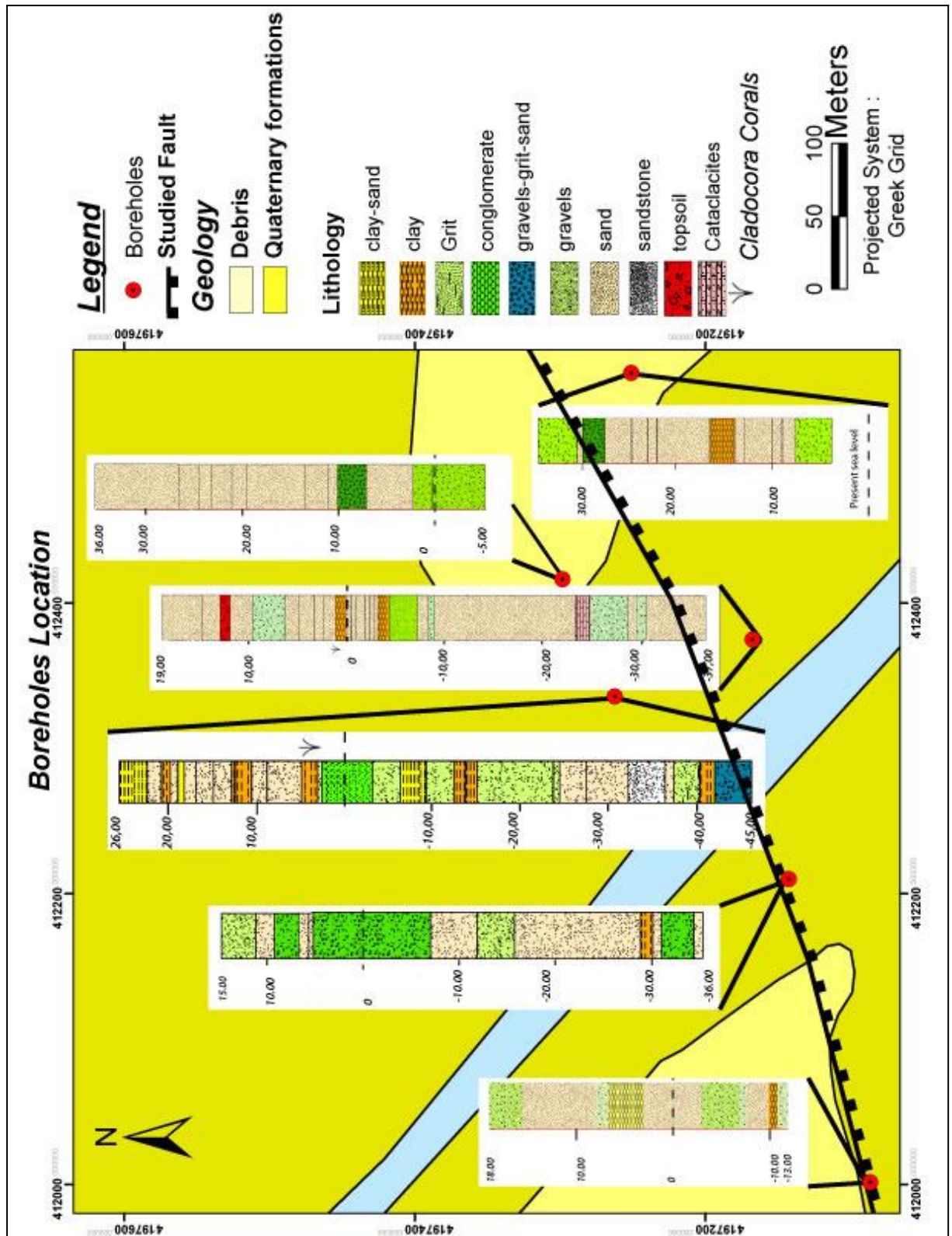


Fig. 4.9 View of lithostratigraphic columns, located in the study area

4.3 Methodology

Approximately 100 samples have been processed for micropaleontological analysis (45 from borehole Bh-3 and 57 from borehole Bh-7). Each sample (20 gr dry weight) was treated with H₂O₂ to remove the organic matter, and subsequently was washed through a 125µm sieve and dried at 60 °C. A subset of each sample was obtained using an Otto microsplitter until aliquots of at least 200 benthic foraminifers. The microfauna have been identified under Leica APO S8 stereoscope. A scanning electron microscope analysis (SEM Jeol JSM 6360, Dept. of Hist. Geology-Paleontology) was used for taxonomical purposes.

The identified foraminiferal species were grouped in euryhaline forms mainly represented by *Ammonia* spp. (mostly *Ammonia tepida*) large and small sized, *Elphidium* spp., *Haynesina* spp. (including *H. germanica* and *H. depressula*), *Aubignyna perlucida* and marine foraminiferal indicators, mostly including miliolids, and in a lesser degree full-marine species grouping *Asterigerinata*, *Neoconorbina*, *Rosalina* spp., *Planorbulina mediterraneensis*, *Bolivina* spp., *Textularia* spp., *Bulimina* spp., *Discorbis* spp.

Foraminiferal assemblages of these species were expressed in relative abundances and statistically analyzed. Using Grapher 5.01 2004, it was able to depict foraminiferal assemblages in each borehole. Euryhaline foraminiferal species indicate a an alternating mesohaline–oligohaline lagoonal environment, while miliolids and the other marine foraminifera indicate a shallow marine environment (Triantaphyllou et al., 2003, Pavlopoulos et al., 2007, Goiran et al., 2011). Since each foraminiferal species implies a different depositional environment, it was able to reconstruct the paleoenvironment of the area and how does it changes through time.

4.4 Micropaleontological analysis

4.4.1 Description

Samples from Bh-3 and Bh-7 were analyzed in order to identify foraminiferal assemblages. The studied benthic foraminiferal assemblages are relatively abundant and moderately preserved. In Bh-3, the interval inbetween 3 and 4,30 m depth is featured by the presence of *Elphidium spp*, *Ammonia* large and small, *miliolids* and to a lesser degree by other full marine species. *Haynesina spp.* and *A. perlucida* were not found there. Beneath this layer till 6.80 m depth, fewer full marine species, *Elphidium spp.* and large- sized *Ammonia* were found, while the sample abounds in small- sized *Ammonia* and in *Haynesina spp.* Beneath this layer, *Haynesina spp*, full marine species and small- sized *Ammonia* were mostly found. From 11.50 till 12.50 meters depth no *Ammonia*, *Haynesina* and *Aubignina* species were found. Till 18.00 meters depth, no foraminiferal species were found, except for few broken specimens.

From 18.00 to 19.00 m depth, samples were abundant in small- sized *Ammonia* and *Haynesina spp.* Up to 21.50 meters depth, the presence of these species is gradually declining while *Elphidium spp.*, milliolids and other marine species assemblages are increased. Approximately at 20.70 m depth, a *Cladocora* corals colony was found in situ. Till 22.50 meters depth samples abounded in small- sized *Ammonia* (more than 93 % of the total foraminiferal assemblage). From that point till 34.00 m depth once again no or few foraminifera was found.

In between 34.00 and 37.00 meters depth no *Haynesina spp.* and *Aubignina spp.* but just few *Ammonia* were found. On the contrary, samples abounded in full marine species, *Elphidium spp.* and in milliolids. Till 50.00 meters depth, no or few foraminiferal species were found. In samples that were taken from 50.00 to 55.00 m

depth, full marine species were dominant (more than 36 % of the total foraminiferal assemblage). Few *Haynesina* spp. specimens were found in each sample, while *Ammonia*, small and large, and were not more than 23 % at 52.30 meters depth.

From that point till the end of the borehole no foraminiferal species were found. Instead of that, ostracod specimens of *Cyprideis* spp. have been detected, followed by echinoderm and *Cladocora* coral fragments, and gastropods that are most probably transferred.

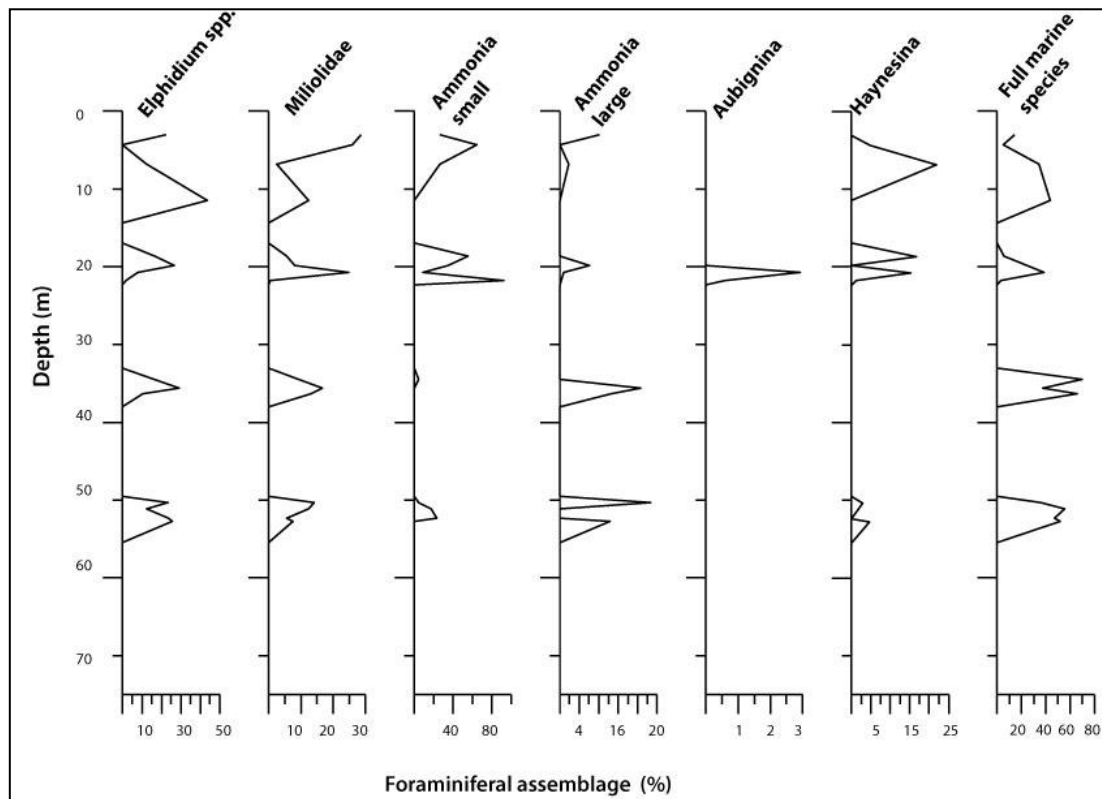


Fig. 4.10 Foraminiferal assemblages calculated as percentage of the total foraminifera counted in borehole 3, grouped in 7 subcategories (*Elphidium* spp., miliolids, small- and large- sized *Ammonia* spp., *Aubignina perlucida*, *Haynesina* spp. and full marine species).

In Bh-7, the samples from 1.50 to 2.50 meters depth were characterized mostly from miliolids, small- sized *Ammonia* spp., *Elphidium* spp. and full marine species. Inbetween 2.50 and 4.50 meters depth miliolids are decreasing. Instead of them *Haynesina* spp. were found. From 4.50 to 5.50 meters depth samples were characterized only by *Elphidium* spp. and small- sized *Ammonia*. Downwards, in-between 6.00 and 7.00 meters, no foraminiferal specimens were found. Beneath this layer, *Ammonia* small- and large- sized specimens prevailed with more than 80 % of the total foraminiferal assemblage. A 1 meter thick layer is following, with no or few broken foraminiferal specimens.

Mostly *Ammonia* small- and large- sized and in a lesser degree miliolids, *Elphidium* spp. and other species were found from 7.00 till 8.00 meters depth. Just below, till 9.00 meters depth only few broken foraminiferal species were found. From 9.00 till 10.00 meters depth, the foraminiferal assemblage was approximately 50% of full marine species and Miliolidae and 50 % of the other euryhaline forms. Deeper, the assemblage of euryhaline foraminifera was gradually increased, while the amount of the other species was declined. At 10.50 meters depth, *Ammonia* and other euryhaline species prevailed against marine species. Till 12.50 meters depth, there was balance between euryhaline and marine species, while at 14.50 euryhaline species prevailed once again. From that point till 18.00 meters depth, fewer *Ammonia*, *Elphidium* and *Haynesina* species were counted while other marine species were dominant⁴. It is significant, though, that *Haynesina* species were present in these samples.

At 19.00 meters depth mostly small- sized *Ammonia* and *Haynesina* spp. were found, while at 19.50 meters depth, it is important the presence of small- sized *Ammonia* and *A. perlucida*. *Haynesina* spp. prevailed from 20.00 till 21.00 meters depth. Miliolids were dominant from 21.50 till 22.00 meters depth but at 22.50 meters depth *Haynesina* spp. prevailed once again. At 23.00 meters depth, the euryhaline species consisted the 100 % of the total sample. Miliolids and other marine species were found at 24.00 meters depth, in balance with the other euryhaline species. From

⁴ At 15.50 meters depth, more than 93% of the total foraminiferal assemblage was miliolids and other marine species.

that point till 26.50 meters depth no or few broken foraminiferal specimens have been observed. At 26.50 meters depth, full marine species were dominant and there was complete absence of small- sized *Ammonia*, *Haynesina* spp. and *A. perlucida*. From that point till the bottom of the borehole at 56.00 meters depth, no significant foraminiferal assemblage was found. At 33.00 till 40.00 meters depth, the deformation zone of the fault has been detected, completely barren of microfauna. At Approximately 50.00 meters depth, the analyzed samples presented scarce foraminiferal specimens. In contrast, the samples were abundant in ostracod valves. (*Cyprideis* spp.).

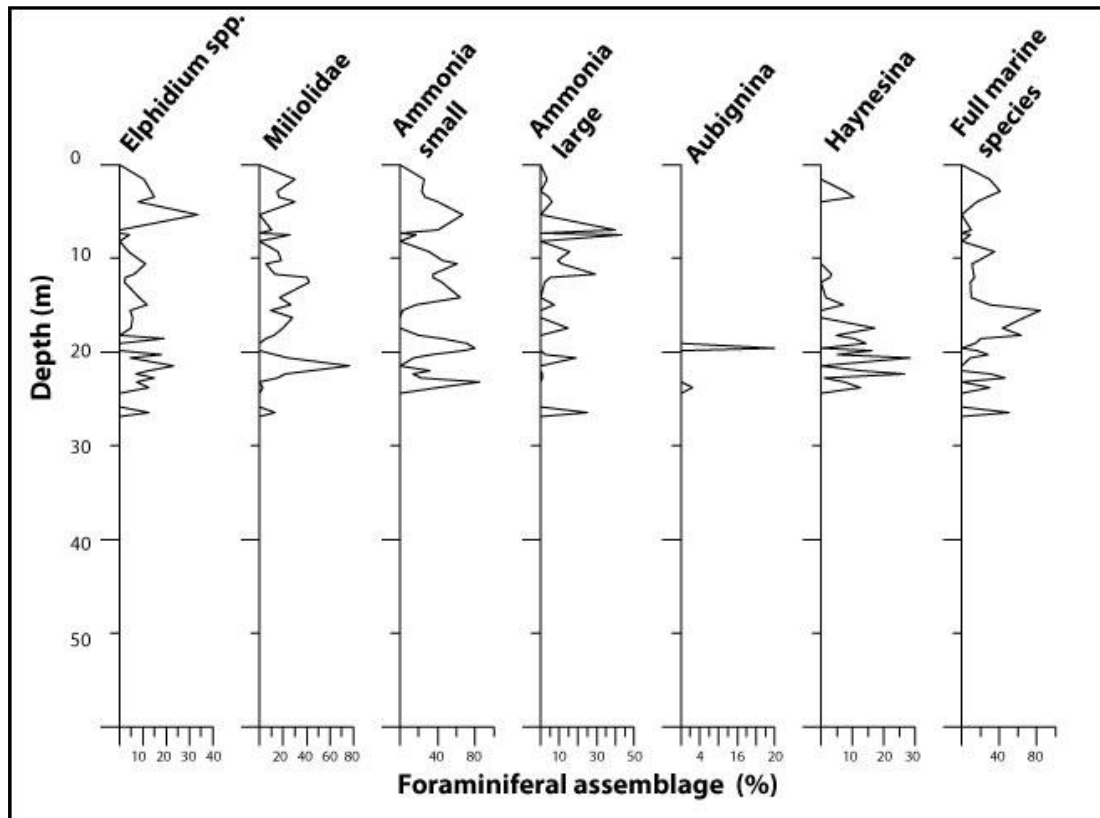


Fig. 4.11 Foraminiferal assemblages calculated as percentage of the total foraminifera counted in borehole 7, grouped in 7 subcategories (*Elphidium*, *Miliolidae*, small- and large- sized *Ammonia*, *Aubignina*, *Haynesina* and full marine species).

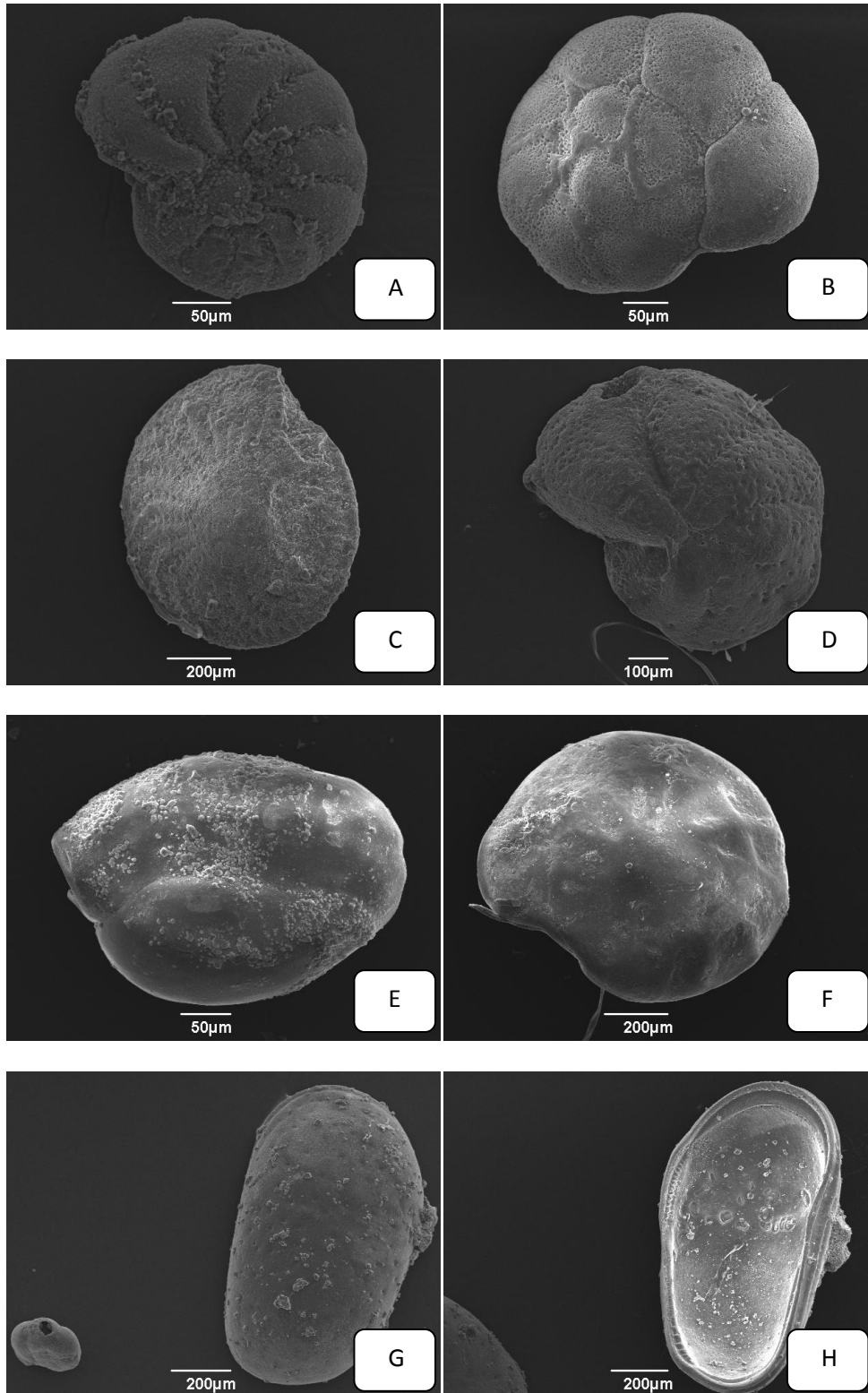


Fig. 4.12 Characteristic microfaunal species that have been identified under Leica microscope. (A) *Elphidium excavatum*. (B) Small- sized *Ammonia tepida*. (C) *Elphidium crispum*. (D) *Lobatula lobatula*. (E) *Triloculina* sp. (miliolid). (F) Large- sized *Ammonia tepida*. (G) *Cyprideis* spp. (outside of a right valve) and *Aubignina perlucida* (down left). (H) *Cyprideis* spp. (inside of a left valve).

4.4.2 Interpretation

Through micropaleontological analysis it is clear that not only lithology has significant variations, but the depositional environment as well. Microfauna that was encountered is used to determine the ecology. *Ammonia tepida* is an opportunistic taxon that flourishes predominantly in a wide range of salinity and temperature near-shore environments; shallow marine, lagoonal and deltaic zones with prominent variation in test size and morphology (e.g. Triantaphyllou et al., 2003, Koukousioura et al., 2011). *Haynesina germanica*, a species tolerant of restricted conditions. Brackish-oligohaline environment is characterized by ostracods such as *Cyprideis* spp.

Triantaphyllou et al. (2009), Koukousioura et al. (2011) point out that assemblages dominated by small-sized *Ammonia tepida*, *Haynesina* spp. (mostly *H. depressula*), *Aubignyna perlucida* and miliolids suggest open lagoonal environmental conditions, whereas foraminiferal assemblages dominated by small-sized *Ammonia tepida* and *Haynesina* spp. (mostly *H. germanica*) correspond to a closed lagoon. In addition large-sized *Ammonia tepida* together with miliolids and higher abundance of full marine species suggests the presence of shallow marine environments. Consequently, through that procedure, it is possible to reconstruct the paleoenvironment of the entire area.

5. Paleoenvironmental Analysis

5.1 Description

Identifying foraminiferal assemblages in each sample has rendered possible the paleoenvironmental analysis in boreholes 3 and 7. A series of different depositional environments were encountered From shallow marine to paralic- back shore environment.

In Bh- 3 the first 1.5 meters was the topsoil and was not examined for microfaunal assemblages. Till 5.00 meters depth microfauna indicated a shallow marine environment with mesohaline features. Few small-sized *Ammonia* were found, while *Milliolids* and other full marine species prevailed. Beneath these strata, the presence of *Haynesina* and *Ammonia* small- and large- sized indicates a mesohaline-oligohaline lagoonal paleoenvironment, till 11.50 meters depth. Beneath these layers strata were described as a paralic or even a backshore environment with no or few broken foraminiferal specimens. At 18.00 meters depth small- sized *Ammonia* and *Haynesina* that dominate against other species, indicate a shallow marine environment that also exhibits lagoonal features. At 20.00 meters depth euryhaline species are fewer where marine species, clearly indicating a deeper marine environment shallow. It is significant to mention that a colony of *Cladocora* corals was found there in situ. At 22.00 meters depth absence of full marine species and the presence of small- sized *Ammonia* more than 90 %, suggest a mesohaline-oligohaline lagoonal environment.

From 23.00 to 34.00 meters depth, few or no foraminifera indicated that was a paralic backshore environment. At 34.50 meters depth, full marine species indicated a shallow marine paleoenvironment. Till 36.00 meters depth paleoenvironment was characterized form the lack of small- sized *Ammonia*. Till 50.00 meters depth few or no foraminiferal species suggested a paralic backshore environment. From 50.50 till 53.00 meters depth foraminiferal species indicated a shallow marine environment that exhibits mesohaline features.

Till the end of Bh-3 at 70.20 meters depth, it was not possible to reconstruct the paleoenvironment due to insufficient foraminiferal assemblage. Till 60.00 meters depth examined samples indicated a paralic-backshore environment. From 60.00

meters till 62.00 meters depth marine species that were found such as corals and gastropods, suggest a marine environment. Till the end of borehole no microfauna assemblage shows a paralic-backshore environment.

In Bh-7 the first 1.50 meters was topsoil and was not examined for microfauna assemblages. From 1.50 till 5.50 meters depth foraminiferal species indicate a shallow marine environment with mesohaline features, ergo a lagoonal paleoenvironment. This is more obvious at 4.50 meters depth where the presence of euryhaline species such as *Haynesina* spp. is clearer. From 5.50 till 7.00 meters depth, sediments were characterized as topsoil and no foraminiferal assemblages were found. This indicates a paralic- backshore paleoenvironment. From 7.00 till 10.50 meters depth full marine species and few miliolids, indicated a shallow marine environment. From that point, till 16.00 meters depth the environment turns to oligohaline lagoonal. The presence of small-sized *Ammonia* and *Haynesina* spp. confirm this hypothesis. Till 19 meters the presence of Miliolidae indicates a shallow marine paleoenvironment. It is important to mention that a *Cladocora* corals colony was found there in situ.

Beneath 19.00 meters depth, environment alters from shallow marine to lagoonal-oligohaline. The presence of *Haynesina* spp. of *Aubignina* spp. and of small- sized *Ammonia*, urged that this was an open lagoon, till 24.00 meters depth.

From 24.00 till 26.00 meters depth, no or few broken foraminifera were found, indicating a paralic backshore environment. At 26.00 meters depth few foraminiferal species indicated a shallow marine environment. From 33.00 till 40.00 meters depth, there is the deformation zone of the fault and no implication about the paleoenvironment can be done. Beneath that sample abound in ostracod valves such as *Cyprideis* spp., suggesting a brackish oligohaline environment. Till the end of borehole at 56.00 meters, few or no foraminifera were found, suggesting a paralic backshore environment.

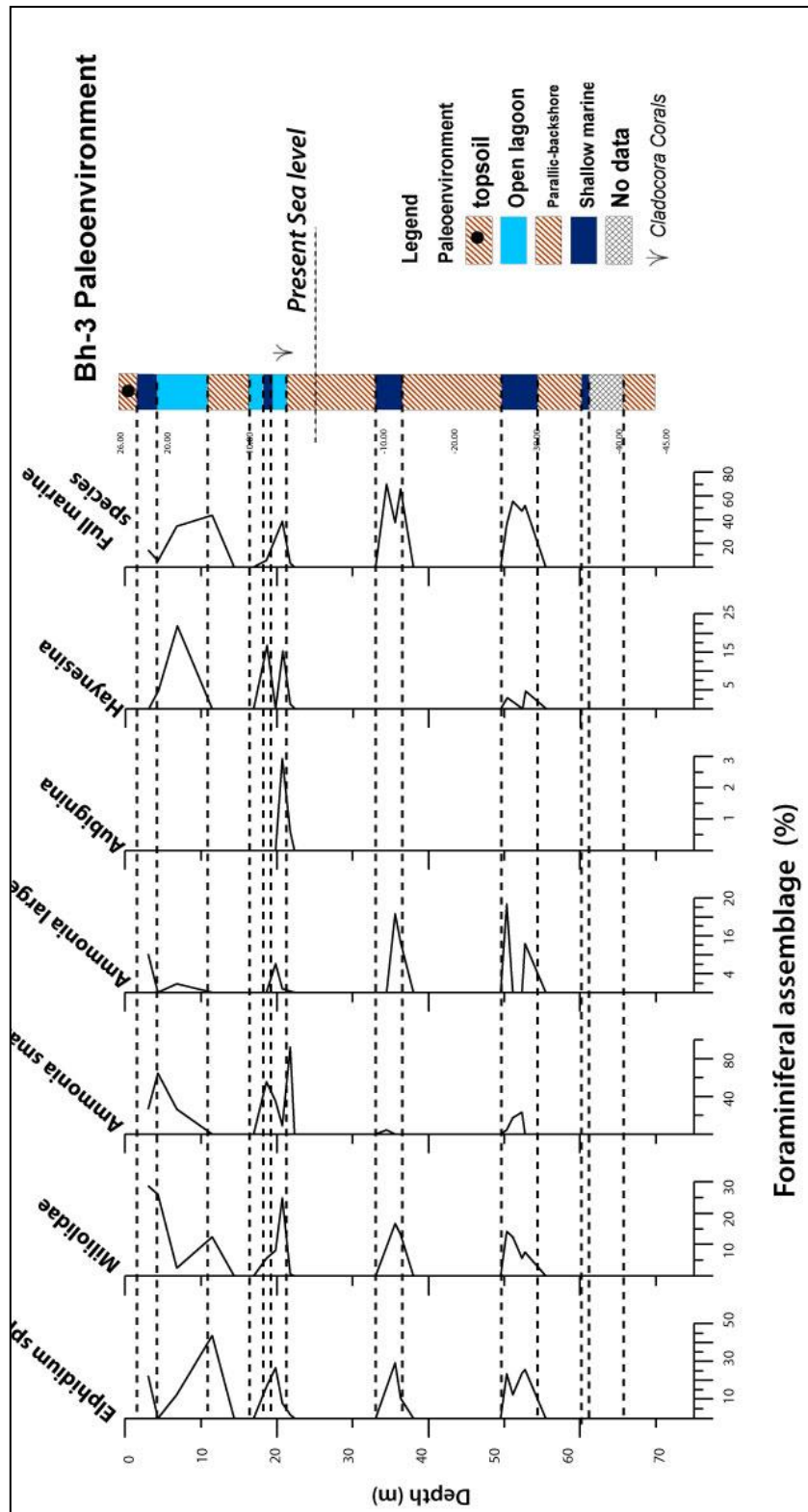


Fig. 5.1 View of the depositional environment of Bh-3 located on the immediate footwall of the studied fault, in correlation with the foraminiferal assemblages.

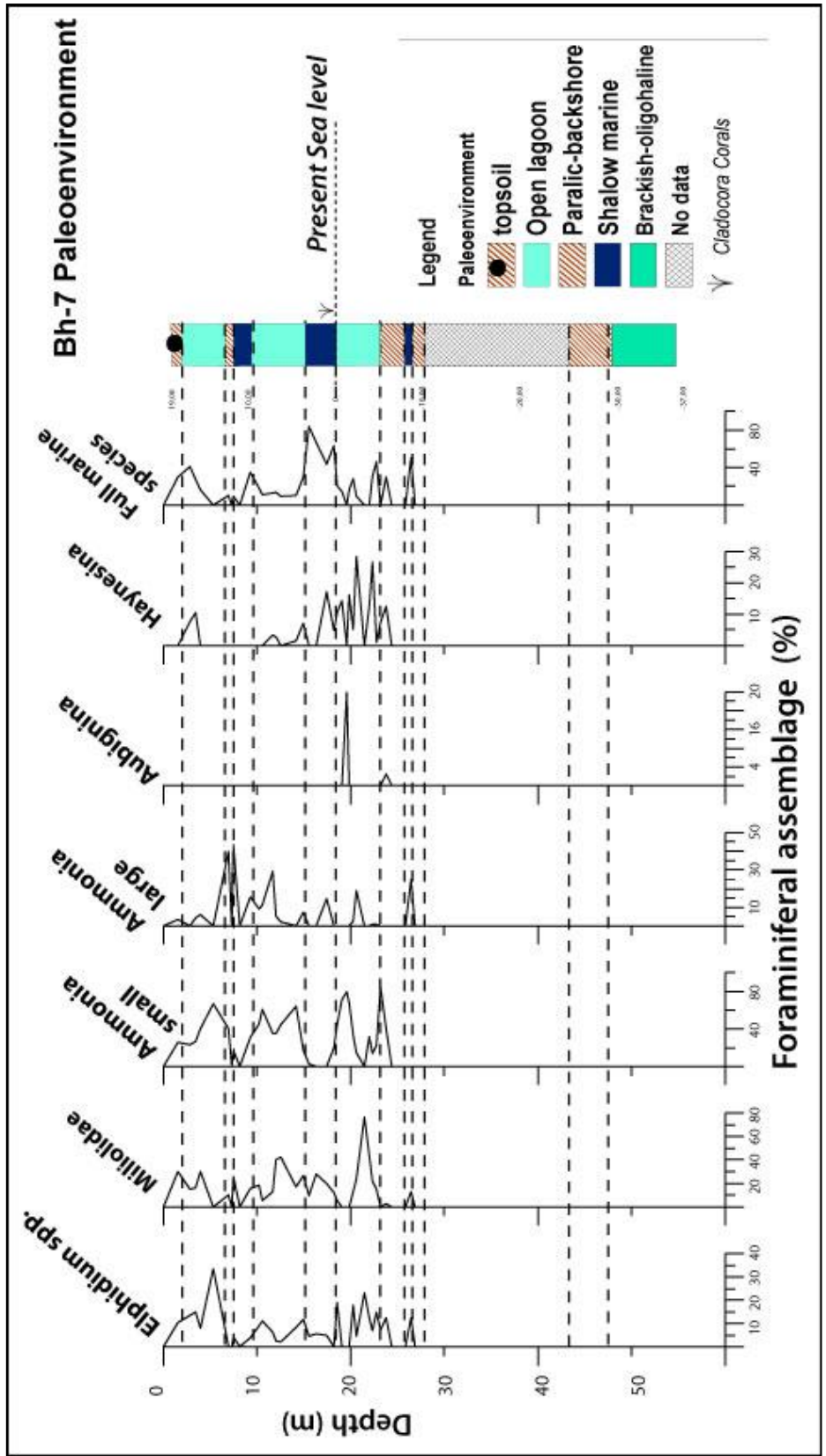


Fig. 5.2 View of the depositional environment of Bh-7 located on the immediate hangingwall of the studied fault, in correlation with the foraminiferal assemblages.

5.2 Interpretation

Through micropaleontological analysis it was able to determine the paleoenvironment and how it has changed through time. The area has changed from shallow marine to oligohaline lagoonal to paralic backshore paleoenvironment several times. Although through lithological analysis no significant correlation could be done, through paleoenvironmental analysis, at least the top layers, seems to have significant relationship with each other. In both boreholes there is a transition from a marine environment to paralic and then marine and finally paralic again. *Cladocora* corals that were found, appears to be at the same depositional environment shallow marine with mesohaline features.

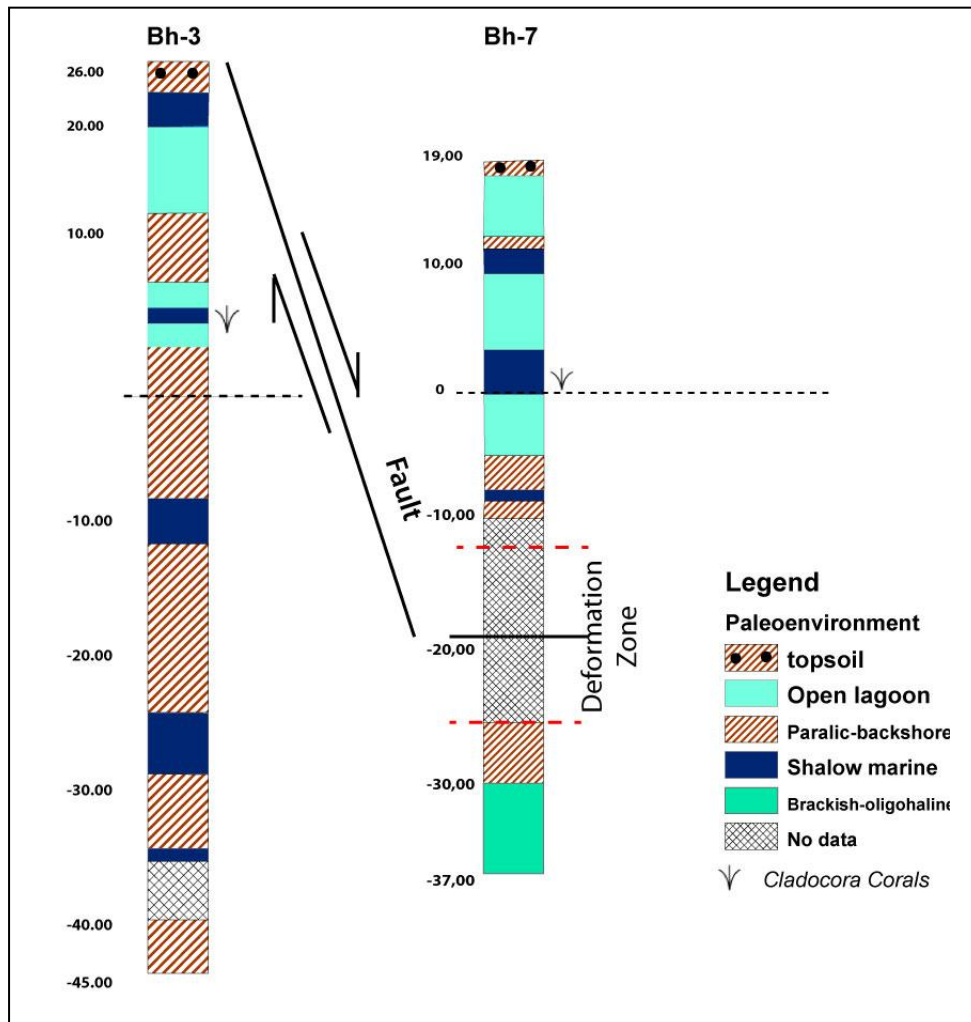


Fig. 5.3 View of the depositional environment of borehole 3 located on the immediate footwall and borehole 7 located on the immediate hangingwall of the studied fault.

The study area is in a very complicated system that influences the paleoenvironment. Three individual factors play vital role to paleoenvironmental evolution of the area. Firstly, the entire area has been uplifted even though that there are several faults which subside the Isthmus canal (see Chapter 3). Secondly, the area is near to the sea level which implies a high energy environment. Fluctuations of global glacioeustatic sea level, have affected the study area. Thirdly, Kalamaki fault has uplifted the area westwards to it (footwall) and has subsided the area eastwards to it (hangingwall). As a result different depositional environment is expected at the footwall and at the hangingwall of the fault.

Paleoenvironmental analysis clearly elucidates that the entire area has been uplifted from Upper Pleistocene until present day. Foraminifera and other marine species were found approximately 20 meters above sea. Furthermore *Cladocora* corals in Bh3 and Bh7 are now 5 and 1 meters above sea level respectively. The goal is to determine the exact uplift rate of the area. According to Collier & Thomson 1991, Collier & Dart 1991, Collier et al. 1992 the uplift rate of Corinth Isthmus is at least 03 mm/yr. Collier, in order to determine the uplift rate has dated corals which the age of these, was 205.000 ± 12.000 years, placing them in isotope stage 7.

Another issue that should be taken under consideration is the fact that global sea level is not stable. It is known that Earth's climate has changed several times during the past from glacial to interglacial, where sea level had changed accordingly. During a glacial period sea level is lower than it is today (lowstand), while during an interglacial period sea level is approximately at the same level that is today (highstand). According to Siddall et al. 2004, there is a glacioeustatic sea level lowstand at 18.000, 150.000 and at 275.000 years. On the contrary glacioeustatic sea level highstand is at 125.000, at 175.000 and at 200.000 years. Presence of shallow marine microfauna and corals shows that marine sediments have been deposit at glacioeustatic sea level highstands. Correlating the known uplift rate with the global glacioeustatic sea level curve it is possible to specify the expected paleoenvironment within the boreholes (Figure 5.3). Consequently, successions of marine and paralic-brackish paleoenvironment are interpreted into lowstand and highstand deposits (Figure 5.4).

Lowstand deposits such as subaerial deposits and top soil are marking unconformities with marine highstand deposits. According to figure 5.3 the marine to subaerial transition is formed when the location emerges above sea level either due to uplift and/or due to falling global sea level. Relative dates for these lowstand and highstand deposits can be derived from the sea level curve. As a result, marine sediments are expected at 125.000 years, then possibly during a short period at 175.000 years, then at a prolonged period 190.000 till 220.000 years, afterwards a period at 230.000, at 275.000 and at 300.000. Ages older than 300.000 are rather unlikely since that imply major erosional processes.

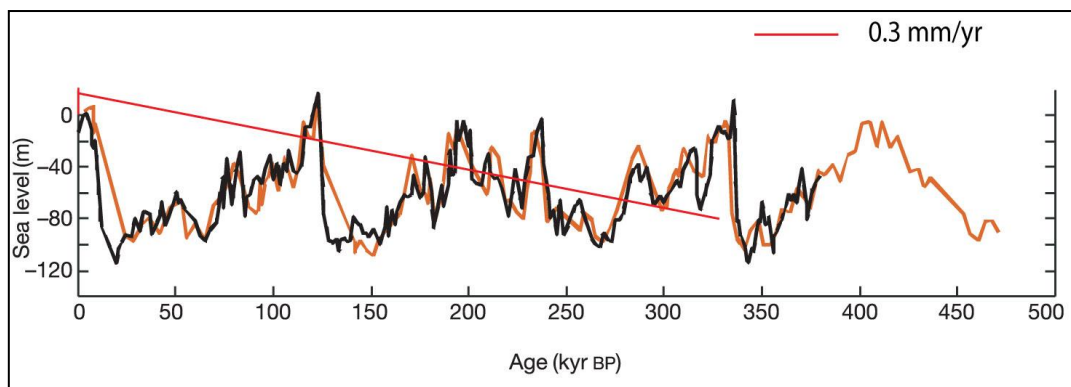


Fig. 5.5 Global sea level curve from Sidall et al. (2004) in correlation with the expected uplift rate, as has been counted by Collier et al. (1992) and Dia et al. (1996), from the neighboring dated corals.

There are difficulties concerning the precise age of each layer was deposited. It is highly important to specify their age in order to calculate throw and the slip rate of the studied fault. As a result, the presence of *Cladocora* corals has been used as reference point. Corals cannot be found everywhere, but only at specific periods, in relation with the glacioeustatic highstands. Therefore, based on the uplift rate of the study area and glacioeustatic highstands, corals would be expected at 125.000, at 175.000, at 200.000, at 225.000, at 240.000 and at 300.000 years. Taking under consideration uncertainties that sea level curve has, corals could also be found at 75.000 years. Consequently, these corals have to be placed in one of these periods.

It is clear in Figure 5.5 that corals may be from 125.000, 175.000 and 200.000 years or even older. Through paleoenvironmental analysis it was clarified that corals are

expected at the second highstand. According to this hypothesis, coral's age is 175.000 to 210.000 years. This age compiles with the age Collier et al. 1992, Dia et al. 1997, have found. These researchers have dated corals that were found at the Corinth canal. Both of them though, have found corals to 40-50 meters altitude. Corals in boreholes 3 and 7 were only at 5 meters. In order to overcome this problem three different scenarios were evaluated. Firstly that corals are not from isotope stage 7, which can be correct considering that Siddall's curve is not absolutely accurate. Secondly that uplift rate is not 0.3 mm/yr as it has been estimated by these researchers. Thirdly that corals are from isotope stage 7 and uplift rate is 0.3 mm/yr but sea level was significantly subsided in relation with the present one.

According to Siddall et al. 2003, the sensitivity of the method that was followed in order to estimate sea level changes has uncertainties of $\pm 12\text{m}$. In this case, corals might be from the isotope stage 5 at 125.000 years and the strata that were found above them could be 75.000 years old. Since the exact age of the corals is not known, it is not possible to specify which scenario between them is correct.

Second scenario, in order to overcome that problem and estimate the age of these strata, is to assume different uplift rates. If corals age is 200.000 then uplift rate is approximately 0.12 ± 0.02 assuming that sea level then was 10 meters below the present one. That uplift rate though, is not compatible with the 0.3 mm/yr rate that was found by Collier et al. 1992, Dia et al. 1997. It is difficult for the uplift rate to be more than 0.4 mm/yr and less than 0.2 mm/yr due to regional uplift. As it is clearly shown in figure 5.6 depositional environment, alters according the hypothetical uplift rate. Firstly, when the uplift rate is 0.2 mm/yr marine sediments are expected at 125.000, then at 200.000, perhaps a short period at 205.000, at 220.000 and finally at 240.000 years. On the other hand when the uplift rate is 0.4 mm/yr, marine sediments are expected at 125.000, a distinct period at 175.000 and then the entire area is almost always below the sea surface.

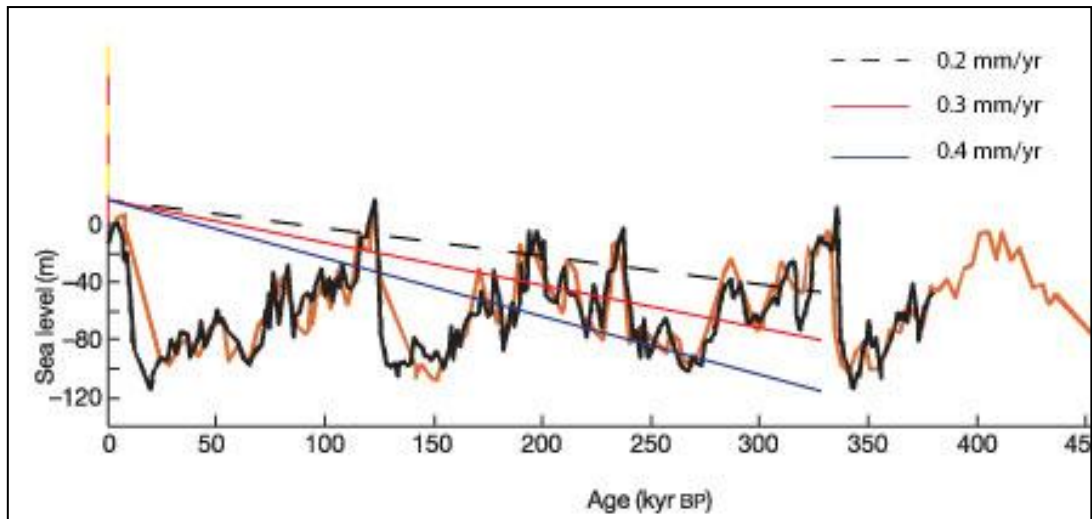


Fig. 5.6 Three scenarios about the uplift rate at the Isthmus canal, in correlation with Siddall's sea level curve.

Through this procedure, depths can be estimated as well. The exact depth of the marine environment cannot be determined, but relative depths can be specified. A lagoonal oligohaline environment is shallower than a mesohaline environment, which is shallower than a shallow marine paleoenvironment. The intersection between the uplift rate and the sea level curve can give a relative sense of depth as well. Uplift rate 0.4mm/yr that has been examined at the previous hypothesis, is rebutted using the depositional paleoenvironment. When uplift rate is 0.4 mm/yr, the expected environment is significant deeper than the expected one. Whether the uplift rate is at 0.3 mm/yr or at 0.2 mm/yr, is irrelevant with the expected date of the corals. In both cases, as it is shown in figure 5.7, corals are expected at 200.000. The purpose of this thesis is not the exact uplift rate, but a relative date of the corals so slip rate can be calculated.

According to Siddall et al. 2004, sea level alters significantly during isotope stage 7 from 175.000 till 225.000 years. For instance at 185.000 years sea level has been subsided approximately 70 meters below the present sea level, while at 205.000 years is approximately where present sea level is. According to this the assumption that when corals have grown sea level was significantly lower than the present one, can be supported.

Another scenario is the hypothesis that corals have not grown at the same period and have other ages. Firstly, through paleoenvironmental analysis, it seems that corals have grown at the same depositional environment⁵. Secondly, if corals were not from the same age means that the slip rate of the fault would be much higher than the expected. This fault has a limited length and is located in the stress shadow of several big faults. Consequently, its slip rate cannot be more than 0.05 -0.1 mm/yr.

Finally, Siddall et al. 2004, is not the only paper that has estimated global glacioeustatic sea level changes. In order to test paleoenvironmental alterations thoroughly, Thompson & Goldstein 2006 sea level curve was examined as well. In figure 5.7 sea level curved was correlated with different uplift rates. The same result was found in both scenarios more or less. Depositional paleoenvironments that was estimated with Siddall's curve, were also found after using the second curve.

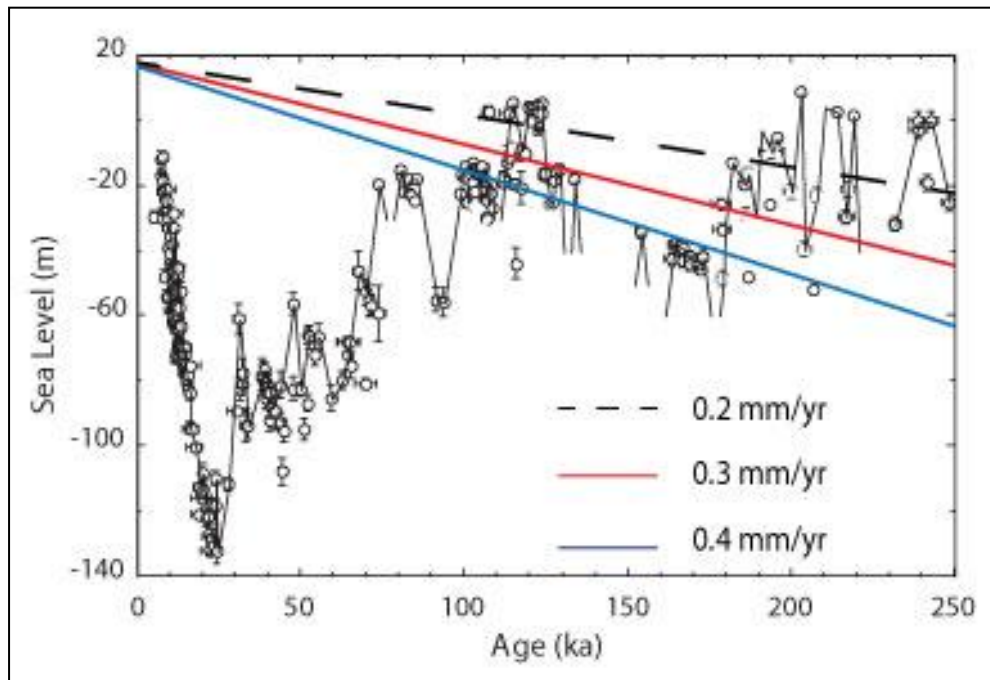


Fig. 5.6 Global sea level curve from Thompson & Goldstein 2006, in correlation with 3 scenarios about the uplift rate. It is obvious that there were no significant differences with Siddall's curve.

⁵ In both samples it was suggested a shallow marine environment with mesohaline characteristics due to fresh water input. Furthermore, paleoenvironment alters with the same pattern in both boreholes, as it changes from shallower to deeper (where the corals have been found) and then shallower marine again.

According to all these scenarios, corals are expected to be at 125.000 or at 200.000 years. It is rather impossible to specify their exact age. Provided that there is an offset approximately 4 ± 2 m between these corals and assumptions for their age have been done, fault's slip rate can be estimated. Since the exact age of corals cannot be found, rates for both scenarios estimated.

6. Seismic hazard assessment

6.1 Introduction

Up to recently, seismic hazard maps were constructing depending on seismic data that have been recorded the previous century. Geological formations and active faults were taken under no consideration, let alone their slip rate. On the contrary, new hazard maps pay less attention to historical seismic data and rely mostly on geology, on faults and characteristics. Features of a fault that are examined in order to determine seismic hazard are its length, its displacement and of course its slip rate. The rate at which a fault slips determines the seismic hazard that it represents. Higher the slip rate is, the more hazardous the fault will be. Practically, faults with a higher slip rate pose greater threat than those that have lower slip rate. For example as slip rates decrease average recurrence intervals tend to increase and several times are longer than the period covered by the historical record. This is why low slip-rate faults are often absent from the historical catalogues and thus from the seismic hazard assessment.

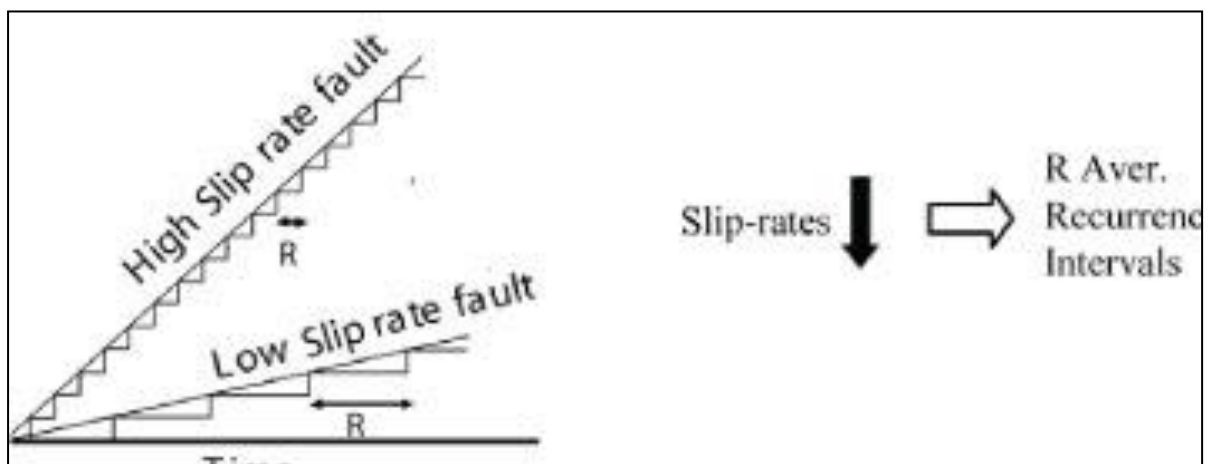


Fig. 6.1As slip rate increases, earthquakes are more frequent (e.g. Cowie & Roberts 2001)

6.2 Slip rate

Using the estimated age of the layers and the measured offset, throw rate can be calculated for the area where these boreholes were drilled. Throw rate is approximately at 0.02 mm/yr. Taking under consideration that the fault dips at 65° to SSE, the slip rate of the fault near the Isthmus canal is approximately 0.022 mm/yr. These values though, have to do only for the section of the fault which is near the Isthmus canal. According to Roberts et al., 2004, Roberts et al., 2002, Gupta & Scholz 2000, the central section of a fault slips more rapidly than the sections located at the tip of the fault. This means that towards its center a fault produce higher displacements and that it accommodates more strain (Figure 6.2_(A)). Consequently, the throw rate is expected to be higher towards the center of a fault than to its tips. This hypothesis corresponds with the geometry of the studied fault. Towards its center this fault has produce topographic variations approximately of 150 meters high, while at the area where boreholes were drilled, topographic variations were not higher than 20 meters.

In order to calculate the maximum slip and throw rate, a triangular displacement profile has been used (Cowie & Shipton. 1998, Roberts et al., 2004)(Figure 6.2_(B)). The maximum displacement of the fault during a certain period of time is (H), while the fault's length is (L). Y is displacement near the area where boreholes were drilled. Y has been found that was 4 ± 2 meters. Using trigonometry, the maximum displacement of a fault is 8.4 ± 2 meters. Throw rate though is different if the age of the corals is at 125.000 or at 200.000 years.

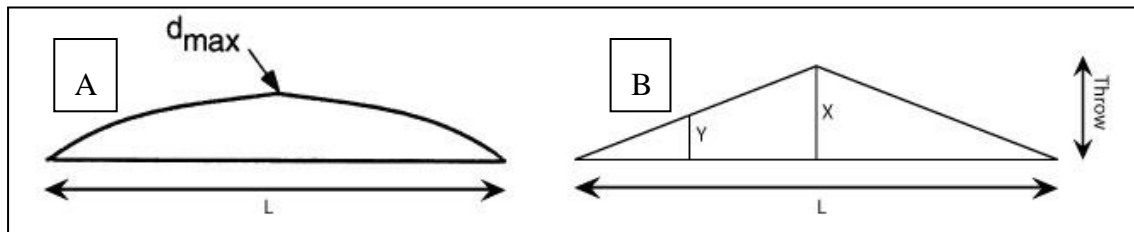


Fig. 6.2 (A) Displacement -Length profile of a fault. (B) A triangular displacement profile. X is the maximum displacement of the studied fault during a period, while Y is displacement near the study area.

If it is assumed that coral's age is at 125.000 indicates that estimated fault's throw rate is approximately 0.067 mm/yr. Otherwise, if it is assumed that the age of corals is at 200.000, indicates that fault's throw rate is approximately 0.041 mm/yr. Throw rate of the fault is estimated at 0.057 ± 0.015 mm/yr. Kalamaki is a very low slip-rate fault, uncertainties of 0.013 mm/yr, at the estimated throw rate are rather insignificant.

6.3 Methodology

Firstly, Fault's throw is taken under consideration since the last major glacial retreat phase (18.000 years ago). The last reported age of small magnitude glacial events is 12.000 ago. Due to the uncertainty on the exact age, the age of 15.000 ± 3.000 years is used for the age of post-glacial scarps. Afterwards, throw rates have been calculated for all faults. Then these rates are translated into earthquakes assuming that each fault ruptures in floating earthquakes of a fixed size shake. This means that throw accumulation is accomplished through a standard mean earthquake magnitude, which depends according to the fault.

According to Wells & Coppersmith 1994, ruptures length are related with maximum displacement and earthquake magnitudes. For this method a triangular displacement profile for faults and ruptures has been assumed (Cowie & Shipton 1998, Roberts et al., 2004), correlating the fault throw with the fault length. Afterwards, the triangle area is filled with hypothetical ruptures (Figure 6.3_(A)). These ruptures are all the necessary earthquake of fixed size⁶ events needed, in order to create a post-glacial

⁶ As far as concern the studied fault, using the empirical relationships of Wells & Coppersmith, the maximum earthquake magnitude that is expected for a 5.5 km fault is approximately 5.6 Ms. Maximum

scarp according to this throw-rate during the last 15.000 ± 3.000 years. All these earthquakes are extracted along the fault. These events are not distributed along the fault randomly. Hypothetical epicenter of each earthquake is located in a specific way so more epicenters will be towards the center of a fault (Roberts 1995, Papanikolaou et al. 2011).

For each epicenter an isoseismal of an expected intensity has been constructed (Figure 6.3_(B)). The distance from the fault is more or less 12 km in the hangingwall of a normal fault, taking under consideration that a fault dips approximately at $30^\circ - 60^\circ$. The range of each isoseismal depends on the expected earthquake magnitude and needed intensity that required to be projected. For instance, the maximum expected magnitude for the studied fault is 5.6 Ms. According to the empirical relationships of Theodoulidis (1991), the maximum intensity is 8 with a mean radius of 5 km, while for intensity 7 the mean radius of isoseismal is 14 km. The distance of each epicenter from the fault, is hypothetically located according to each fault's geometry at 10 to 8 km to the hangingwall. This assumption has to do with the fact that earthquakes, especially the large ones, tend to be generated near the seismogenic layer at 10 -15 km depth. According to Wyss et al., 2008, for the area of Corinth epicenters are more or less at 10 km depth, which lead to the requested distance.

expected magnitude in the area is 6.9 caused by South Alkyonides fault system, provided that it will rupture at its total length.

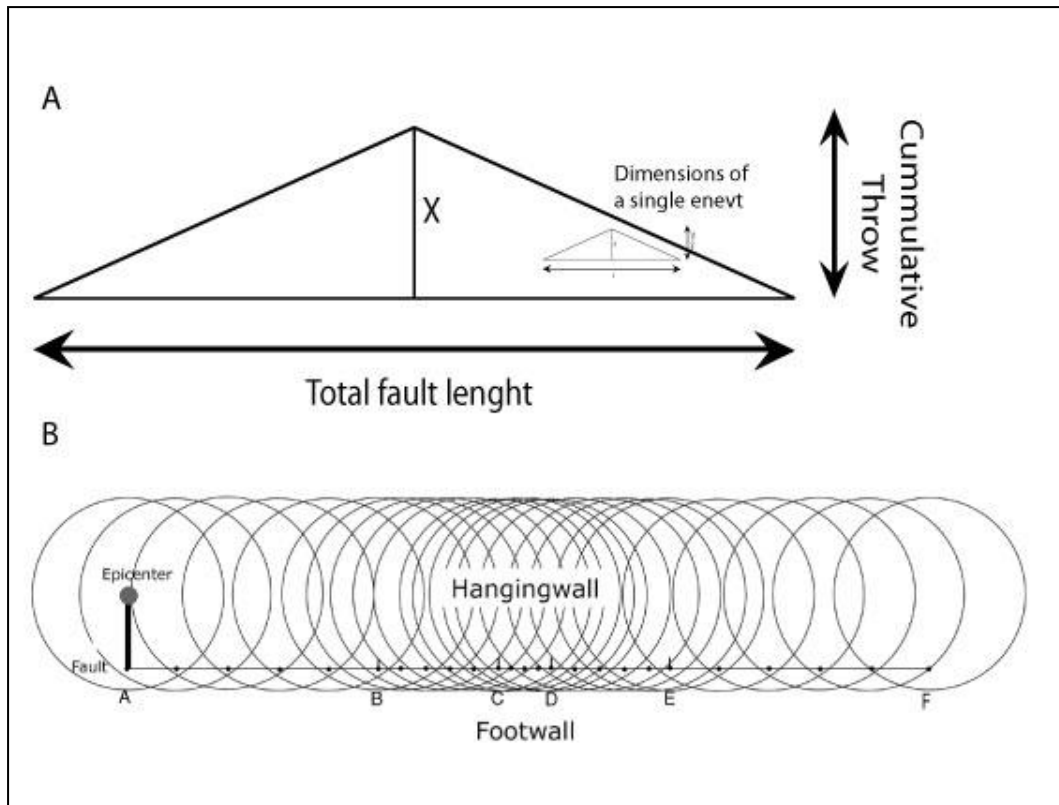


Fig. 6.3 Cumulative throw of a fault and displacement caused by a single event (A). Most hypothetical epicenters are plotted at the hangingwall, towards the center of the fault (redrawn from Roberts et al., 2004).

These isoseismals are without taking under consideration geological formations and how these influence the area and the intensity. The expected intensity alters compared with the geological formations in the area. For the purpose of this thesis, formations have been grouped in three categories in order to represent how these react in case of an earthquake. Igneous formations, limestones and marbles are the first group, schist with Pliocene sediments and flysch are the second group and Quaternary sediments are the third group. The first group (hard rock) subsides the expected intensity for one degree, while the second group (soft rock) does not affect the expected intensity. On the contrary, Quaternary sediments amplify the intensity for one degree.

There are several scales that can be used for estimating the impact from an earthquake. Effects from these hypothetical earthquakes, have been assessed according to the Environmental Seismic Intensity scale, ESI 2007 (Michetti et al. 2005, 2007, Papanikolaou et al. 2007). Other scales such as MS (Mercalli- Sieberg)

or EMS (European Macroseismic Scale), have disadvantages as far as the attribute of the effects of an earthquake concern. ESI has the advantage that describes the effects to the environment and does not take under consideration the effects on humans and infrastructures. Consequently is more objective than the other scales are.

6.4 *Seismic Hazard maps*

According to this methodology each fault affect a specific area and with a maximum intensity. A map that presents the seismic hazard of the area has to include all the faults that may affect a region. As it has been clarified before, in the area several faults can generate significant earthquakes with destructive results. The fault that has been studied in detail in this thesis is one of the many that can pose a threat for the Isthmus canal and all the communities that are there. For the purpose of this study, Kalamaki fault, Loutraki fault, South Alkyonides fault, Kechries fault Agios Vassileios fault have been taken under consideration in order to estimate seismic threat.

6.4.1 Kalamaki fault

Along the Corinth canal several faults have been identified but only this displays a clear fault plane up to the surface and controls the topography of the area. As it has been described before, its total length is approximately 5.5 km. It can uplift the Corinth canal and subside the westernmost section of the Saronic Gulf (Figure 6.4). Its limited length renders it incapable to produce earthquake of significant intensities as the previous faults could. According to the empirical relationships of Wells and Coppersmith (1994), this fault can give a maximum magnitude 5.6 Ms and according Theodoulidis (1991), the maximum intensity will be VII. The radius of these hypothetical epicenters are estimated at 16 km. In Subchapter 6.2, fault's throw rate toward its center has been estimated. Due to uncertainties considering the rate, two

different values have been estimated. In order to estimate the seismic hazard of the area, the highest throw rate will be taken under consideration. Thus the worst case scenario will be estimated. With this throw rate, the last 15.000 ± 3.000 years 7 hypothetical earthquakes might have occurred according to the methodology that has been described before.



Fig. 6.4 View of the studied fault, where the tip and center of the fault are shown.

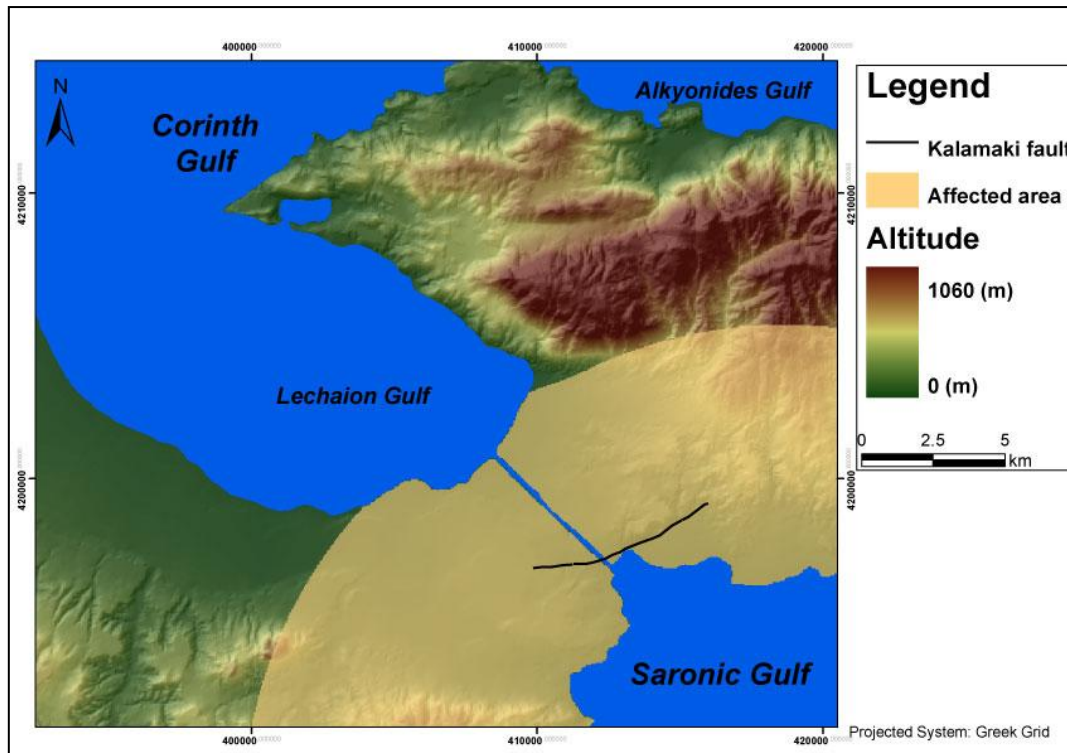


Fig. 6.5 *The area that can be influenced with intensity VII from the studied fault, assuming an homogeneous bedrock geology,*

This fault can influence the entire area of Corinth canal, with intensity VII, also the westernmost area of the Saronic Gulf, the south section of Perachora peninsula and the area where the cities of Corinth, Kechries and Isthmia are located (Figure 6.5). It is assumed that the entire surface slip for the 15.000 ± 3.000 years is the result of floating earthquakes of 5.7 magnitude, which can produce 0.14 m coseismic throw of 5.5 km rupture length according to Well & Coppersmith (1994). As a result, a number of expected earthquakes for this fault during this period are estimated. Figure 6.6 shows which area receives enough energy to shake at intensity IX, during the last 15.000 ± 3.000 years. The central area of Corinth Isthmus receives 7 times enough energy to shake during this period.

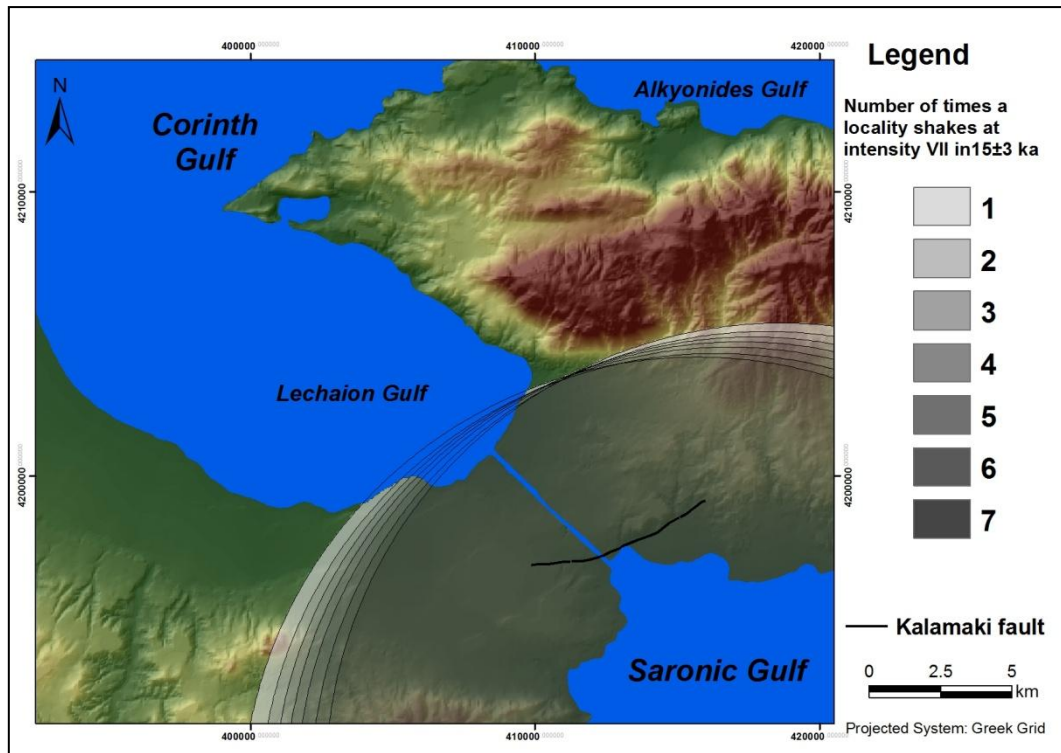


Fig. 6.6 Earthquake recurrence of intensity VII in the studied fault. During the last 15.000±3.000 years 7 hypothetical earthquakes are expected.

Bedrock geology can influence the maximum expected intensity caused by an earthquake. Semi cohesive sediment that compile the central part of Corinth canal can amplify the expected intensity to VIII. On the contrary, few marl formations and limestones at the north or at the south sections of the area, subside the expected intensity to VI.

Correlating expected intensities and geological amplification can clearly show which is under a greater threat. The central part of Corinth Isthmus and the area where the cities of Corinth, Lechaion Kechries and Isthmia are located, receive more energy. If an earthquake occurs there, maximum expected intensity is VIII (Figure 6.8).

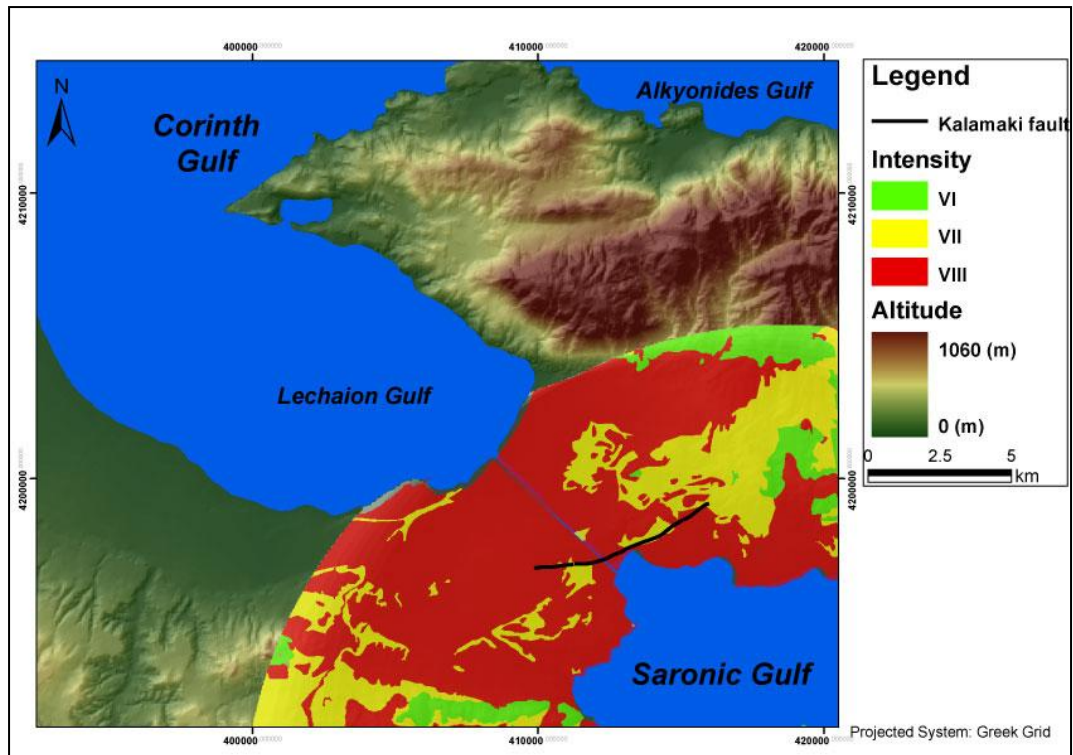


Fig. 6.7 Map showing the maximum expected intensity generated by Kalamaki fault

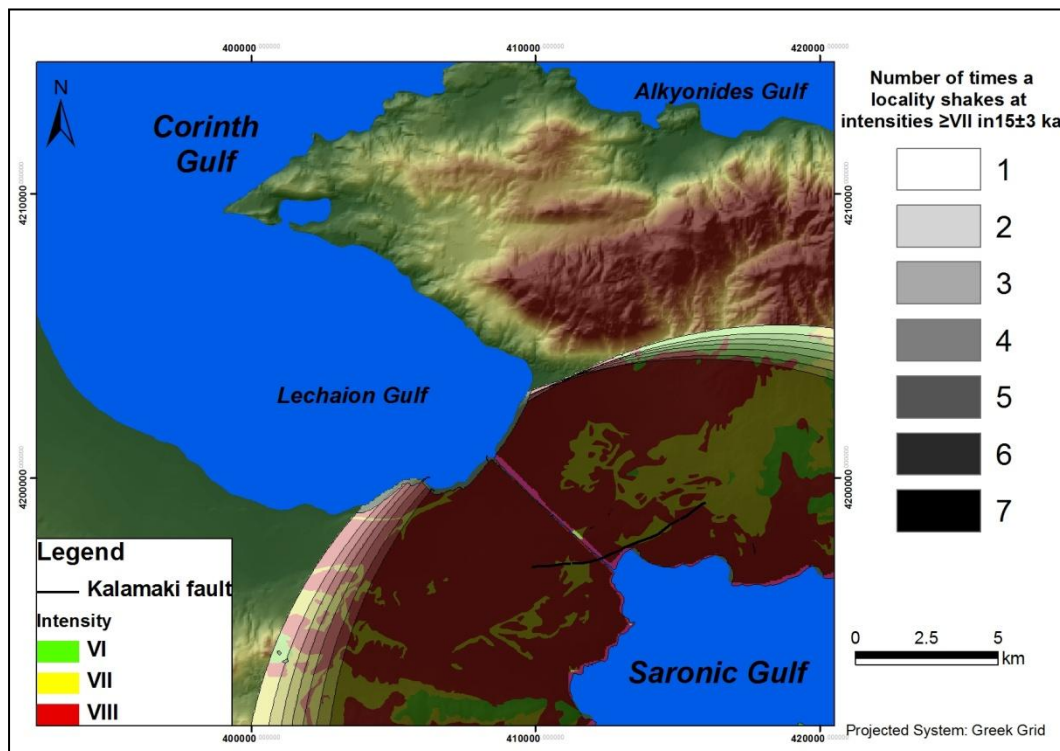


Fig. 6.8 Map that shows the maximum expected intensities after considering the amplification due to the surface geology.

6.4.2 The Kechries fault

Kechries is a E-W trending fault that dips to the north and subsides the Corinth canal. Onshore this fault has approximately 10 km length (Figure 6.9). This fault has a segment that is offshore (Papanikolaou et al. 1988). The exact length is not known, but is at least more than 10 to 15 km. For the purpose of this thesis, a minimum total length of 24 km has been estimated, in order to calculate the seismic threat. It has created obvious topographic variations more than 300 m. It bounds Quaternary sediments and has uplifted Mesozoic limestones. According to Roberts et al. (2011), even though it is clearly active since it offsets recent layers, there is no obvious postglacial scarp, while according to Turner et al. 2010, the fault is inactive.

This implies that it is a very low slip-rate fault maximum at 0.4mm/yr. and throw rate is approximately 0.25 mm/yr. Using the empirical relationships of Wells & Coppersmith the maximum magnitude from this fault is 6.7. Since the last glaciation 6, hypothetical earthquakes might have occurred according to the methodology that has been described. Finally, according to Theodoulidis 1991, the Kechries fault can be responsible for an earthquake that has intensity IX with an estimated radius at 10 km.



Fig. 6.9 View of the Kechries fault plane from Google Earth (Roberts et al. 2011).

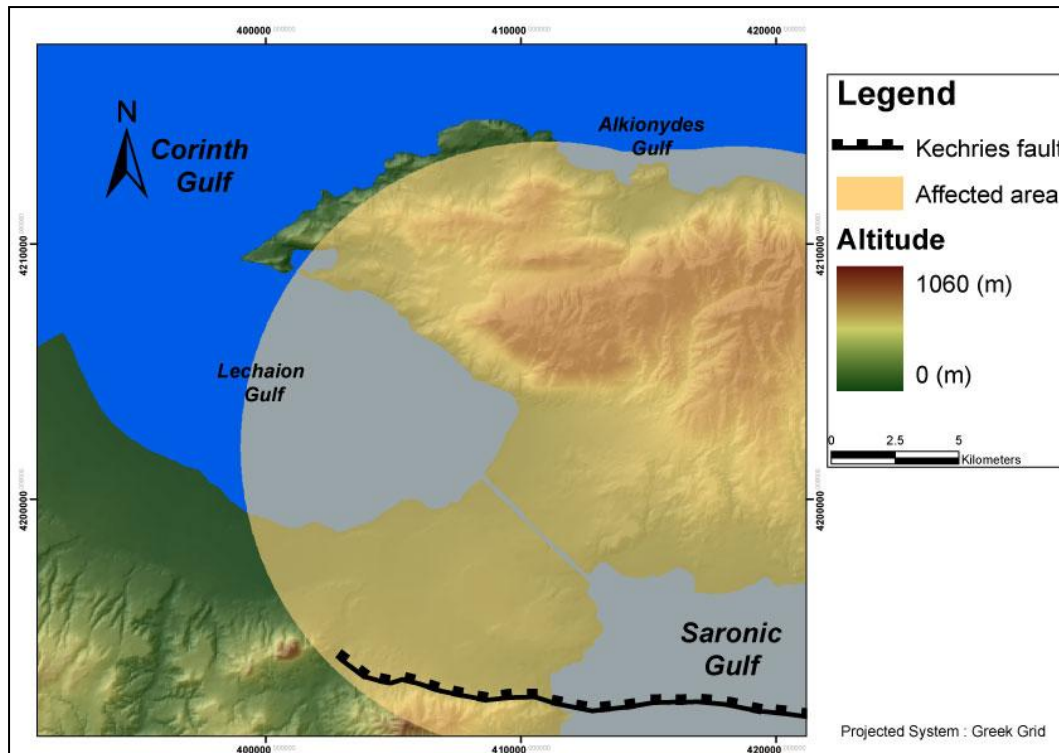


Fig. 6.10 The area that is expected to be influenced by Kechries fault with intensity IX, assuming an homogenous bedrock geology

As it is shown in figure 6.10 this fault can influence the north section of Corinth region, the entire Perachora peninsula, the Lechaion gulf, the easternmost area of the Saronic Gulf, the Megara and the southernmost section of Attica region with intensity IX. It is assumed that the entire surface slip for the 15.000 ± 3.000 years is the result of floating earthquakes of 6.5 magnitude, which can produce 1 m coseismic throw of 15 km rupture length according to Well & Coppersmith. In figure 6.11 shows how many times each area receives enough energy to shake at intensity IX the last 15.000 ± 3.000 years. Areas that are near the centre of the fault receive more energy. In this case the westernmost section of Perachora peninsula receives 6 times enough energy to shake at intensities IX. Neither in this case has geological influence been estimated. $\geq \pm$

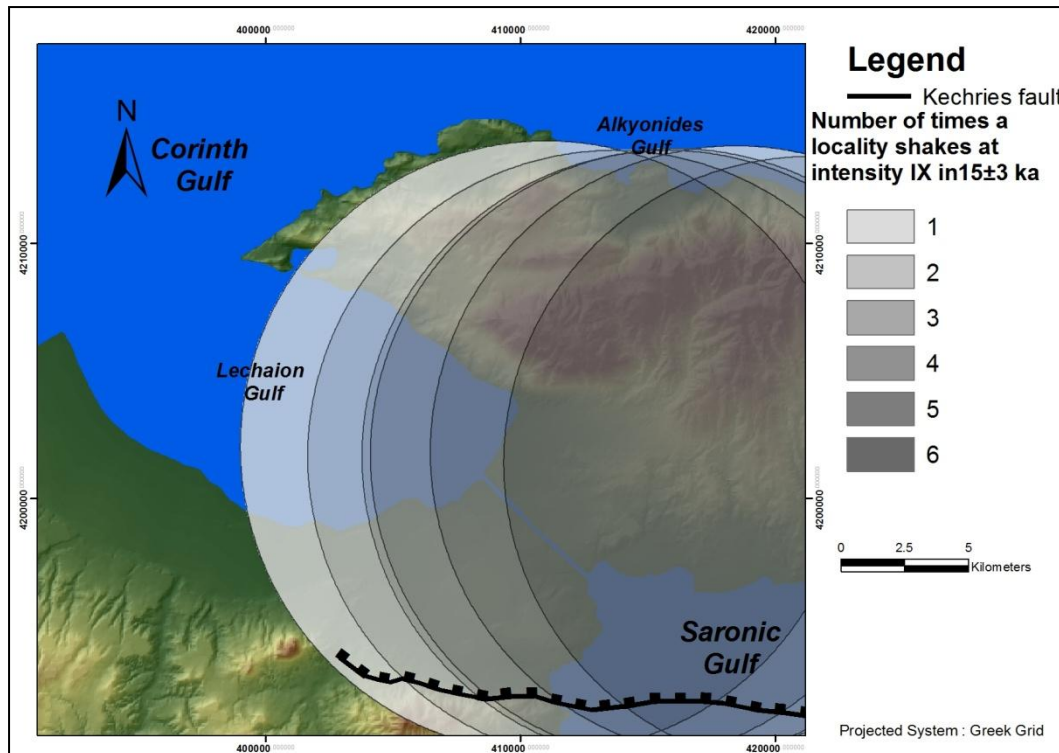


Fig. 6.11 Earthquake recurrence. During the last 15.000±3.000 years 6 of intensity IX in Kechries fault hypothetical earthquakes are expected

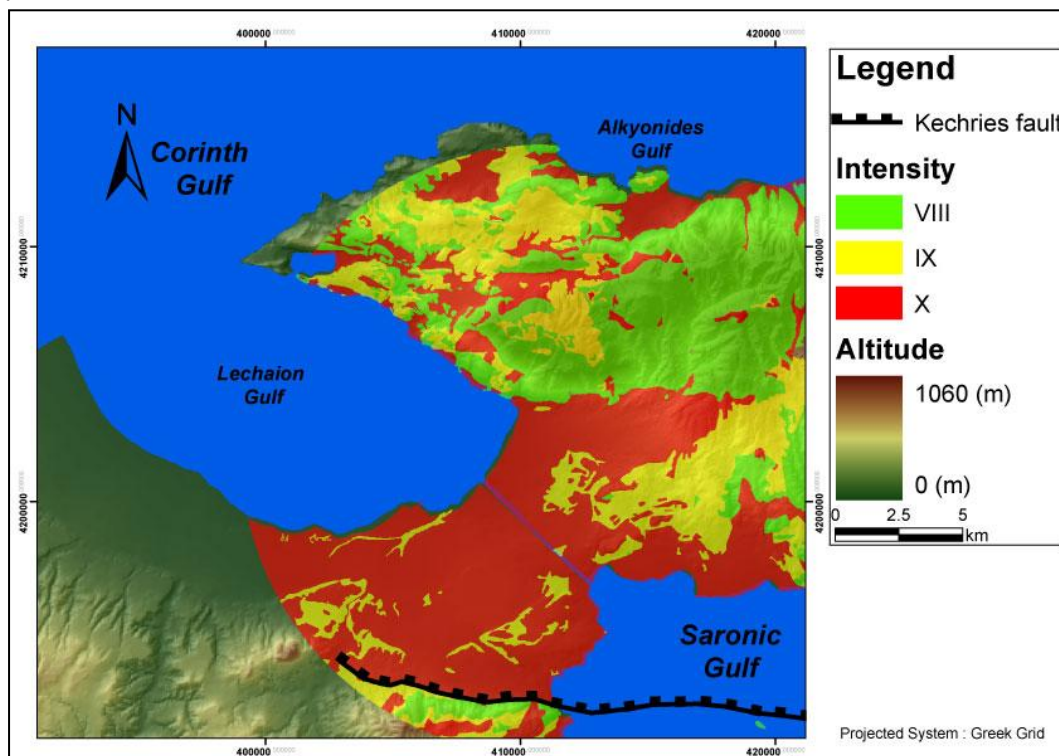


Fig. 6.12 The intensity alters in relation with the geological formations, from X till VIII.

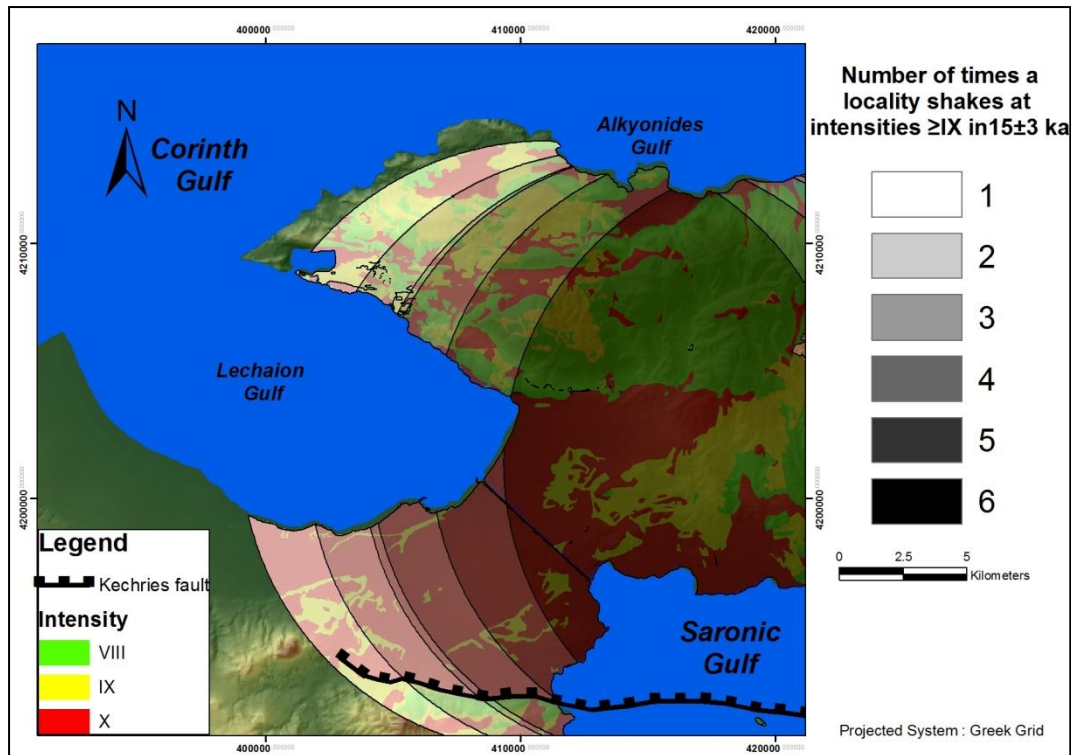


Fig. 6.13 Earthquake recurrence in relation with the geological amplification. The area that is at a greater risk is westernmost section of the Corinth canal.

Geological formations can amplify or lessen the expected intensity approximately for one degree. Consequently, expected intensities from the Kechries fault are from X till VIII (Figure 6.12). The northernmost section of the study area where ophiolites and limestones are, intensity is less (VIII). Few sparse areas that intensity has been amplified, is mostly due to the recent fluvial deposits. On the contrary, the Corinth canal is less safe since strata are composed mostly from recent marine sediments and manmade artificial deposits from the Upper Pliocene and intensity X is expected there. The central part of Corinth Isthmus can receive enough energy to shake at intensities IX the last 15.000 ± 3.000 years. The same area will be shacked with intensity X. Consequently, the Kechries fault poses greater threat for the area where the Corinth canal, the Loutraki and the Isthmia are (Figure 6.13).

6.4.3 The Loutraki fault

The Loutraki fault is the only south-dipping fault in the study area. Characteristic of this fault is the fact that it is composed by several segments more or less parallel to each other (Rontoyanni et al. 2008, Turner et al. 2011). The first segment bounds Loutraki basin and continues offshore (Lykousis et al. 2007, Goldsworthy & Jackson 2001, Zygouri et al. 2008). The other segment lays 1.5 km to the north and its length is approximately 5 km. The Loutraki fault has contributed to the uplift of Gerania Mountains. A clear postglacial scarp approximately 9 m height near to the Osios Potapios monastery, (Figure 6.14), clearly indicates that the fault is active (Roberts et al. 2011). This scarp indicates that the fault has a throw rate, approximately 0.5 mm/yr. With the empirical relationships of Wells & Coppersmith maximum magnitude from this fault is 6.6. During the last 15.000±3.000 years 10 hypothetical earthquakes might have occurred according to the methodology that has been described. Furthermore according Theodoulidis (1991), the Loutraki fault can be responsible for an earthquake that has intensity IX with an estimated radius at 10 km



Fig. 6.14 View of the postglacial scarp of the Loutraki fault. This scarp is from the segment northwards the main fault, near the monastery of Osios Potapios.

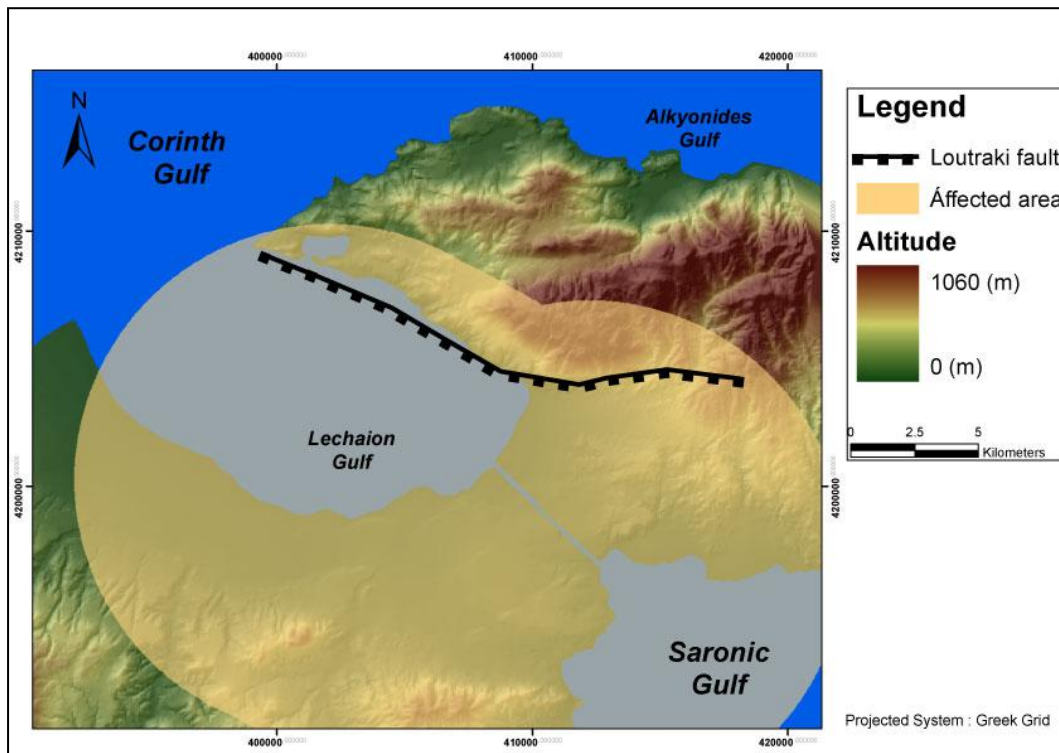


Fig. 6.15 The area that is expected to be influenced by the Loutraki fault with intensity IX, without taking under consideration the bedrock geology or the earthquake recurrence.

The Loutraki fault influences the southernmost area of the Perachora peninsula, the entire Corinth canal, the Lechaion and the easternmost area of the Saronic Gulf and the city of Corinth (Figure 6.15). This area though, is without taking under consideration bedrock or the earthquake's frequency. It is assumed that the entire surface slip for the 15.000 ± 3.000 years is the result of floating earthquakes of 6.5 magnitude, which can produce 1 m coseismic throw of 15 km rupture length according to Well & Coppersmith (1994). A number of expected earthquakes for this fault during this period are estimated. figure 6.8 shows which area receives enough energy to shake at intensity IX the last 15.000 ± 3.000 years. The frequency is 10 times towards the center of the Isthmus and diminishes towards the tips (Figure 6.16).

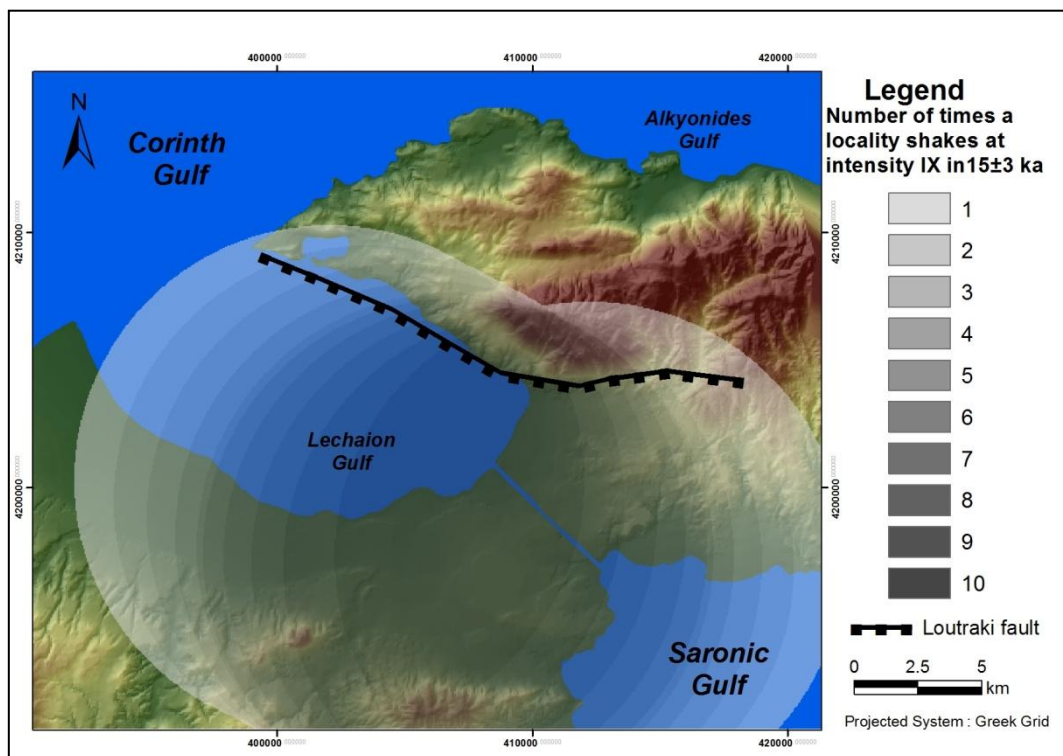


Fig. 6.16 Earthquake recurrence of intensity IX in Loutraki fault. Since the last glaciation, 10 hypothetical earthquakes might have occurred.

The expected intensity from the Loutraki fault range from X till VIII (Figure 6.17), considering the bedrock geology. The north area, where limestones and ophiolites are, maximum expected intensity is less (VII). Corinth canal and the south bay of Lechaion gulf where consists of marine terraces and sediments that increase intensity at one degree.

. The west-central part of Corinth Isthmus and the area where the cities of Corinth, Lechaion and Loutraki are located, can receive enough energy to shake at intensity Xi the last 15.000 ± 3.000 years and are in an area that the maximum expected intensity is X (Figure 6.18).

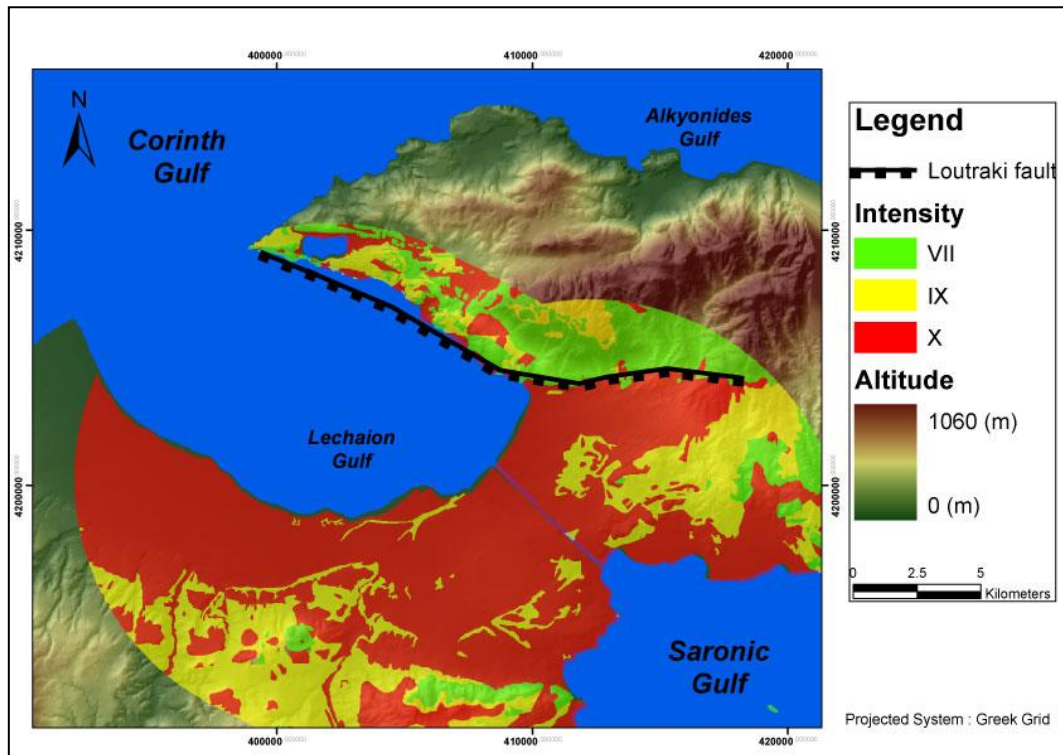


Fig. 6.17 The maximum expected intensity and how does it alters in relation to the bedrock geology.

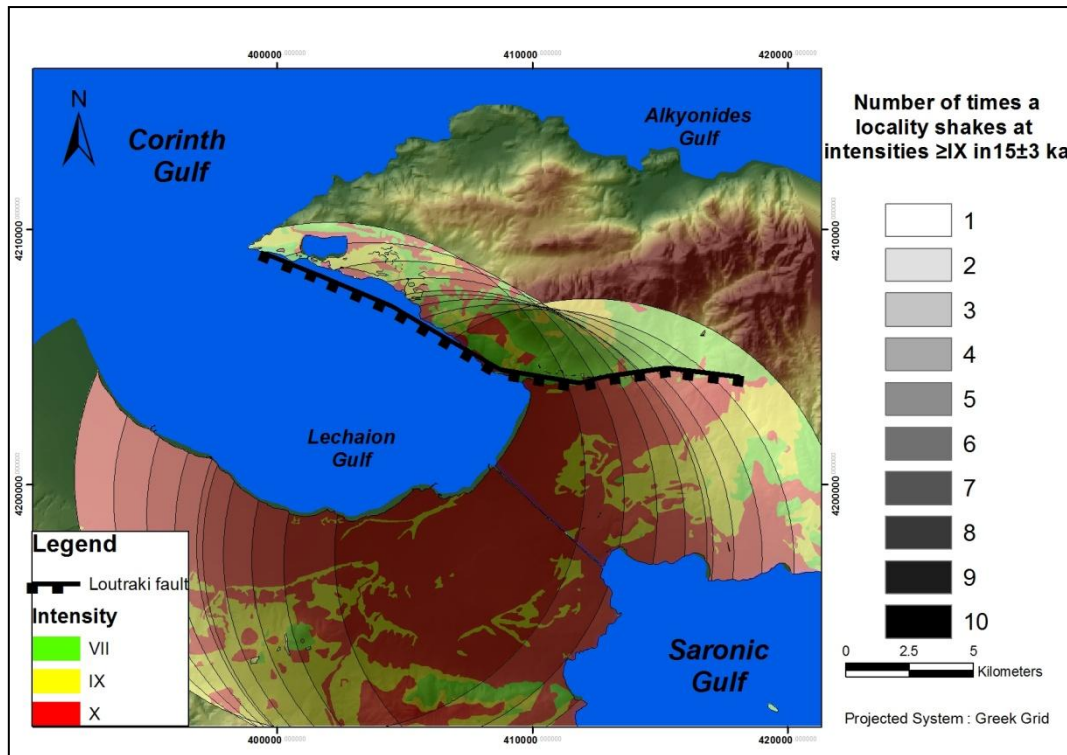


Fig. 6.18 Earthquake recurrence in relation to the geological amplification. The area that is at a greater risk is the central area of the Corinth canal, is characterized by higher recurrence.

6.4.4 The South Alkyonides fault system

This fault system is probably the most well studied fault at the eastern end of Corinth gulf due to the 1981 earthquake sequence. The peculiarity of the South Alkyonides fault system is that it is composed by several minor faults parallel or sub parallel with each other. The most significant of them is the offshore south Alkyonides fault and the onshore Schinos and Pisia faults (Figure 6.19). Each of these segments is approximately 15 km long and composes a fault system more or less 35 km long (Leeder et al. 2002, Pantosti 1996, Collier et al. 1998, Papanikolaou et al. 2009, Roberts et al. 2011, Morewood and Roberts 1999).

It is active since it was ruptured during the 1981 earthquake sequence. Surface ruptures were mapped then, almost at entire faults length (Mariolakos et al. 1982, Jackson et al. 1982, Hubert et al. 1996). In 1981 three earthquakes occurred, two of them are ascribed in this fault system, while the third was caused by Kaparelli fault which is a few km to the north. Until now uncertainties remain though, whether surface ruptures in Perachora peninsula should be ascribed to one or both shake events. The fact is that both Schinos and Pisia have activated during that earthquakes, producing extensive surface ruptures⁷ (Papanikolaou et al. 2009, Pantosti 2011).

The maximum cumulative throw of this fault system is approximately 2.5-3 km (Roberts et al. 2011). Throw rate has been calculated by Pantosti et al. 1996, Collier et al. 1998, from trenching in area Bambakies, where is an active alluvial fan. According to them minimum throw rate was estimated at 1 mm/yr, while minimum rate is between 1.2 to 2.2 mm/yr towards the centre of the fault. Estimated throw rate from trenching is always considered as the minimum. There is the possibility that researchers did not find an earthquake event that would increase the expected rate. For the purpose of this thesis throw rate was considered to be 2 mm/yr, in order to estimate the “worst case scenario” that can affect the area. Through empirical relationships (Well & Coppersmith 1996) maximum magnitude from this fault is 6.9 Ms. Since the last glaciation 23 hypothetical earthquakes might have occurred according to the methodology that has been described. Furthermore according to Theodoulidis 1991, the SAFS can be responsible for an earthquake that has intensity IX with an estimated radius of 16 km (Figure 6.20).

⁷ Maximum displacements were approximately 150 cm to Pisia fault and 100 cm to Schinos fault.

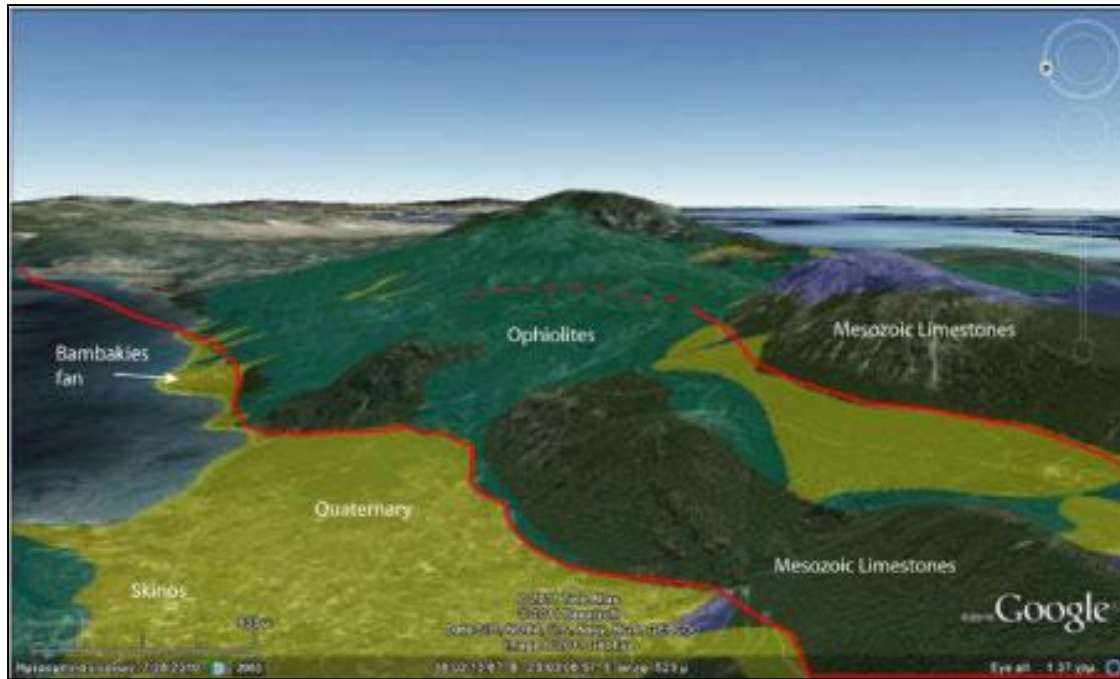


Fig. 6.19 View of the Schinos and Pisia segments fault from Google Earth(Roberts et al. 2011).

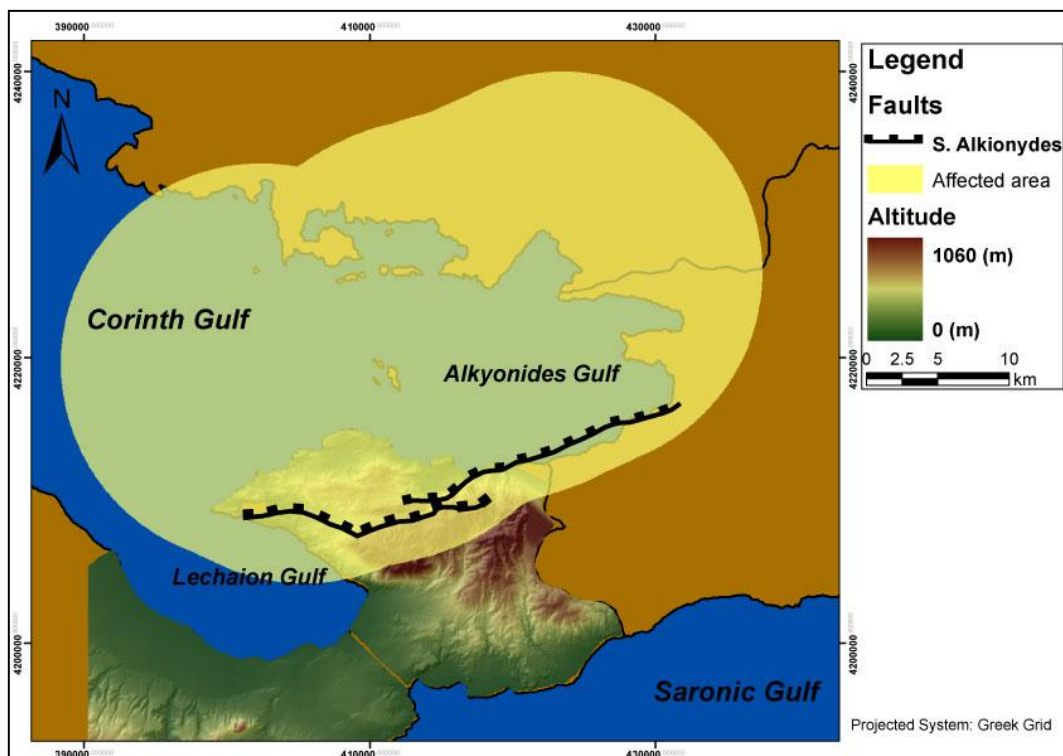


Fig. 6.20 The area influenced by the South Alkyonides fault system with intensity IX, considering an homogenous bedrock geology.

This fault system can shake with intensity IX, the north section of the Perachora peninsula, the entire Alkyonides gulf and an area of Attica and Voiotia region. The difference between the other faults that have been examined in this study is the fact that does not influence directly the Canal Isthmus. It is assumed that the entire surface slip for the 15.000 ± 3.000 years is the result of floating earthquakes of 6.7 magnitude, which can produce 1.5 m coseismic throw 25 km rupture length according to Well & Coppersmith. During the 1981 earthquake 1.5m was the maximum displacement and 25 km the total surface ruptures that has been observed. As a result a number of expected earthquakes for this fault during this period are estimated. Figure 6.19 shows which area receives enough energy to shake at intensity IX the last 15.000 ± 3.000 years. The central part of SAFS receives 23 times enough energy to shake at intensity IX during this period (Figure 6.21).

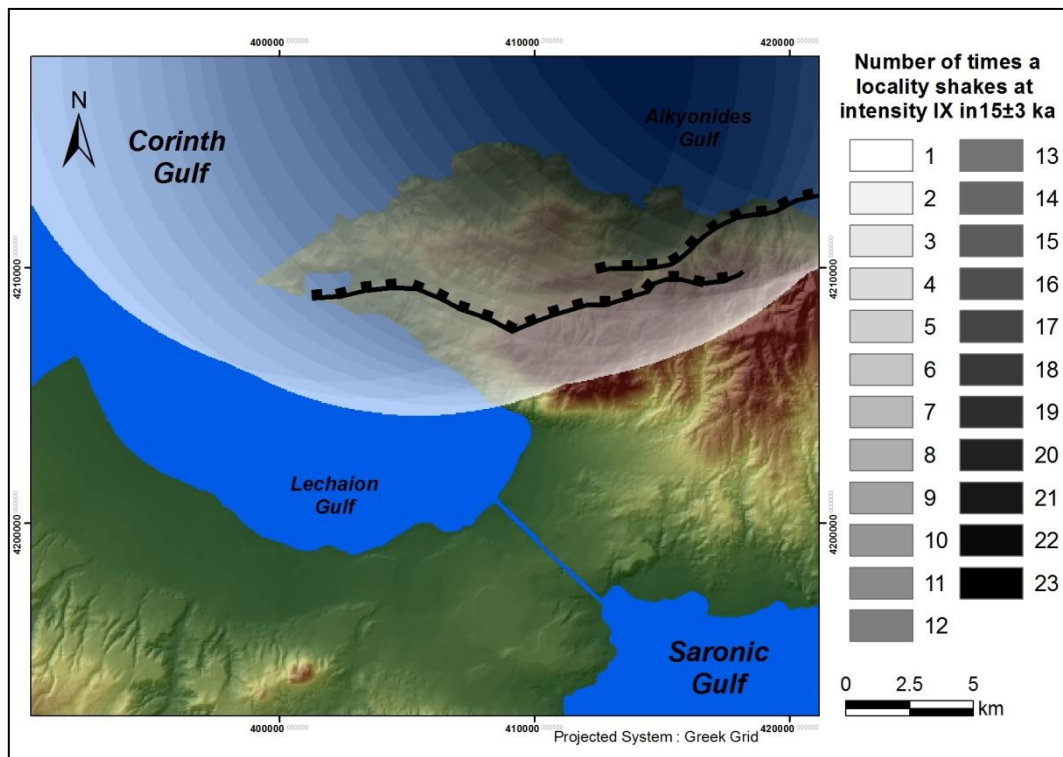


Fig. 6.21 Earthquake recurrence of intensity IX in South Alkyonides fault system. During the last 15.000 ± 3.000 years 23 hypothetical earthquakes are expected.

Geology bedrock mostly lessens the expected intensity. Geological formations that prevail in this area are limestones and ophiolites. In few sparse areas that intensity has been amplified, is mostly due to recent fluvial sediments (Figure 6.22). The central area of SAFS except that receives more energy to shake at intensity IX the last 15.000±3.000 years, maximum intensity X is expected there (Figure 6.23).

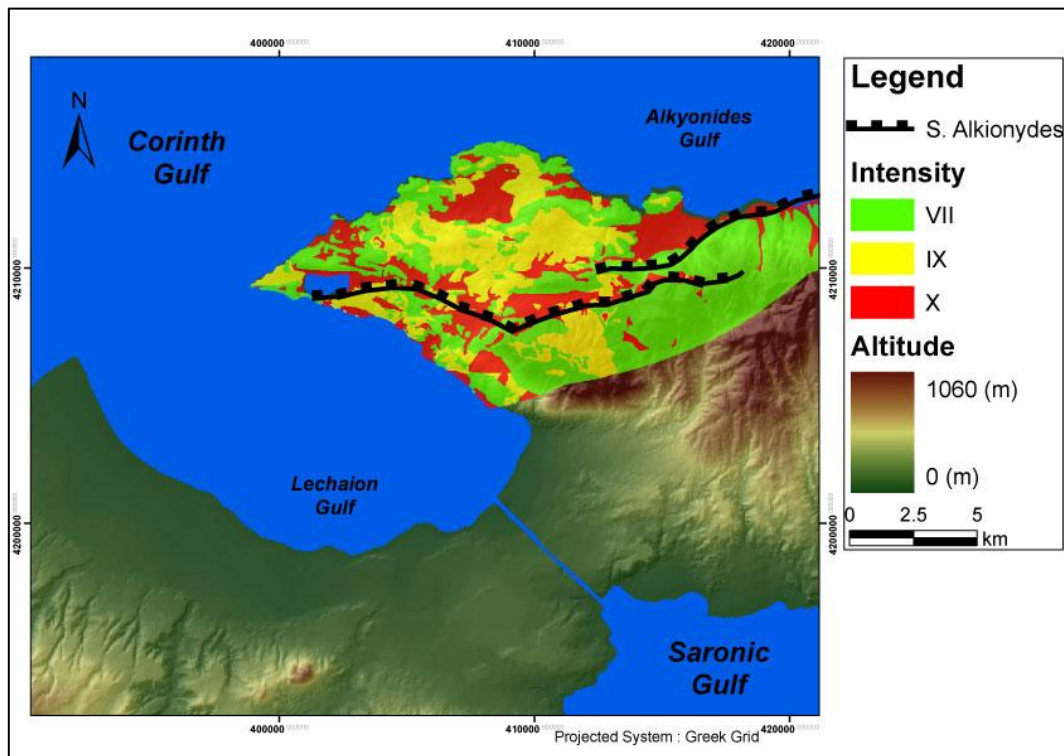


Fig. 6.22 The maximum expected intensity and how does it alters in relation to the bedrock geology.

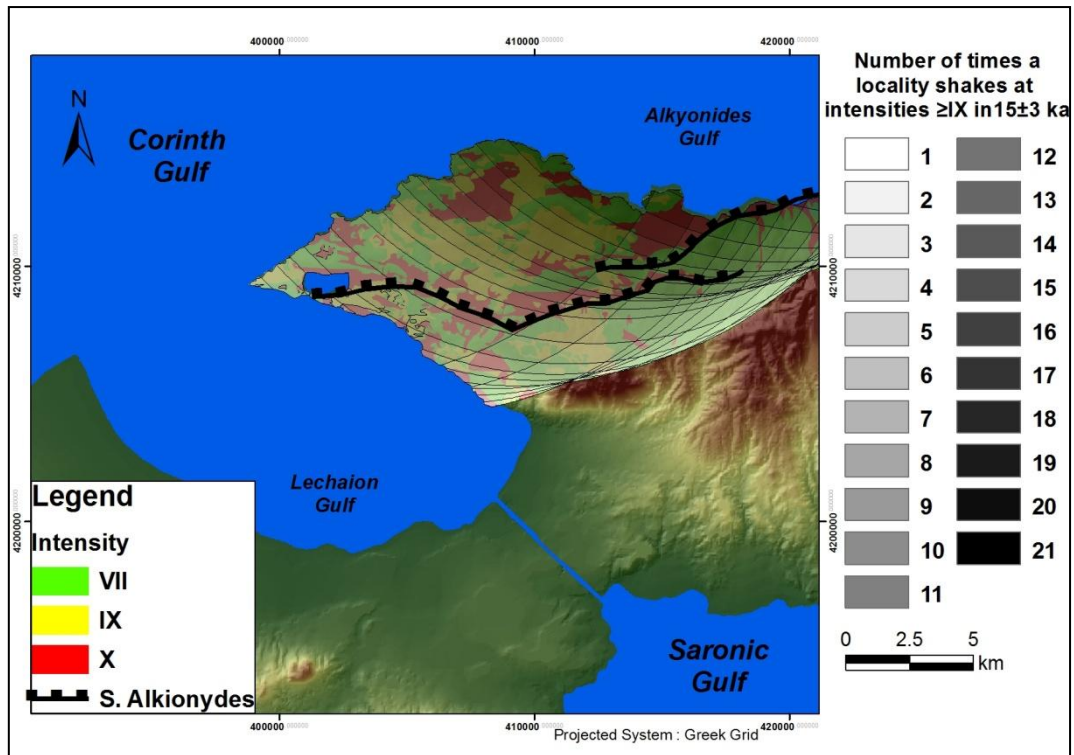


Fig. 6.23 Earthquake recurrence in relation to the geological amplification. The northern section of the Perachora peninsula receives higher energy.

6.4.5 The Agios Vasilios fault

The Agios Vasilios is a major E-W trending and north dipping fault that subsides the Corinth canal. Its onshore length is approximately 38 km and it might extend offshore (Lykousis et al. 2007, Zygouri et al. 2008, Roberts et al. 2011). It has created a topographic variation of approximately 1 km towards its center and it bounds recent Pleistocene sediments. This fault is active, but it is considered to have very low slip rate less than 0.5 mm/yr, since it exhibits no postglacial scarp. According to the empirical relationships of Wells & Coppersmith (1994), the maximum magnitude from this fault is 6.9 and according to Theodoulidis (1991), this fault can be responsible for an earthquake that has intensity IX with an estimated radius of 16 km. The Agios Vasilios fault can influence with intensity IX, the entire Corinth region, including

Lechaion and the westernmost section of the Saronic Gulf (Figure 6.24). In this figure though, geology amplification was not estimated..

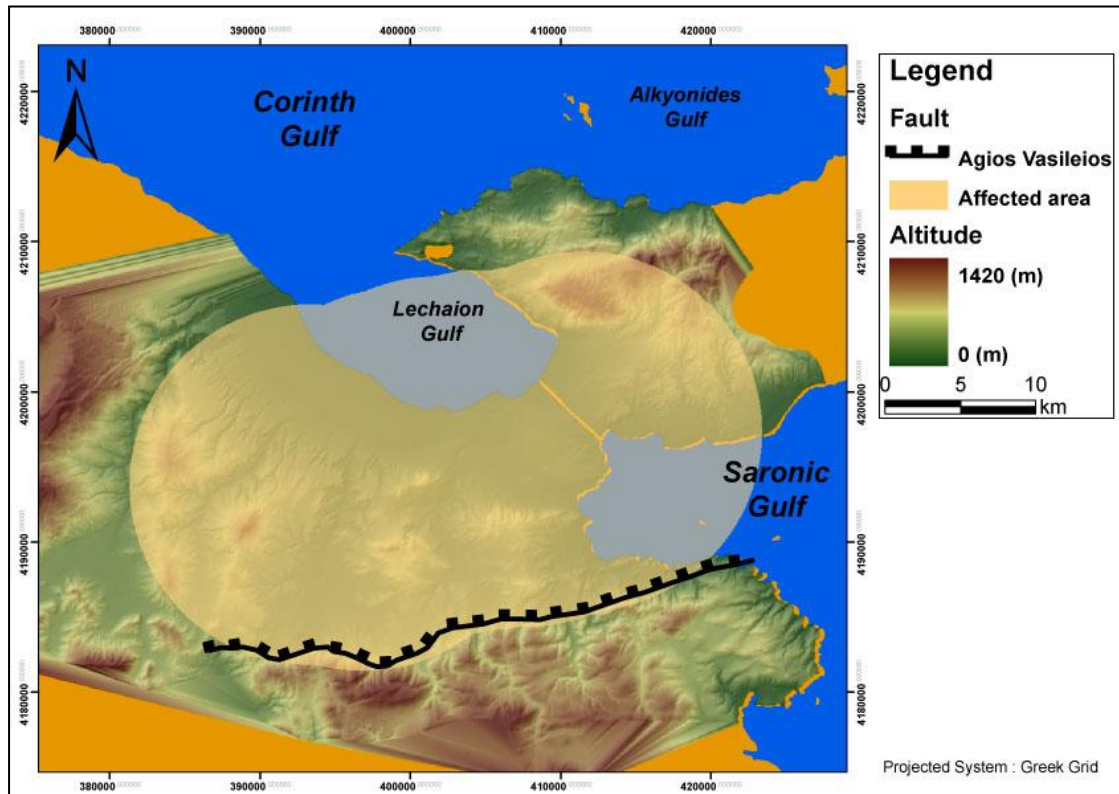


Fig. 6.24 The area that is expected to be influenced by the Agios Vassilios fault with intensity IX, considering an homogenous bedrock geology.

It is assumed that the entire surface slip for the 15.000 ± 3.000 years is the result of floating earthquakes of 6.5 magnitude, which can produce 1 m coseismic throw of 15 km rupture length according to Well & Coppersmith (1994). As a result, is estimated a number of expected earthquakes for this fault during this period. Figure 6.25 shows how many times each area receives enough energy to shake at intensity IX the last 15.000 ± 3.000 years. Agios Vassilios fault can shake the area 8 times during that period. Maximum earthquake recurrence is westwards the Corinth canal. Geological bedrock was not estimated.

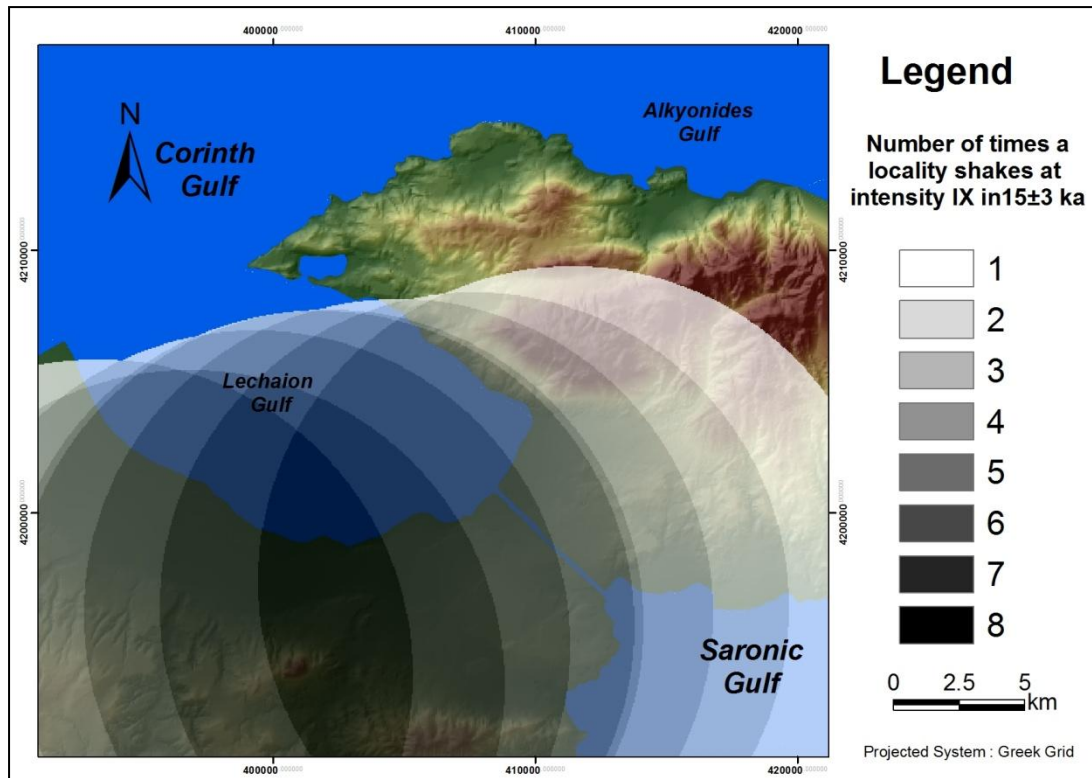


Fig. 6.25 Earthquake recurrence of intensity IX in Agios Vassilios fault. Since the last glaciation, 8 hypothetical earthquakes might have occurred.

The maximum expected intensity range from X till VIII (Figure 6.26). The north and south sections of the study area consist of marls, limestones and igneous formations and the maximum expected intensity is VIII. On the contrary, the central part of the area consists of semicoherent sediments that amplify the intensity (X). The south bay of Lechaion Gulf is regarded the locality with the highest hazard from this fault, having the highest frequency and expected intensity (Figure 6.27).

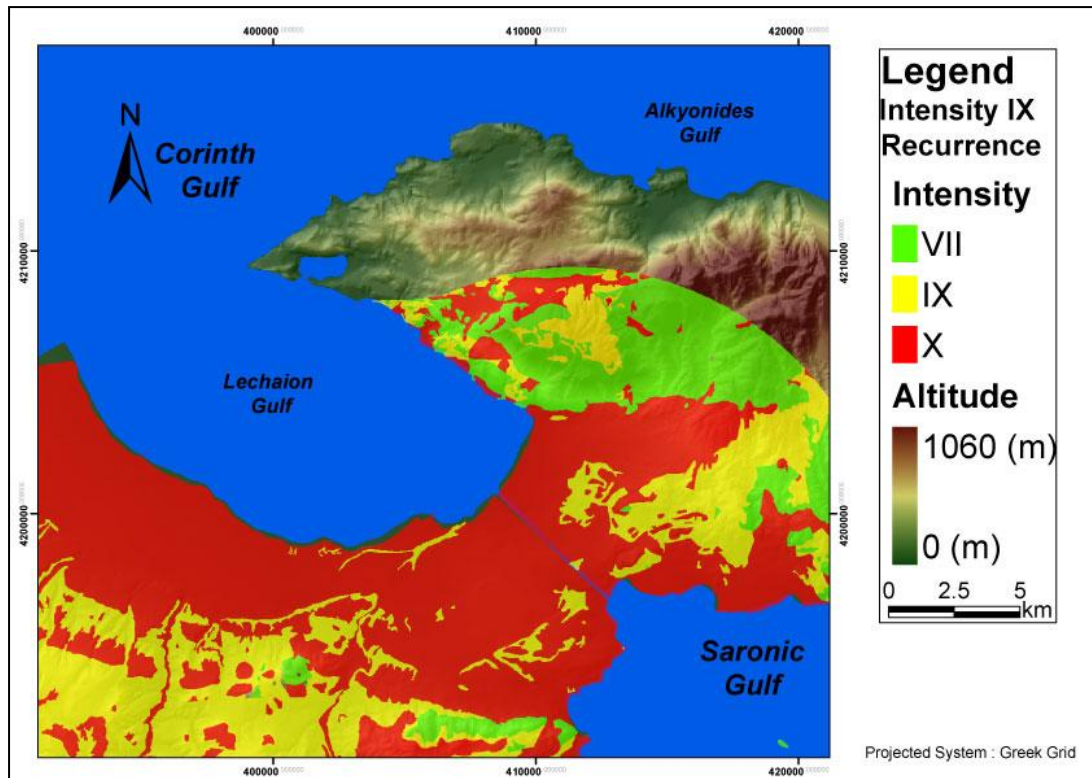


Fig. 6.26 The maximum expected intensity after considering the bedrock geology

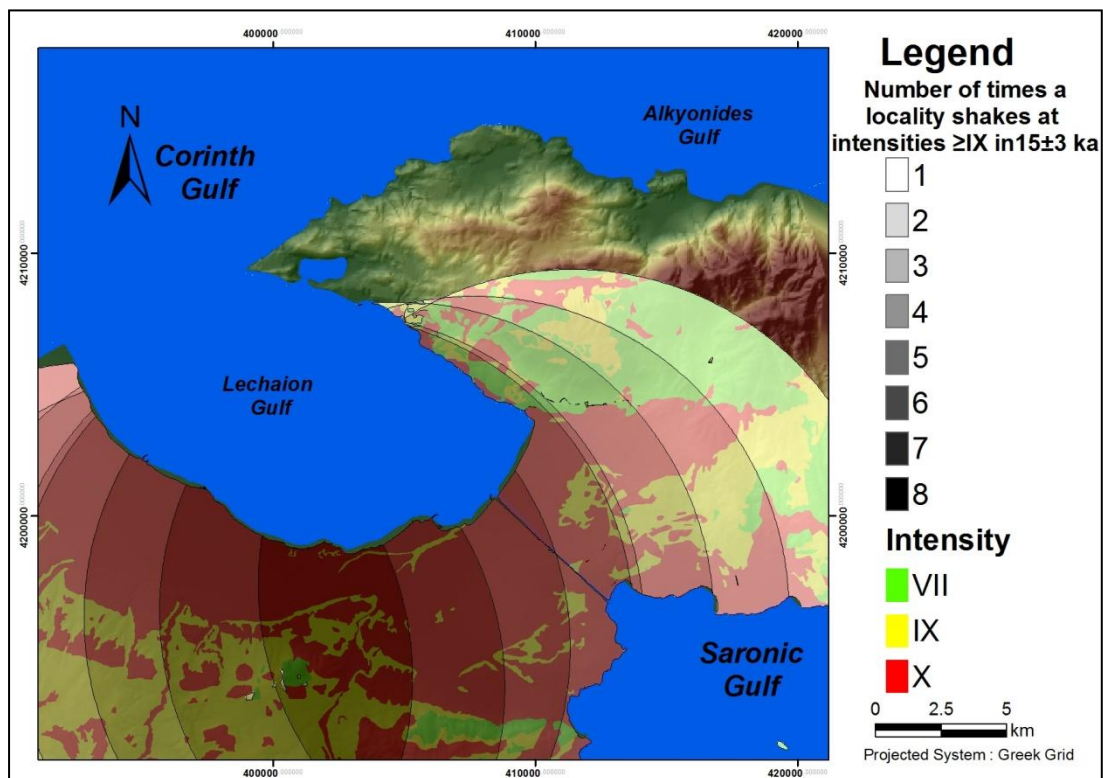


Fig. 6.27 Earthquake frequency in relation to the bedrock geology. The area westwards the Corinth canal, receives the highest frequency.

7. Discussion

7.1 *Effects from the studied fault*

The studied fault is active according to Collier et al. (1991), Papanikolaou et al. (2011). It has produced topographic variations, it bounds recent Pleistocene sediments and striations have been measured, facts that clearly indicate recent activity. Maximum throw rate is approximately 0.057 ± 0.013 mm/yr towards its center. This value though is showing that this is a very low slip rate fault. During the last 15.000 ± 3.000 years 7 hypothetical earthquakes might have occurred as it has been described before. Consequently, an earthquake of magnitude 5.7 due to this fault may occur every 2140 ± 430 years. This means that for an earthquake to occur now, the last time an earthquake was provoked from this fault should have been, more or less, 2140 years ago. The problem is that abundant earthquakes of such a magnitude occurred during this period. This is one of the most tectonically active region of Greece. Furthermore, several destructive earthquakes have occurred there, of magnitude higher than 6 Ms (Armijo et al. 1996, Tsapanos et al. 2011). The latter implies that an earthquake of magnitude 5.7 is considered to be a common phenomenon in this area therefore, it is unlikely such an earthquake to be correlated with this fault. Furthermore historical data are incomplete and possible for an earthquake of magnitude 5.7 Ms, not to have been recorded at all.

As far as the seismic threat is concerned, it is important to mention that this fault lies to the stress shadow of other faults such as the Loutraki, the Kechries and the South Alkyonides system fault. Each time that one of this fault ruptures, stress drops at the studied fault and strain accumulation is reduced (Cowie & Roberts 2001, Cowie

1998, Papanikolaou et al. 2005). As a result, there is a clock delay mechanism⁸. Finally, this fault will rupture less and less until it will be practically inactive.

There is evidence that during the 1981 earthquake, where South Alkyonides fault has been ruptured, this fault has passively ruptured (Figure 7.1). In several benchmarks the army had accurately calculated the exact difference at the altitude due to the earthquake. Mariolakos & Stiros (1987), noticed that the 1981 earthquake has uplifted the central part of the Corinth canal for almost 2 cm. The most interesting observation was that while the area at benchmark 79 was uplifted, near benchmark 77 was not only uplifted but subsided for 4 cm as well (Figure 7.1).

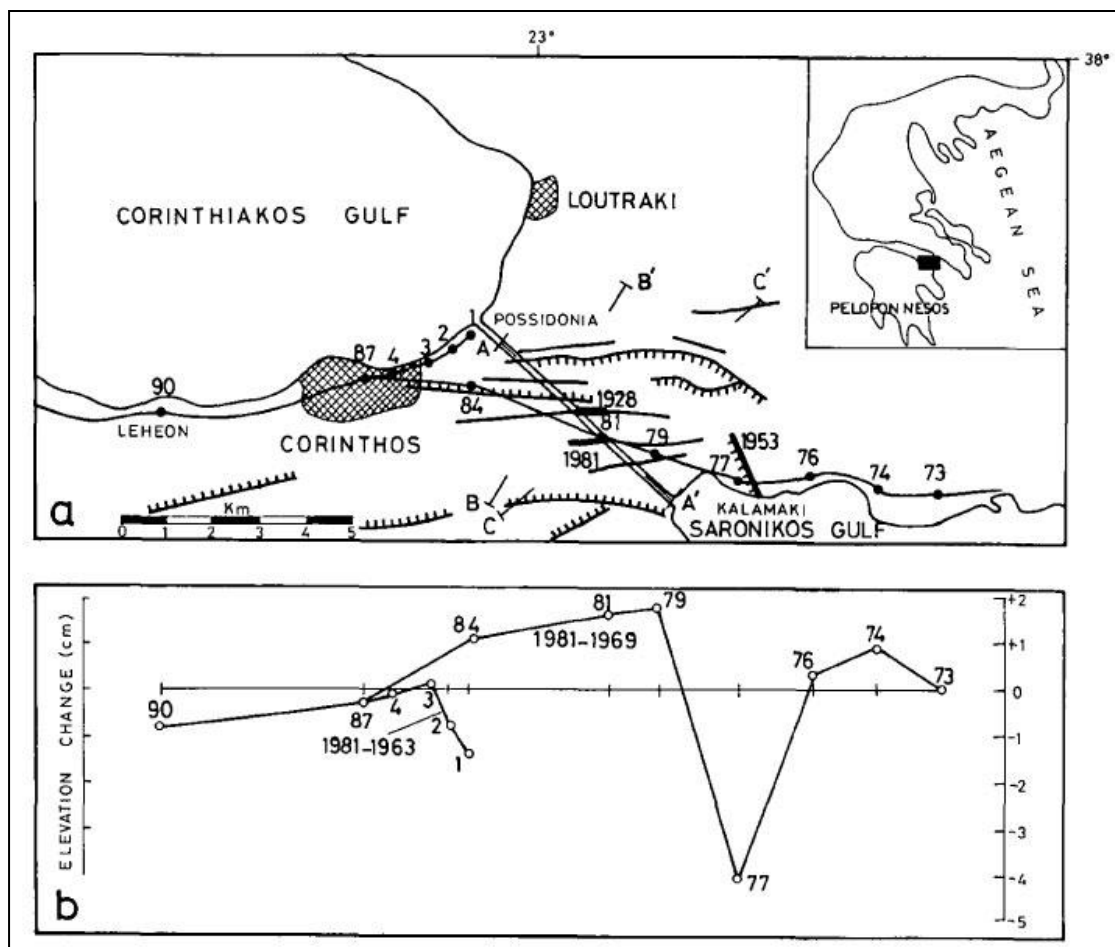


Fig. 7.1 Location map and leveling benchmarks where displacement was estimated (Mariolakos & Stiros 1987).

⁸ This process is like having an alarm clock that is set to ring at a specific time and every time that an earthquake occur the clock is rewind a few minutes before.

These researchers could not explain why did this happen, since they did not know the existence of the fault. This fault was unmapped until when Collier in 1991 has recognized this fault and defined it as an active fault. After 1981, an earthquake of such magnitude did not occur in this area. This fact strongly supports the idea that this fault has been activated during 1981 earthquake. Furthermore the fact that benchmarks 76, 74 and 73 have not subsided but have uplifted indicates that the fault did not rupture on its own but has passively moved. Otherwise, these benchmarks would have been subsided as well (Figure 7.2).

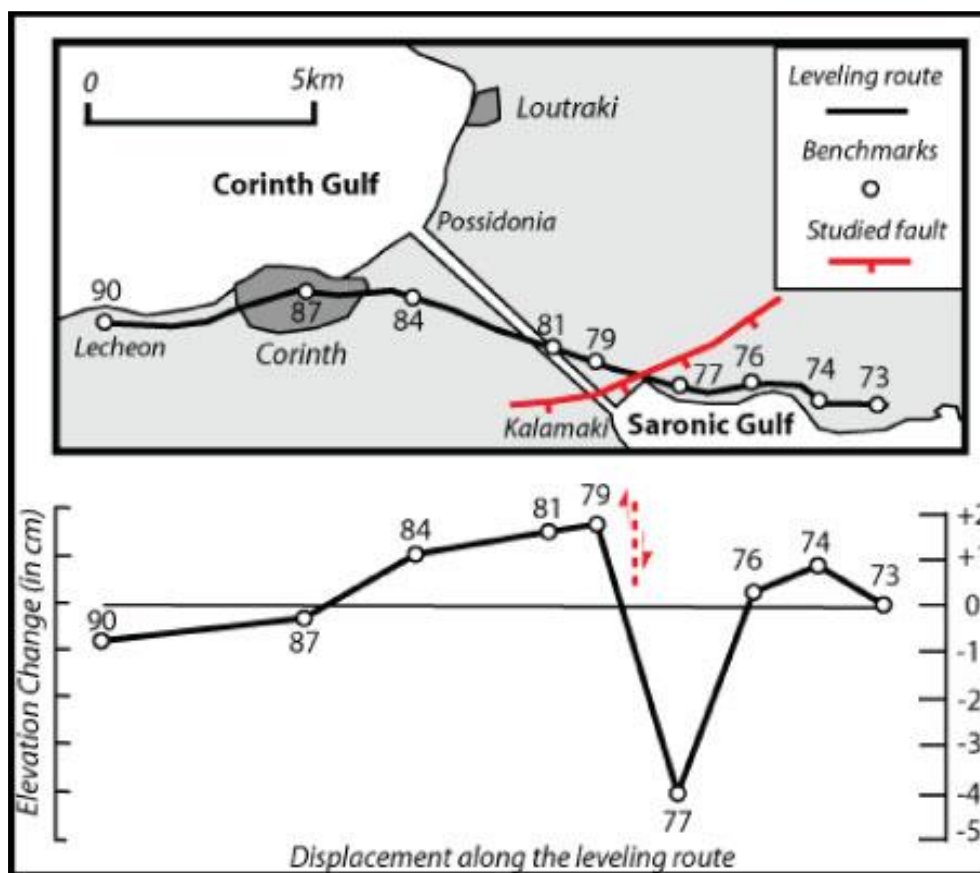


Fig. 7.2 Location map showing the leveling route, the benchmarks and their post-1981 displacements (redrawn from Mariolakos and Stiros 1987). Benchmark 77 the only one that subsided by 4cm, lies at the immediate hangingwall of the fault and benchmark 79 that was uplifted by 2cm on its immediate footwall, implying that our studied fault may have been passively ruptured during the 1981 earthquake.

As far as the seismic hazard assessment is concerned, this fault has limited length, approximately 5.5 km. Such a fault can barely produce surface ruptures if any. Maximum intensity considering geology's amplification is VIII. Furthermore since this fault has passively ruptured during the 1981 earthquake means that cumulative strain has partially relieved. Consequently this fault has few possibilities to give an earthquake.

In chapters 4 and 5 through micropaleontological analysis, several paleoenvironmental alterations have been identified within Bh-3 and Bh-7. Foraminiferal species can show, not the exact sea depth but fluctuations in salinity and through them relative assumptions could be made concerning depth alterations. This fault has undoubtedly influenced these alterations but at a much lesser degree than other factors. Cumulative throw is approximately 4 ± 2 m, as it was measured by a *Cladocora* corals colony. It was clarified that marine sediments are expected at 125.000, at 175.000 and at 200.000 years. Two scenarios were estimated, considering their age 125.000 or 200.000 years. If corals are from isotope stage 7, implies that offset between these corals at 125.000 years should have been approximately at 2 ± 2 m. Such differences in depth can barely affect the paleoenvironment. Shallow marine environment from instance, is referred to a depth that fluctuates from several meters to several dozens of meters. Even though, for the isotope stage 5, 125.000 years ago, implications about the paleoenvironment can be made (see subchapter 7.3).

7.2 Seismic hazard of Corinth canal

The Loutraki, Kechries, South Alkyonides and Agios Vasilios faults that have been examined before are considered to be the four major seismic sources that can pose a threat to the Corinth canal and the nearby region (Figure 7.3). All these faults can shake this area with earthquakes of magnitude at least 6.5 Ms. Earthquake recurrence differentiates though, the energy that an area receives. The central part of Isthmus receives 23 times energy to shake at intensities IX during the last 15.000 ± 3.000 years. The latter implies that the canal is unsafe as far as concern seismic hazard assessment. The Loutraki area receives 29 times enough energy to shake at intensities IX during

the same period. The area that is less safe according to figure 7.3 is the Perachora peninsula. Near to Perachora village, the area receives 34 times enough energy to shake at intensities IX during the same period, while near to Bambakies fan (where Pantosti had estimated the throw rate from trenching for South Alkyonides system fault), 29 times. This fact is logical considering that this is the central segment of the most active fault in the area. However, other offshore faults, within the Alkyonides Gulf have not been estimated. Earthquake recurrence would be higher considering these faults' effect.

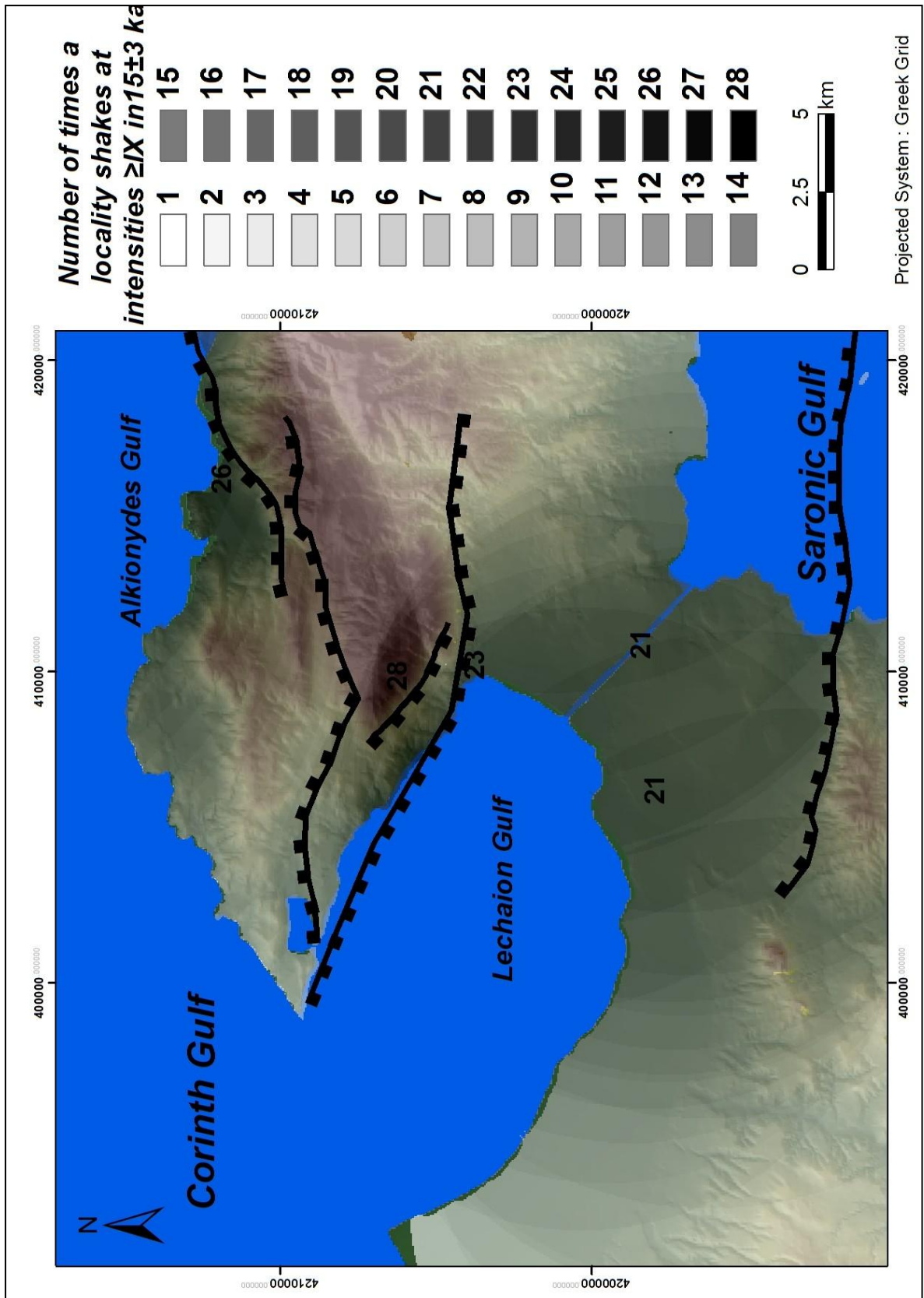


Fig. 7.3 Earthquake recurrence to Corinth canal and Perachora peninsula, taking under consideration the SAFS, the Loutraki, the Kechries and the Agios Vasilios faults

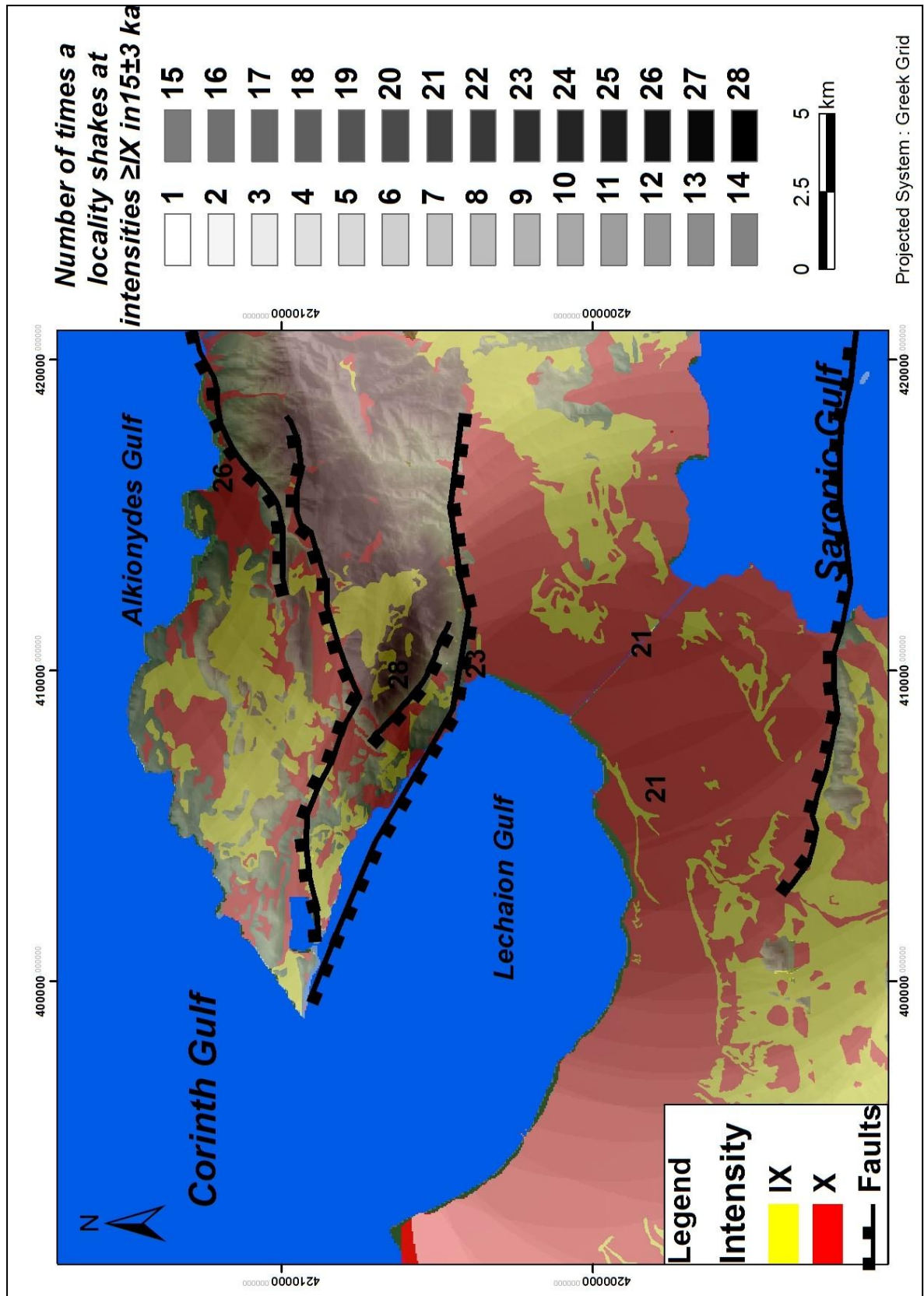


Fig. 7.4 Combined earthquake recurrence from the three major faults that pose a threat for the Isthmus canal, correlated with geological formations.

Towards the Corinth Isthmus and westwards from it, maximum intensity X is expected. Southwards the canal, expected intensity due to marls and limestones formations is less, IX or VIII. The same applies for the north section of the area, to Perachora peninsula. Few sparse areas where intensity is amplified, is due to alluvial formations deposited mostly by the drainage system (Figure 7.4).

Map in figure 7.3 which area an earthquake affects, not the probability for an earthquake to occur. In order to determine that paleoseismological data for the area are necessary. In this case, apart from South Alkyonides fault system that has been studied in detail, few recorded data exist. Several historical earthquakes count on their slip-rates that have been recorded cannot be correlated satisfyingly with these faults, but only implications can be made.

During the last 15.000 ± 3.000 for each fault have been calculated several hypothetical epicenters. Based on that an earthquake event is expected every 652 ± 130 for the South Alkyonides fault system, every 1500 ± 300 years for the Loutraki fault, 2500 ± 500 years for the Kechries fault and 1875 ± 375 years for the Agios Vassilios fault. Several historical earthquakes have been recorded to the easternmost section of Corinth gulf where the most known are at 77, 543, 1756, 1775, 1858, 1928, 1930 and at 1981 (Armijo et al. 1996, Rontoyanni et al, 2008, Maroukian et al. 2008, Tsapanos et al. 2011, Papanastasiou et al. 1994, Roberts et al. 2011, Gaki-Papanastasiou et al. 1996).

The 1858 (hypothetical magnitude 6.5) and 1928 (magnitude 6.3) earthquakes, are associated with the Kechries fault (Tsapanos et al. 2011, Papanikolaou & Roberts 2011), where the 1981 earthquake is well studied and has been attributed to Schinos-Pisia fault. Agios Vassilios is associated with an historical event at 1756⁹ and another possible at 400 AD (Papanikolaou et al. 2011). This fact renders an imminent earthquake from these faults less possible. On the other hand, according to Roberts & Papanikolaou 2011 no historical earthquake can be associated to the Loutraki fault. This fact renders the Loutraki fault as the biggest threat for the canal. As it has been described in subchapter 7.1 though, cumulative strain was partially relieved after the

⁹ This event's magnitude is estimated approximately at 7.0 Ms

1981 earthquake. Loutraki fault lies to the footwall of Alkyonides fault, which means that it is in its stress shadow. It is possible that after 1981, Loutraki might delay to generate an earthquake. This fault threatens mostly the Corinth canal and the city of Loutraki that are located at the immediate hangingwall and towards its center.

The fact that the Kechries and the Kalamaki fault have lower slip rate than the South Alkyonides fault system renders them less hazardous for the area. However, these faults still remain a threat for the area. During the 1981 shake sequence Kaparelli fault ruptured, even though it was considered to be inactive for approximately 10,000 years (Turner et al. 2010). Another fault that was considered to be inactive, was Parnitha's fault that ruptured at 1999. This fault has many similarities with the studied one, since both of them can barely create surface ruptures and are very low slip rate faults.

The Corinth canal is an area that several landslides have occurred. According to Anagnostopoulos et al. 1990, from 1987 till the Second World War 14 major landslides happened and afterwards, several minor. Slopes have steep inclination, approximately 75° , which render the slopes hazardous for another landslide to occur. A seismic event can trigger such an event. Furthermore, an earthquake caused by a major fault such as Loutraki, can cause surface ruptures to other minor faults¹⁰. Moreover, it must be considered that every fault may passively rupture during an earthquake.

Considering all the above data, it is clear that the Corinth canal is prone and vulnerable to seismic hazards despite the fact that no major active fault crosses the area except from the Kalamaki fault. The Kalamaki fault is considered a secondary structure. Earthquake recurrence is 23 and expected intensity X, while surface ruptures and landslides can affect the canal as well. It is important to mention though that the national highway and railroad, intersect the canal and a landslide or surface ruptures caused by an earthquake, might destroy these infrastructures. The city of Corinth is located in an area that intensity X is expected and earthquake recurrence is 22. Furthermore, previous earthquakes have repeatedly destroyed the city and were reconstructed approximately at the same area. It is crucial that the city should be

¹⁰ For instance, the studied fault has passively ruptured during the 1981 earthquake.

protected, since it is the economical and administrative center of the region. The area that is under greater risk is Perachora village. This village was completely leveled during the 1981 earthquake sequence and has been reconstructed. Earthquake recurrence is 34, the highest in the study area and alluvial deposits can amplify the expected intensity up to X (figure 7.5).

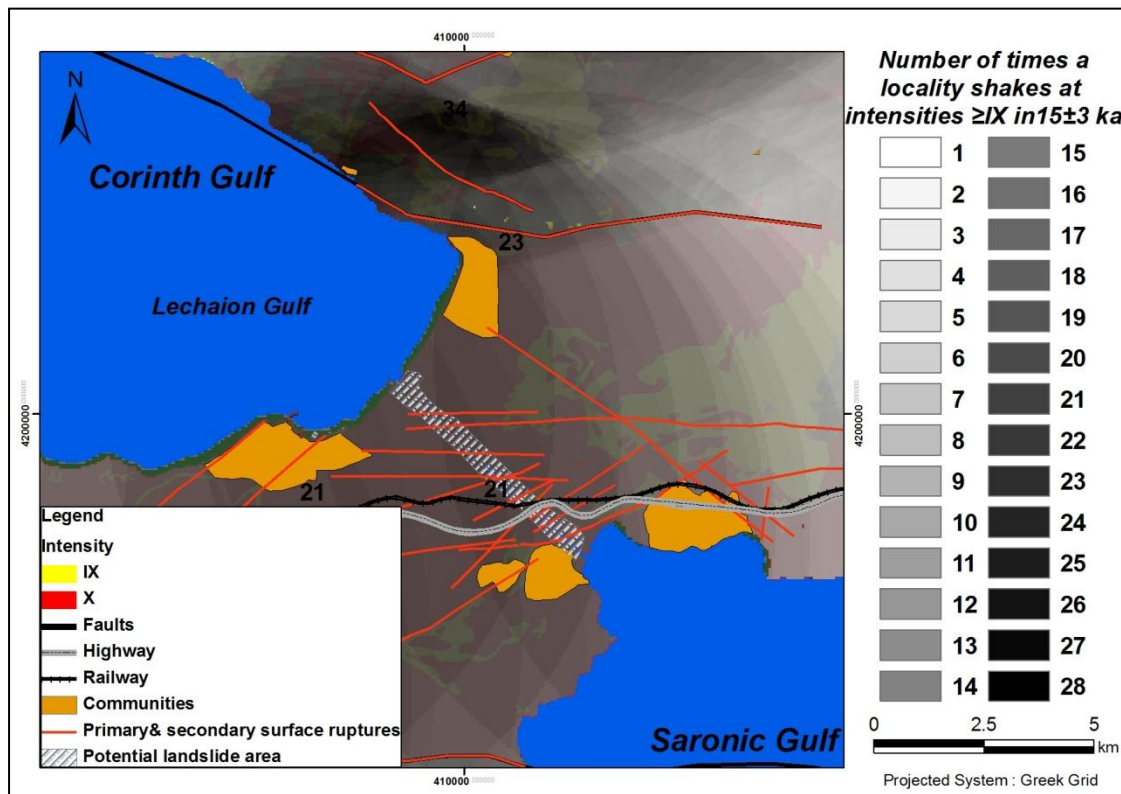


Fig. 7.5 Primary, secondary effects in Corinth basin and communities that are under greater threat.

Another interesting outcome from the map in figure 7.2, is the influence of South Alkyonides fault system to the study area. As it has been described before, the Corinth basin is constantly uplifted at least during the last 800.000 to 1.000.000 years. Three of the four major structures that have been examined (Kechries, Loutraki and Agios Vasilios faults), subside the area, while South Alkyonides fault system uplift the area. Despite the fact that more seismic sources can subside the canal, the Alkyonides fault

system is the most active fault of all, is activated more often than the others and therefore prevails against the others. Herein, it should be noticed that there is an regional uplift that is estimated by most researchers at 0.20 mm/yr.

7.3 Paleoenvironmental reconstruction

Several researchers have tried to reconstruct the paleoenvironment using an estimated uplift rate for the Corinth Gulf and sea level fluctuations during the Upper Pleistocene (Collier et al. 1991, Leeder et al. 2002, Roberts et al. 2009). It is certain that several times during this period sea level was much lower than the present day, while others it was slightly higher. It is also believed that Corinth Gulf was isolated from the Aegean Sea and was a lake during the glacioeustatic sea level lowstands (Roberts et al. 2009). Corinth gulf has two channels that can communicate with the sea. The one is the Rio straits and the other one is the Isthmus of Corinth. The Gulf could be a lake if both of these channels were above sea level. According to Roberts et al. (2009), at 140, 185 and at 275 lowstand Corinth Gulf might was Corinth lake. According to the same author though at 125.000 years Corinth canal was below sea level and the Gulf communicated with the Saronic. In order for this to happen, he implied that uplift rate of the Isthmus have to be at least at 0.6 mm/yr during the last 125.000 years because the SAFS speeded up. This does not correspond, though with previous researchers.

During the isotope stage 7, according to the previous researcher, Corinth could function as a channel. This hypothesis corresponds with Collier et al. (1991), who had also reconstructed the paleoenvironment approximately 200.000 years ago. Collier et al. (1991), used observations concerning transverse and linear dunes in Corinth basin and dated corals in order to attribute the paleogeography. Finally, mapped geological formations also support the hypothesis that during that period, this area was subsided. Marine sediments that construct Corinth basin, are considered to be from 350.000 till 125.000 years (Figure 7.6). This fact enhances the hypothesis that if there was a channel connecting Corinth with Saronic Gulf that would be in the area where the Canal is located now, directing to the south.

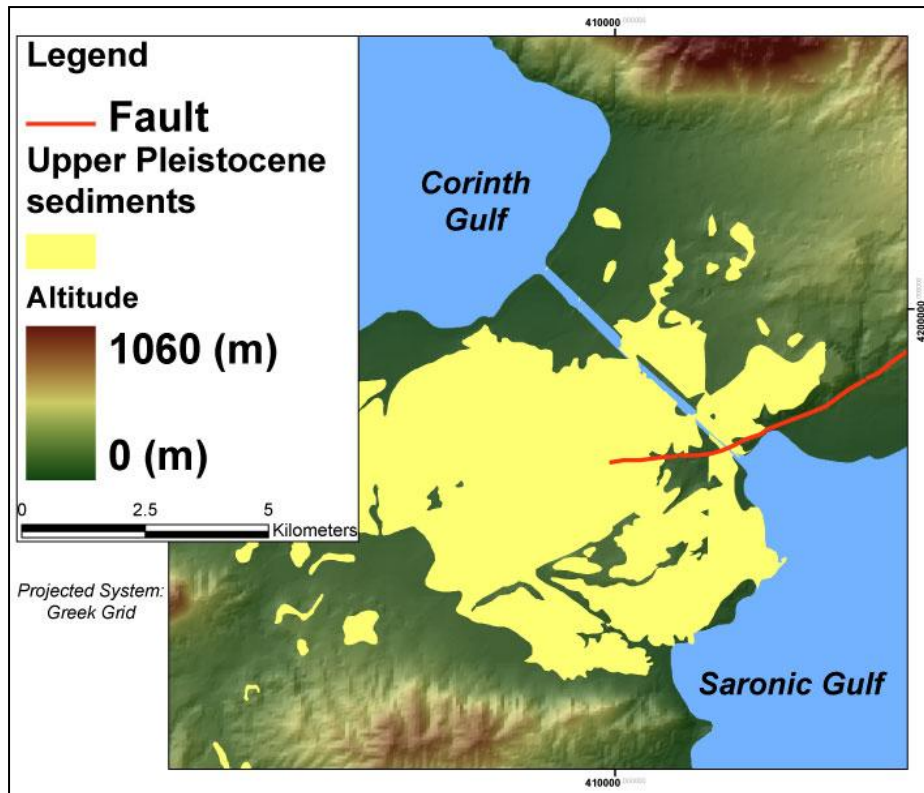


Fig. 7.6 Marine sediments in Corinth basin dated from the Upper Pleistocene

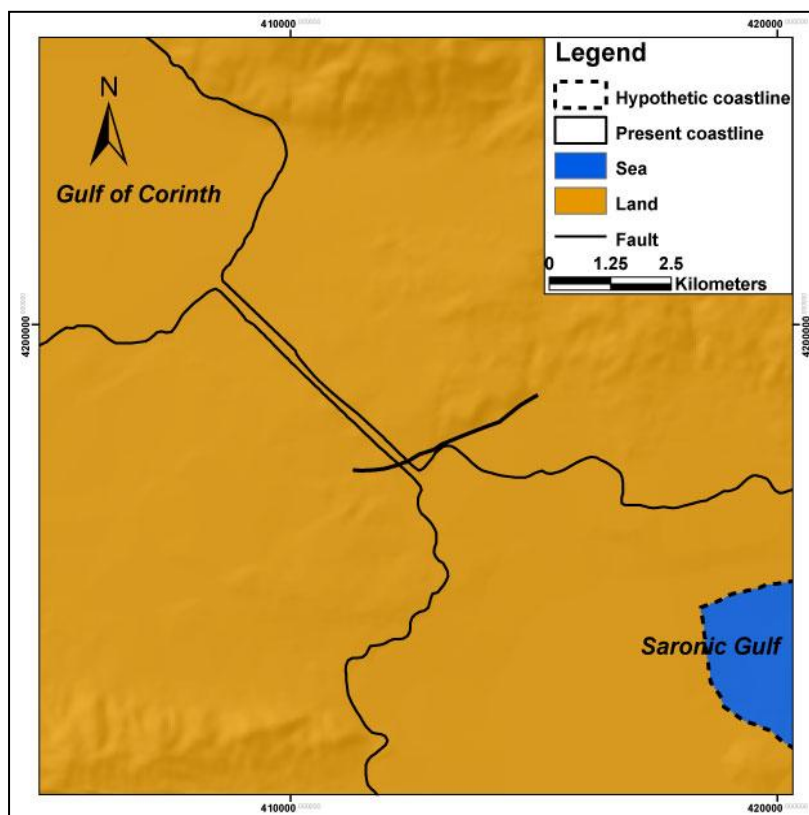


Fig. 7.7 Expected paleogeography of Corinth 18.000 years ago.

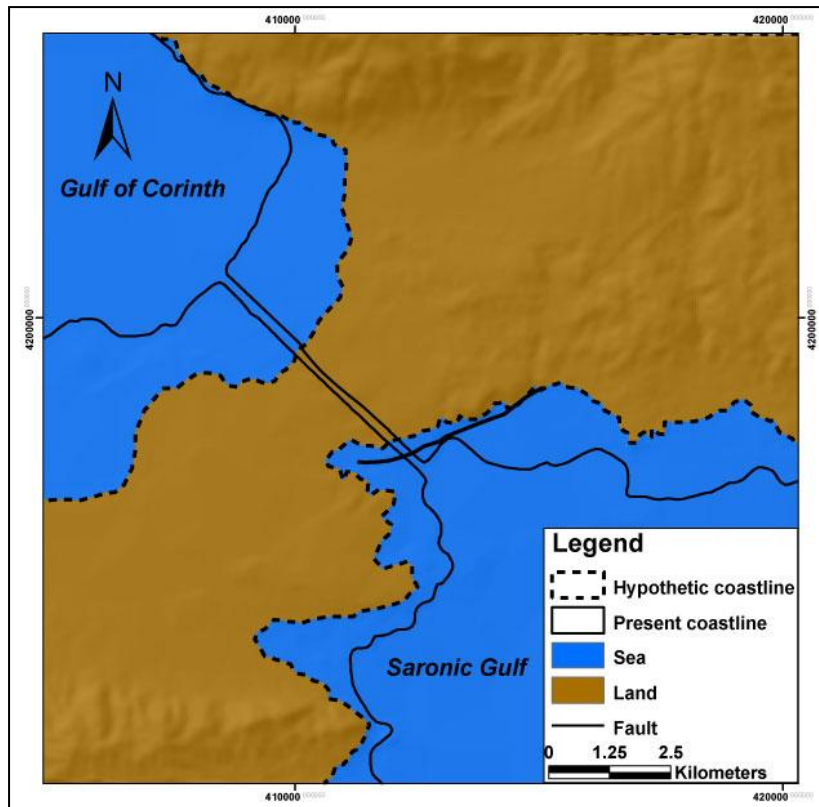


Fig. 7.8 Expected paleogeography of Corinth 125.000 years ago.

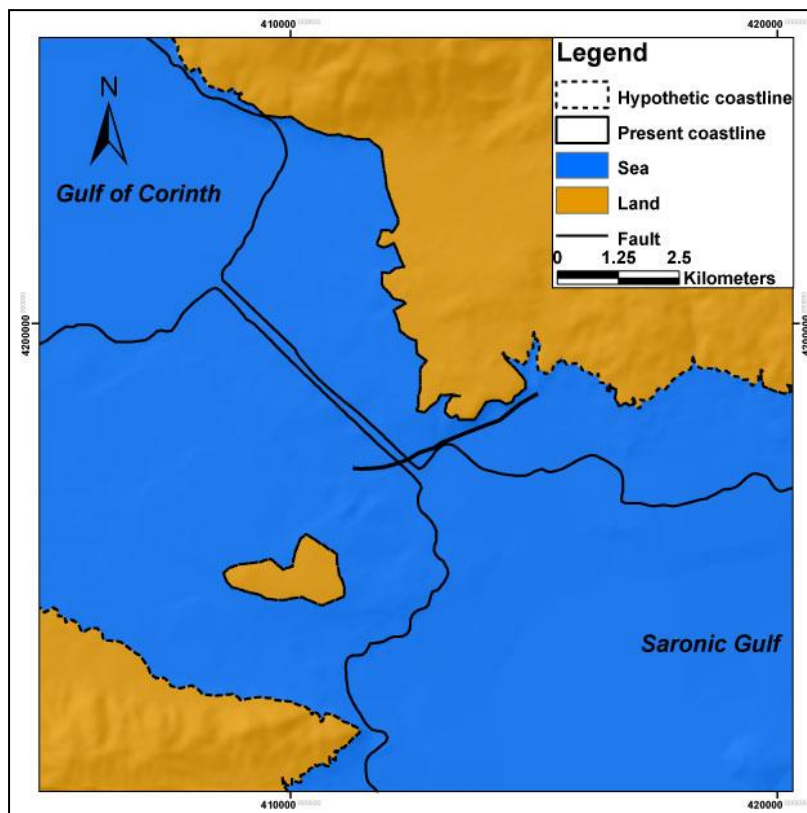


Fig. 7.9 Expected paleogeography of Corinth 200.000 years ago.

According to Siddall et al. (2004), Thompson et al. (2006), 18.000 years ago, sea level was approximately 125 m below than today. The uplift rate is 0.3 mm/yr towards the centre of Corinth canal and approximately 0.44 mm/yr 2 km southern of it (Collier et al. 1991, 1992). Consequently, coastline was 120 m below than today. Corinth basin was not a narrow isthmus, but a wider area that separated, the Corinth Lake from Saronic gulf (Figure 7.7). During the isotope stage 5e 125.000 years ago, sea level was approximately 6 ± 12 m above today. According to these uplift rates, the entire area was subsided 40 to 60 m compared with present altitude. Consequently Corinth was an isthmus where the coastline formed an isthmus, but narrower than it is today (Figure 7.8). Maximum altitude in Corinth basin should have been 15 m. Considering that spatial resolution of the map is 20m and uncertainties Siddall et al. (2004) has, it is possible that Roberts et al. (2009), be correct. Even though it is debatable if these Gulfs could communicate.

On the contrary, during the isotope stage 7, therefore approximately 200.000 ± 20.000 years, it is possible for these gulfs that could be as one (Figure 7.9). Sea level was several meters below the present one. According to the uplift rates the area was subsided 60 to 70 m. Coastline would not formed an isthmus, but a strait. From isotope stage 7 and backwards, it is highly possible that there should be a connection between both gulfs, during every glacioeustatic sea level highstand.

Paleomorphology of the area is predominately influenced from the global glacioeustatic sea level changes and then by the rate of tectonic uplift. The activation of a single fault can influence the paleomorphology but in a lesser degree and for short period of time. Kalamaki fault has a minor effect, despite that it is the larger fault in the Canal and it has a minor influence on the paleogeography. It has a 4 ± 2 m offset, implying that the uplift caused by its activity in the center of the Isthmus will not exceed 2-3 m.

8. Conclusions

It is not easy to determine slip and throw rate of a fault. It is significant though to find the rate in order to estimate how active a fault is. In this thesis the requested was to determine slip rate of a fault that is considered to be the most active fault that intersects the Corinth canal. This fault has created a topographic variation of 150 m towards its center (Collier et al. 1991, Papanikolaou et al. 2011), but its initiation age is unknown. Only after that borehole data were used, relative values could be estimated. Through lithostratigraphic and micropaleontological analysis it was possible to estimate the throw and slip rate. Due to uncertainties though, Two different scenarios were considered, therefore two different throw rates were estimated. According to the first scenario throw rate is 0.041 mm/yr, while according to the second scenario throw rate is at 0.067 mm/yr. Consequently, throw rate of the fault is estimated at 0.057 ± 0.015 mm/yr. Due to the fact that Kalamaki is a very low slip-rate fault, uncertainties at the estimated throw rate are insignificant. Foraminiferal species were deployed for identifying the paleoenvironment and through this, horizons within the boreholes were correlated. These horizons were correlated with late Pleistocene oxygen-isotope stages of sea-level highstands and consequently, with global sea-level fluctuations. Throw rate has been estimated there at 0.020 mm/yr during the last 200.000 ± 10.000 yr but the segment of the fault where the boreholes were recovered is at its tip. Towards its center a total offset of 8.4 m has been estimated for the same period, a fact that gives a maximum throw rate at 0.041 mm/yr.

Throw rate and geometrical features of a fault, were used for estimating earthquake recurrence, expected magnitude and intensity. This procedure was repeated not only for Kalamaki fault, but Loutraki, Kechries, South Alkyonides fault system and Agios Vassileios fault. Despite the fact that South Alkyonides system is the most active of them all, but Loutraki fault is the one that threatens Corinth Isthmus the most, since the isthmus is located at the immediate hangingwall and towards its center. Several Hazard maps were compiled for each fault showing earthquake recurrence and maximum expected intensity. A final map that combines threat posed by All these fault was made showing which area is under greater threat. Moreover, considering

the uplift rate of the area and the sea level curve, paleogeographical evolution of the Corinth basin was reconstructed for the last 200.000 years. 18.000 years ago Corinth was not an Isthmus but a wide area. At 125.000 years, isthmus was a narrower than the present one. At 200.000 years or even earlier the Corinth Isthmus was a strait and Saronic Gulf could communicate with Corinth.

9. References

- Anagnostopoulos, A.,G., Kalteziotis, N., Tsiambaos, C.,K., (1991). Geotechnical properties of the Corinth Canal marls, *Geotechnical and Geological Engineering*, 9, 1-26.
- Armijo, R., Meyer, B., King, G.C.P., Rigo. A., Papanastassiou, D., (1996). Quaternary evolution of the Corinth Rift and its implications for the Late Cenozoic evolution of the Aegean, *Geophys. J. Int.*, 126, 11 –53,
- Billiris, H., et al. (1991). Geodetic determination of tectonic deformation in central Greece from 1900 to 1988. *Nature*, 350, 124– 129, doi:10.1038/350124a0.
- Bornovas, J., Lalechos, N. and Filipakis, N. (1972). 1:50.000 scale geological map, Sheet “Korinthos”. Institute of Geology and Mineral Exploration
- Briole, P., A. Rigo, H. Lyon-Caen, J. C. Ruegg, K. Papazissi, C. Mitsakaki, A. Balodimou, G. Veis, D. Hatzfeld, and A. Deschamps,(200). Active deformation of the Corinth rift, Greece: Results from repeated Global Positioning System surveys between 1990 and 1995, *J. Geophys. Res., Solid Earth*, 21, 25,605– 25,625
- Collier, R. E. L., and C. J. Dart (1991). Neogene to Quaternary rifting, sedimentation and uplift in the Corinth Basin, Greece, *J. Geol. Soc.*, 148, 1049– 1065, doi:10.1144/gsjgs.148.6.1049.
- Collier, R. E. L., and J. Thompson (1991). Transverse and linear dunes in an upper Pleistocene marine sequence, Corinth Basin, Greece, *Sedimentology* 38, 1021– 1040.
- Collier, R.E.L., Leeder, R.M., Rowe, P. and Atkinson, T. (1992). Rates of tectonic uplift in the Corinth and Megara basins, Central Greece, *Tectonics*, 1159-1167.
- Collier, R.E.Ll., D. Pantosti, G.D'Addezio, P. M. De Martini, E. Masana, and D. Sakellariou (1998). Paleoseismicity of the 1981 Corinth earthquake fault: Seismic contribution to extensional strain in central Greece and implications for seismic hazard. *J. Geophys. Res.*, 103, 30001-30019.

Cooper, F. J., G. P. Roberts, and C. J. Underwood (2007). A comparison of 10^3 – 10^5 year uplift rates on the South Alkyonides Fault, central Greece: Holocene climate stability and the formation of coastal notches, *Geophys. Res. Lett.*, 34, L14310, doi:10.1029/2007GL030673.

Dia, A. N., A. S. Cohen, R. K. O’Nions, and J. A. Jackson (1997). Rates of uplift investigated through ^{230}Th dating in the Gulf of Corinth (Greece), *Chem. Geol.*, 138, 171–184, doi:10.1016/S0009-2541(97)00010-7.

Evelpidou, N., Pavlopoulos, K., Vassilopoulos, A., Triantaphyllou, M., Vouvalidis, K., Syrides, G., (2010). Yria (western Naxos island, Greece): Sea level changes in Upper Holocene and paleogeographical reconstruction, *Geodinamica Acta* 23/5-6, 233-240.

Ferranti, L., Pagliarulo, R., Antonioli, F., Randisi, A., (2011). “Punishment for the Sinner”: Holocene episodic subsidence and steady tectonic motion at ancient Sybaris (Calabria, southern Italy), *Quaternary International* 232, 56-70.

Freyberg, V. (1973). *Geologie des Isthmus von Korinth*, Erlangen Geologische Abhandlungen, Heft 95, Junge und Sohn, Universitats Buchdruckerei Erlangen, 183pp.

Gaitanakis, P., Mettos, A., and Fytikas, M. (1985). 1:50.000 scale geological map, Sheet “Sofikon”. Institute of Geology and Mineral Exploration.

Gaki-Papanastassiou, K., Papanastassiou, D., Maroukian, H., (1996). Geomorphic and Archaeological — Historical evidence for past earthquakes in Greece. *Annali di Geofisica* 39 (3), 589–601.

Goiran, J.P., Pavlopoulos, K., Fouache, E., Triantaphyllou, M.V., Etienne, R., (2011). Piraeus, the ancient island of Athens: Evidence from Holocene sediments and historical archives. *Geology*, doi:10.1130/G31818.1.

Gupta, A., and Scholz, C.H. (2000). A model of normal fault interaction based on observations and theory. *Journal of Structural Geology* 22, 865-879.

Jackson, J.A., J. Gagnepain, G. Houseman, G.C.P. King, P.Papadimitriou, C. Soufleris, and J. Virieux (1982). Seismicity, normal faulting, and the geomorphological development of the Gulf of Corinth (Greece): The Corinth

earthquakes of February and March 1981, *Earth Planetary Science Letters*, 57, 377-397.

Hayward, B.,W., Grenfell, H., R., Sabaa, A.,T., Carter, R., Cochran, U., Lipps, J., H., Shane, P.,R., Morley, M.,S., (2006). Micropaleontological evidence of large earthquakes in the past 7200 years in southern Hawke's Bay, New Zealand, *Quaternary Science Reviews* 25,1186-1207.

Houghton, S. L., G. P. Roberts, I. D. Papanikolaou, J. M. McArthur, and M. A. Gilmour (2003). New ²³⁴U-²³⁰Th coral dates from the western Gulf of Corinth: Implications for extensional tectonics, *Geophys. Res. Lett.*, 30(19), 2013, doi:10.1029/2003GL018112.

Hubert, A., G. C. P. King, R. Armijo, B. Meyer, and D. Papanastassiou (1996). Fault reactivation, stress interaction and rupture propagation in the 1981 Corinth earthquake sequence, *Earth Planet. Sci. Lett.*, 142, 573– 585, doi:10.1016/0012-821X(96)00108-2.

IGME: Institute of Geological and Mining Research, (1984). Geologic map — Perachora sheet, 1:50.000.

Trikolas, K., Koskeridou, E., Tsourou T., Drinia, C., Alexoudi-Leivaditi, A., (2004). Marine Pleistocene formations at the area of Aigialeia., (N. Peloponnesus), *Bulletin of the Geological Society of Greece* vol. XXXVI, Proceedings of the 10th International Congress, Thessaloniki,

Kouli, K., Triantaphyllou, M., Pavlopoulos, K., Tsourou, T., Karkanis, P., Dermizakis, M.D., (2009). Palynological investigation of the Holocene palaeoenvironmental changes in the coastal plain of Marathon (Attica, Greece). *Geobios* 42, 43–51.

Koukousioura O., Triantaphyllou M.V., Dimiza M.D., Pavlopoulos K., Syrides G., Vouvalidis K., (2011), Benthic foraminiferal evidence and paleoenvironmental evolution of Holocene coastal plains in the Aegean Sea (Greece), *Quaternary International*,doi:10.1016/j.quaint.2011.07.004

Krstic, N., Dermizakis, M.D., (1981). Pleistocene Fauna from a section in the channel of Corinth (Greece). *Ann. Geol. du Pays Hellen.* 30 (2): 473-499.

Leeder, M.R., Collier, R.E., Abdul Aziz, L.H., Trout, M., Ferentinos, G., Papatheodorou, G., Lyberis, E., 2002. Tectono-sedimentary processes along an active marine/lacustrine margin: alkyonides Gulf, E. Gulf of Corinth, Greece. *Basin Res.* 14, 25–41.

Leeder, M. R., L. C. McNeill, R. E. L. Collier, C. Portman, P. J. Rowe, J. E. Andrews, and R. L. Gawthorpe (2003), Corinth rift margin uplift: New evidence from Late Quaternary marine shorelines, *Geophys. Res. Lett.*, 30(12), 1611, doi:10.1029/2003GL017382.

Leeder, M.R., Mack, G.H., Brasier, A.T., Parrish, R.R., McIntosh, W.C., Andrews, J.E. & Duermeijer, C.E. 2008. Late-Pliocene timing of Corinth (Greece) rift-margin fault migration. *Earth and Planetary Science Letters*, 274, 132–141.

Lykousis, V., Sakellariou, D., Moretti, I., Kaberi, H., 2007. Late Quaternary basin evolution of the Gulf of Corinth: Sequence stratigraphy, sedimentation, fault–slip and subsidence rates. *Tectonophysics* 440, 29–51.

Marinos, P. and Tsiambaos, G. (2008). The Geotechnics of Corinth Canal: A review. *Bulletin of the Geological Society of Greece XXXXI/I*, 7-15.

Mariolakos, I., Papanikolaou, D., Symeonidis, N., Lekkas, S., Karotsieris, Z., & Sideris, Ch. (1982). The deformation of the area around the eastern Korinthian gulf, affected by the earthquakes of February-March 1981. *Proc. Inter. Symp. On the Hellenic Arc and Trench (H.E.A.T.)* 1, 400-420.

Mariolakos, I. and Stiros, S.C. (1987). Quaternary deformation of the Isthmus and Gulf of Corinth (Greece). *Geology* 15, 225-228.

Maroukian, H., Gaki-Papanastasiou, K., Karymbalis, E., Vouvalidis, K., Pavlopoulos, K., Papanastasiou, D., Albanakis, K., (2008), Morphotectonic control on drainage network evolution in the Perachora Peninsula, Greece, *Geomorphology* 102, 81-92.

Michetti, A.M., Esposito, E., Guerrieri, L., Porfido, S., Serval, L., Tatenossian, R., Vittori, E., Audemard, F., Azuma, T., Claque, J., Commerci, V., Gurpinar, A., McCalpin, J., Mohammadioun, B., Corner, N.A., Ota, Y., and Roghazin, E. (2007). Intensità scale ESI 2007. In Guerrieri L. and Vittori, E. (Eds): *Mem. Descr.*

Carta Geol. d' Italia 74, Servizio Geologico d' Italia-Dipartimento Difesa del Suolo, APAT, Rome Italy.

Morewood, N. C., and G. P. Roberts (1997), The geometry, kinematics and rates of deformation in a normal fault segment boundary, central Greece, *Geophys. Res. Lett.*, 24, 3081– 3084, doi:10.1029/97GL03100.

Morewood, N.C., Roberts, G.P., (1999). Lateral propagation of the surface trace of the South Alkyonides normal fault segment, central Greece: its impact on models of fault growth and displacement–length relationships. *J. Struct. Geol.* 21, 635–652.

Murata, A., Takemura, K., Miyata, T., Lin, A., (2001), Quaternary vertical offset and average slip rate of the Nojima Fault on Awaji Island, Japan, *The Island Arc* 10, 360-367.

Pantosti, D., R. Collier, G. D'Addezio, E. Masana, and D. Sakellariou (1996). Direct geological evidence for prior earthquakes on the 1981 Corinth fault (central Greece), *Geophys. Res. Lett.*, 23, 3795-3798.

Papanastassiou, D., Gaki-Papanastassiou, K. (1994). Geomorphological observations in the Kechries – Ancient Corinth region and correlation with seismological data. *Proc. of the 3rd Panellenic Geographical Congress* 2, 210-223.

Papanikolaou, D., Chronis, G., Lykousis, V., Pavlakis, P., Roussakis, G., and Syskakis, D. (1989). 1:100.000 scale, Offshore Neotectonic Map the Saronic Gulf. Earthquake Planning and Protection Organization, National Centre for Marine Research, University of Athens.

Papanikolaou, D., Logos, E., Lozios, S. and Sideris, Ch. (1996). 1:100.000 scale Neotectonic Map of Korinthos Sheet, Earthquake Planning and Protection Organization, Athens.

Papanikolaou, I. D., Roberts, G. P., and Michetti, A. M. (2005): Fault scarps and deformation rates in Lazio-Abruzzo, Central Italy: Comparison between geological fault slip-rate and GPS data, *Tectonophysics*, 408, 147–176.

Papanikolaou, I.D. and Roberts G.P., (2007). Geometry, kinematics and deformation rates along the active normal fault system in the Southern Apennines: implications for fault growth. *Journal of Structural Geology* 29, 166-188.

Papanikolaou I.D., Roberts, G., Deligiannakis, G., Sakellariou, A., Vassilakis, E., (2011). The Sparta fault, southern Greece : Tectonic geomorphology, seismic hazard mapping and conditional probabilities. *Earthquake Geology and Archaeology: Science, Society and Critical facilities. 2nd INQUAIGCP 567 International Workshop, Corinth (Greece)*, 178-181.

Papanikolaou I.D., Triantaphyllou, M., Pallikarakis A., Migiros, G. (2011). Active faulting towards the eastern tip of the Corinth Canal: Studied through surface observations, borehole data and paleoenvironmental interpretations. *Earthquake Geology and Archaeology: Science, Society and Critical facilities. 2nd INQUAIGCP 567 International Workshop, Corinth (Greece)*, 182-185.

Papantoniou, L., Rozos, D., Migiros, G. (2008). Engineering geological conditions and slope failures along the Corinth Canal. *Bull. Geol. Soc. Greece*, Vol. XXXVI/I, 17-24.

Papazachos, B.P. and Papazachou, C.B. (1997). *The earthquakes of Greece*. Ziti Editions, 304pp, Thessaloniki.

Pavlopoulos, K., Theodorakopoulou, K., Bassiakos, Y., Hayden, B., Tsourou, T., Triantaphyllou, M., Kouli, K., Vandarakis, D., (2007). Paleoenvironmental evolution of Istron (N.E. Crete), during the last 6000 years: depositional environment, climate and sea level changes. *Geodinamica Acta* 20 (4), 219e229.

Pavlopoulos, K., Triantaphyllou, M., Karkanias, P., Kouli, K., Syrides, G., Vouvalidis, K., Palyvos, N., Tsourou, T., (2010). Paleoenvironmental evolution and prehistoric human environment, in the embayment of Palamari (Skyros Island, Greece) during Middle-Late Holocene. *Quaternary International* 216, 41e53.

Roberts, G. P., (1996) Variation in fault-slip directions along active and segmented normal fault systems, *J. Struc. Geol.*, 18, 835– 845.

- Roberts, G. P., Cowie, P., Papanikolaou, I. & Michetti, A. M.(2004). Fault scaling relationships, deformation rates and seismic hazards: An example from the Lazio-Abruzzo Apennines, central Italy. *Journal of Structural Geology*, 26, 377–398.
- Roberts, G. P., S. L. Houghton, C. Underwood, I. Papanikolaou, P. A. Cowie, P. van Calsteren, T. Wigley, F. J. Cooper, and J. M. McArthur (2009). Localization of Quaternary slip rates in an active rift in 105 years: An example from central Greece constrained by ²³⁴U-²³⁰Th coral dates from uplifted paleoshorelines, *Journal of Geophysical Research*, 114, B10406, doi:10.1029/2008JB0058
- Roberts, G., Papanikolaou, I., Vott, A., Pantosti, D., Hadler, H., (2011). Field Trip Guide. *Earthquake Geology and Archaeology: Science, Society and Critical facilities*. 2nd INQUAIGCP 567 International Workshop, Corinth (Greece), 11-30, 40-41, 66-68.
- Rondoyanni Th., Marinos P., (2008). The Athens-Corinth highway and railway crossing a tectonically active area in Greece. *Bull. Eng. Geol. Environ*, 67, 259-266,
- Rondoyanni, Th., Livaditi, A. and Mettos, A. (2008). Eastern Corinthia: Structure and characteristics of an active geological environment. *Bulletin of the Geological Society of Greece XXXXI/I*, 35-42 (In Greek).
- Siddall, M., E. J. Rohling, A. Almogi-Labin, C. Hemleben, D. Meischner, Schmelzer, and D. A. Smeed (2003), Sea-level fluctuations during the last glacial cycle. *Nature* 423, 853 – 858.
- Theodorakopoulou, K., Pavlopoulos, K., Triantaphyllou, M., Kouli, K., Tsourou, T., Bassiakos, Y., Zacharias, N., Hayden, B., (2009). Geoarchaeological studies in the coastal area of Istron-Kalo Chorio (gulf of Mirabello- Eastern Crete): landscape evolution and paleoenvironmental reconstruction. *Zeitschrift für Geomorphologie* 53 (1), 55e70.
- Theodoulidis, N.P., (1991). Contribution to the study of strong motion in Greece. Ph.D. Thesis, University of Thessaloniki, 500pp.
- Thompson, W.G. & Goldstein, S.L. (2006). A radiometric calibration of the SPECMAP timescale. *Quaternary Science Reviews*, 25, 3207–3215.

Triantaphyllou, M.V., Pavlopoulos, K., Tsourou, Th. & Dermitzakis M.D., (2003). Brackish marsh benthic microfauna and paleoenvironmental changes during the last 6.000 years on the coastal plain of Marathon (SE Greece). *Rivista Italiana Paleontologia et Stratigrafia*, 109 (3), 539-547.

Triantaphyllou, M.V., Kouli K., Tsourou, T., Koukousioura, O., Pavlopoulos, K., Dermitzakis, M.D., (2010). Paleoenvironmental changes since 3000 BC in the coastal marsh of Vravron (Attica, SE Greece). *Quaternary International*, doi:10.1016/j.quaint.2009.08.019.

Turner, J. A., Leeder, M. R., Andrews, J. E., Rowe, P. J., Van Calsteren, P., Thomas, L. (2010). Testing rival tectonic uplift models for the Lechaion Gulf in the Gulf of Corinth. *Journal of the Geological Society of London*, 167, 1237-1250.

Wells, D.L., Coppersmith, K.J., (1994). New empirical relationships among magnitude, rupture length, rupture width and surface displacement. *Bulletin of the Seismological Society of America* 84, 974–1002.

Zygouri, V., Verroios, S., Kokkalas, S., Xypolias, P., Koukouvelas, I., and Papadopoulos, G. (2008). Growth of faults within the gulf of Corinth. *Bulletin of the Geological Society of Greece* XXXXI/I, 25- 33

List of figures

Fig. 1.1 The eastern end of Corinth Gulf (A), where the Corinth canal is (B) and the boreholes were drilled (C) _____	7
Fig. 3.1 View from Google Earth, where Kechries and the studied fault are shown. The area where boreholes were drilled is also shown (redrawn from Roberts et al. 2011) _____	22
Fig. 3.2 View of the main fault plane about 50m northwards the Canal. On this plane striations have been measured. This is a high angle normal fault dipping 65o towards the SSE. _____	23
Fig. 3.3 View of the fault about 650m southwards the Canal. Arrows point to the fault plane displayed in the photo towards the right. It trends 070o-250o and dips 70o towards the SSE. _____	24
Fig. 3.4 View of the secondary fault plane of the principal fault on the southern part of the Canal. It also created a landslide in the past. _____	24
Fig. 3.5 DEM of the area. _____	25
Fig. 3.6 Slope map of study area. The north section is much steeper than the central and south part. _____	26
Fig. 3.7 Simplified geology of study area. _____	29
Fig. 3.8 Active faults and lithological formations resistant to erosion are clearly associated with steep slopes. _____	30
Fig. 4.1 Lithostratigraphic view of borehole 3. Borehole was 70.00 m deep _____	33
Fig. 4.2 Lithostratigraphic view of borehole 7. Borehole was 56.00 m deep. _____	35
Fig. 4.3 Lithostratigraphic view of borehole 1. Borehole was 31.00 m deep. _____	36
Fig. 4.4 Lithostratigraphic view of borehole 2. Borehole was 50.00 m deep _____	37
Fig. 4.5 Lithostratigraphic view of borehole 4. Borehole was 30.50 m deep. _____	38
Fig. 4.6 Lithostratigraphic view of borehole 6. Borehole was 40.50 m deep. _____	39
Fig. 4.7 The exact location of each borehole. The distance between Bh-1 to Bh-4 is 580 meters and from Bh-6 to Bh-7 is 145 meters _____	41
Fig. 4.8 View of the stratigraphic columns of borehole 3 located on the immediate footwall and borehole 7 located on the immediate hangingwall of the studied fault. _____	42
Fig. 4.9 View of lithostratigraphic columns, located in the study area _____	43

Fig. 4.10 Foraminiferal assemblages calculated as percentage of the total foraminifera counted in borehole 3, grouped in 7 subcategories (Elphidium spp., miliolids, small- and large- sized Ammonia spp., Aubignina perlucida, Haynesina spp. and full marine species).	46
Fig. 4.11 Foraminiferal assemblages calculated as percentage of the total foraminifera counted in borehole 7, grouped in 7 subcategories (Elphidium, Miliolidae, small- and large- sized Ammonia, Aubignina, Haynesina and full marine species).	48
Fig. 4.12 Characteristic microfaunal species that have been identified under Leica microscope. (A) Elphidium excavatum. (B) Small- sized Ammonia tepida. (C) Elphidium crispum. (D) Lobatula lobatula. (E) Triloculina sp. (miliolid). (F) Large- sized Ammonia tepida. (G) Cyprideis spp. (outside of a right valve) and Aubignina perlucida (down left). (H) Cyprideis spp. (inside of a left valve).	49
Fig. 5.1 View of the depositional environment of Bh-3 located on the immediate footwall of the studied fault, in correlation with the foraminiferal assemblages.	53
Fig. 5.2 View of the depositional environment of Bh-7 located on the immediate hangingwall of the studied fault, in correlation with the foraminiferal assemblages.	54
Fig. 5.3 View of the depositional environment of borehole 3 located on the immediate footwall and borehole 7 located on the immediate hangingwall of the studied fault.	55
Fig. 5.4 View of the paleoenvironment of borehole 3 located on the immediate footwall and borehole 7 located on the immediate hangingwall of the suited fault, in correlation with global sea level high- and lowstand.	57
Fig. 5.5 Global sea level curve from Sidall et al. (2004) in correlation with the expected uplift rate, as has been counted by Collier et al. (1992) and Dia et al. (1996), from the neighboring dated corals.	58
Fig. 5.6 Global sea level curve from Thompson & Goldstein 2006, in correlation with 3 scenarios about the uplift rate. It is obvious that there were no significant differences with Siddall's curve.	61
Fig. 6.1 As slip rate increases, earthquakes are more frequent (e.g. Cowie & Roberts 2001)	63
Fig. 6.2 (A) Displacement -Length profile of a fault. (B) A triangular displacement profile. X is the maximum displacement of the studied fault during a period, while Y is displacement near the study area.	64
Fig. 6.3 Cumulative throw of a fault and displacement caused by a single event (A). Most hypothetical epicenters are plotted at the hangingwall, towards the center of the fault (redrawn from Roberts et al., 2004).	67
Fig. 6.4 View of the studied fault, where the tip and center of the fault are shown.	69

Fig. 6.5 The area that can be influenced with intensity VII from the studied fault, assuming an homogeneous bedrock geology,	70
Fig. 6.6 Earthquake recurrence of intensity VII in the studied fault. During the last 15.000±3.000 years 7 hypothetical earthquakes are expected.	71
Fig. 6.7 Map showing the maximum expected intensity generated by Kalamaki fault	72
Fig. 6.8 Map that shows the maximum expected intensities after considering the amplification due to the surface geology.	72
Fig. 6.9 View of the Kechries fault plane from Google Earth (Roberts et al. 2011).	73
Fig. 6.10 The area that is expected to be influenced by Kechries fault with intensity IX, assuming an homogenous bedrock geology	74
Fig. 6.11 Earthquake recurrence. During the last 15.000±3.000 years 6 of intensity IX in Kechries fault hypothetical earthquakes are expected	75
Fig. 6.12 The intensity alters in relation with the geological formations, from X till VIII.	75
Fig. 6.13 Earthquake recurrence in relation with the geological amplification. The area that is at a greater risk is westernmost section of the Corinth canal.	76
Fig. 6.14 View of the postglacial scarp of the Loutraki fault. This scarp is from the segment northwards the main fault, near the monastery of Osios Potapios.	78
Fig. 6.15 The area that is expected to be influenced by the Loutraki fault with intensity IX, without taking under consideration the bedrock geology or the earthquake recurrence.	78
Fig. 6.16 Earthquake recurrence of intensity IX in Loutraki fault. Since the last glaciation, 10 hypothetical earthquakes might have occurred.	79
Fig. 6.17 The maximum expected intensity and how does it alters in relation to the bedrock geology.	80
Fig. 6.18 Earthquake recurrence in relation to the geological amplification. The area that is at a greater risk is the central area of the Corinth canal, is characterized by higher recurrence.	81
Fig. 6.19 View of the Schinos and Pisia segments fault from Google Earth(Roberts et al. 2011).	83
Fig. 6.20 The area influenced by the South Alkyonides fault system with intensity IX, considering an homogenous bedrock geology.	83
Fig. 6.21 Earthquake recurrence of intensity IX in South Alkyonides fault system. During the last 15.000±3.000 years 23 hypothetical earthquakes are expected.	84
Fig. 6.22 The maximum expected intensity and how does it alters in relation to the bedrock geology.	85

<i>Fig. 6.23 Earthquake recurrence in relation to the geological amplification. The northern section of the Perachora peninsula receives higher energy.</i>	86
<i>Fig. 6.24 The area that is expected to be influenced by the Agios Vassilios fault with intensity IX, considering an homogenous bedrock geology.</i>	87
<i>Fig. 6.25 Earthquake recurrence of intensity IX in Agios Vassilios fault. Since the last glaciation, 8 hypothetical earthquakes might have occurred.</i>	88
<i>Fig. 6.26 The maximum expected intensity after considering the bedrock geology</i>	89
<i>Fig. 6.27 Earthquake frequency in relation to the bedrock geology. The area westwards the Corinth canal, receives the highest frequency.</i>	89
<i>Fig. 7.1 Location map and leveling benchmarks where displacement was estimated (Mariolakos & Stiros 1987).</i>	91
<i>Fig. 7.2 Location map showing the leveling route, the benchmarks and their post-1981 displacements (redrawn from Mariolakos and Stiros 1987). Benchmark 77 the only one that subsided by 4cm, lies at the immediate hangingwall of the fault and benchmark 79 that was uplifted by 2cm on its immediate footwall, implying that our studied fault may have been passively ruptured during the 1981 earthquake.</i>	92
<i>Fig. 7.3 Earthquake recurrence to Corinth canal and Perachora peninsula, taking under consideration the SAFS, the Loutraki ,the Kechries and the Agios Vasilios faults</i>	95
<i>Fig. 7.4 Combined earthquake recurrence from the three major faults that pose a threat for the Isthmus canal, correlated with geological formations.</i>	96
<i>Fig. 7.5 Primary, secondary effects in Corinth basin and communities that are under greater threat.</i>	99
<i>Fig. 7.6 Marine sediments in Corinth basin dated from the Upper Pleistocene</i>	101
<i>Fig. 7.7 Expected paleogeography of Corinth 18.000 years ago.</i>	101
<i>Fig. 7.8 Expected paleogeography of Corinth 125.000 years ago.</i>	102
<i>Fig. 7.9 Expected paleogeography of Corinth 200.000</i>	102

